A NOVEL LYSOPHOSPHATIDYLETHANOLAMINE DEHYDROGENASE FROM

MYXOCOCCUS XANTHUS

by

MADHAVI SITARAMA AVADHANI

(Under the Direction of LAWRENCE J. SHIMKETS)

ABSTRACT

Myxococcus xanthus serves as a prokaryotic paradigm to study multicellularity in bacteria. Nutrient limitation initiates a developmental program in which the cells exhibit spatially and temporally regulated, morphologically distinct behaviors. The developmental program is coordinated by a series of intercellular signals. The most significant among them is the contact-dependent signal termed the C-signal which is absolutely essential for completion of development. The protein responsible for C-signaling, CsgA, belongs to the short-chain alcohol dehydrogenase (SCAD) family of enzymes. CsgA is proteolytically processed into a 17 kDa form. Much debate has focused on whether intercellular signaling occurs because of the enzymatic activity of the full length form or if the 17 kDa form is itself the signal. The genetic basis for the enzymatic role of CsgA comes from isolation of overexpression suppressor mutants. Overexpression of SocA, a SCAD with 28% identity to CsgA almost exclusively in the enzyme active site, not only suppresses the C-signaling defect, but also restores C-signaling to *csgA* mutants upon extracellular complementation.   In addition, conserved residues of CsgA are shown to be essential for C-signaling. The potential role of SocA in generating the C-signal was exploited to determine the biochemical basis for C-signaling.

We developed a dehydrogenase assay based screen coupled with mass spectrometry to identify SocA substrates. Our results indicate that SocA performs a novel biochemical reaction in oxidizing lysophoaphatidylethanolamine. Oxidized lysophosphatidylethanolamine does not function as an intercellular signal in *M. xanthus*.

INDEX WORDS: *Myxococcus xanthus*, Intercellular signaling, Short chain alcohol

    dehydrogenase, Lysophosphatidylethanolamine

A NOVEL LYSOPHOSPHATIDYLETHANOLAMINE DEHYDROGENASE FROM

MYXOCOCCUS XANTHUS

by

MADHAVI SITARAMA AVADHANI

M. Sc., Bangalore University, India, 1997

A Dissertation Submitted to the Graduate Faculty of The University of Georgia in Partial

Fulfillment of the Requirements for the Degree

DOCTOR OF PHILOSOPHY

ATHENS, GEORGIA

2005

A NOVEL LYSOPHOSPHATIDYLETHANOLAMINE DEHYDROGENASE FROM

MYXOCOCCUS XANTHUS

by

MADHAVI SITARAMA AVADHANI

Major Professor:	Dr. Lawrence J. Shimkets
Committee:	Dr. Harry Dailey
	Dr. Claiborne Glover
	Dr. Timothy Hoover
	Dr. Robert Maier

Electronic Version Approved:

Maureen Grasso
Dean of the Graduate School
The University of Georgia
May 2005

TABLE OF CONTENTS

LIST OF TABLES

LIST OF FIGURES

CHAPTER 1

INTRODUCTION AND LITERATURE REVIEW

A variety of environmental stimuli elicit collective or multicellular responses from bacterial populations. The effects of multicellularity range from colony morphogenesis, chemotaxis, and genetic exchange to formation of complex structures like biofilms or fruiting bodies (118). For example, flagellated, free-living *Pseudomonas aeruginosa* form surface-attached multicellular communities called biofilms within which cells differentiate into non-flagellated, mushroom-shaped structures called microcolonies. The cells forming the stalk of the microcolony are non-motile, while the mushroom cap is formed by migration of cells *via* twitching motility (78). The microcolony also shows remarkable resistance to antibiotics (25, 132). Thus, multicellularity enables cell survival under adverse conditions because of structural and functional differentiation of individual cells.

An essential feature of coordinated multicellular behavior is intercellular signaling. The mechanism of signaling is not universal, and bacterial signals encompass chemically diverse molecules. Acylated homoserine lactones (AHL) mediate cell density (quorum) sensing in many gram-negative bacteria, while oligopeptides are the canonical signaling molecules in gram positive bacteria. Signaling molecules that may not be as widely represented across the phylogenetic tree have been identified in both gram positive and gram-negative bacteria. Adenosine, β-lactam derivatives, and γ-

butyrolactones are produced by several species of *Streptomyces* and *Norcardia*. Quinolone from *P. aeruginosa* and hydroxy ketone from *Stigmatella aurantica* have not been reported to be produced by any other gram negative bacteria (117). Thus, bacterial signals appear to follow a phylogenetic pattern of distribution with most signals, though some are not as widely represented as others.

Intercellular signaling can also occur upon physical contact between adjacent cells. For example, the invasion of human mucosal epithelia by pathogenic *Neisseria* involves the interaction between the bacterial type IV pili and the human CD46 receptors on the host cell surface that triggers an immune response (102). Although tactile responses enable growth, differentiation, and movement during development of higher organisms (38, 73), not much is known about contact-dependent communication between bacteria.
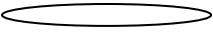
Multicellularity in *Myxococcus xanthus*:

M. xanthus is a gram-negative soil bacterium that serves as a prokaryotic paradigm to study social behavior and multicellularity in bacteria. The *M. xanthus* life style (Figure 1.1) involves cooperative group behavior (34). During vegetative growth, long slender rods glide over solid surfaces in large swarms, secreting hydrolytic enzymes that kill prey bacteria. The hydrolyzed protein and lipid from the prey serves as the primary source of carbon, nitrogen, and energy (33). The population feeds more efficiently than individual cells. Rosenberg et al. showed that cells at a high density hydrolyzed casein more efficiently than cells at a low density because of more efficient use of extracellular proteases (113).

Figure 1.1. Life cycle of *M. xanthus*. Cells, enzymes, fruiting bodies, and spores are not to scale.

Devouring Prey
Secreted hydrolytic enzymes including proteases

Spore
Germination

Fruiting body formation
and sporulation

**Developmental
cycle**

Starvation

**Predation
(Vegetative growth cycle)**

Rippling

Aggregation

Killing Prey
Peptidoglycan hydrolases
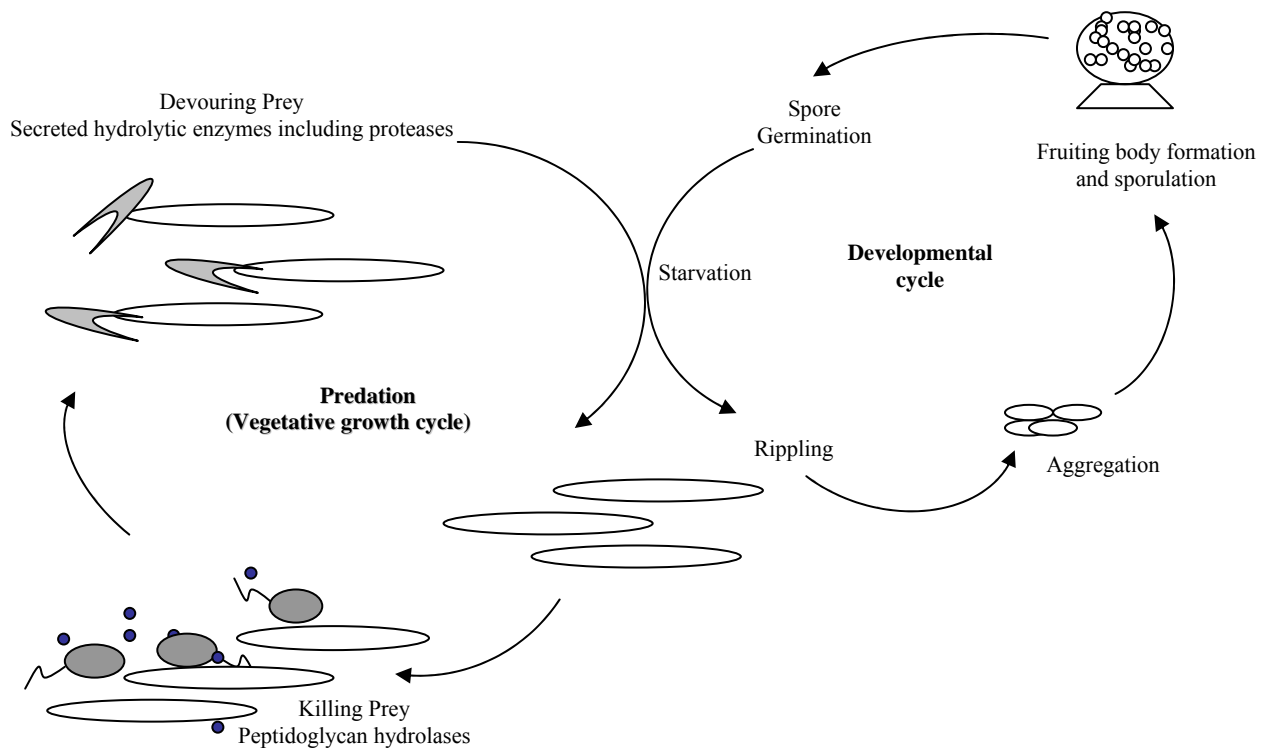
Key:

Vegetative *M. xanthus*;   Prey Cell;   Lysed Prey Cell

Peptidoglycan hydrolases;   Aggregating *M. xanthus*;   Myxospores

Nutrient limitation triggers a developmental program during which the cells exhibit a series of spatially and temporally regulated behaviors with a characteristic multicellular dependence (34). Rippling, so called because of its resemblance to ripples on the surface of water, is the first of the behavioral changes. Rippling is the coordinated movement of ridges of cells that propagate as waves outward in a recurring pattern from the center of a domain. Rippling is induced by peptidoglycan and some of its individual components (126, 127). Sager and Kaiser observed two sets of wave patterns moving in opposing directions with the same velocity and wavelength. They suggested that rippling causes an end-to-end collision between waves of cells stimulating cell reversal (116). Welch and Kaiser studied the properties of rippling cells using time-lapse microscopy which showed that while the opposing crests appeared to pass right through each other, in fact they reflected off of each other (138).

Welch and Kaiser studied the behavior of fluorescent rippling cells (138). Green fluorescent protein (GFP) expressing cells were mixed with non-fluorescent cells at a ratio of 1:500. The labeled cells in a wave crest were aligned perpendicular to the direction of wave movement and moved in the direction of the crest. They reversed their direction upon encountering the opposing crest head on. This led Igoshin et al to propose the existence of a biochemical oscillator that controls the reversal of gliding direction (59). The biochemical nature and mechanism of the proposed oscillator will be discussed in a separate section. Rippling is proposed to play a role in the spacing of fruiting bodies. However, equally spaced fruiting bodies have been seen in submerged culture experiments where rippling has not been observed. Also, rippling is not essential for completion of the developmental program. Hence the exact need for rippling has yet to

be deciphered.

Aggregation is the movement of cells into foci where they organize into fruiting bodies. Cells exhibit gliding motility in the direction of their long axis with periodic reversals in the gliding direction. Aggregation is proposed to be initiated and sustained by contact-dependent C-signaling between individual cells (62, 63). The details of this model will be discussed in a later section.

Kaiser (66) suggested a signal-independent mechanism of aggregate formation. According to this model, the high cell density in the crests of rippling cells is the key to aggregate formation. Collision between cells in countermigrating ripples is proposed to inhibit cell movement, trapping the cells in an aggregation center. Time-lapse microscopy reveals fusions between aggregates due to cell movement within and outside the aggregates resulting in the formation of macroscopic fruiting bodies.

The fruiting bodies mature with the differentiation of 10-20% of the rod-shaped vegetative cells into spherical structures called myxospores that are environmentally resistant and metabolically dormant. Another 10% of the initial population differentiates into specialized peripheral rods that show differential gene expression but never enter the fruiting body or sporulate. Peripheral rods are proposed to play a protective role in guarding the immature aggregates against consumption by other microbes. The majority of the cells undergo developmental autolysis, which is proposed to provide nutrients when cellular metabolism has slowed due to nutritional stress (34, 122).

The underlying feature of fruiting body development is intercellular signaling, which is suggested by six extracellular complementation groups (A, B, C, D, E, and S). The developmental defect in a mutant in one complementation group can be corrected by

codevelopment with wild-type cells or a mutant in another complementation group (50, 101). The vegetative cells recovered from the germinated spores of such mutants retain their developmental defects and mutant genotype suggesting that complementation is not due to the transfer of genetic material.

While the biochemical basis of extracellular complementation is at least partially understood in the A, C, and S groups by addition of specific cellular fractions, the mechanisms of B, D, and E signaling remain to be elucidated (122). Table 1.1 summarizes the different signaling systems along with what is known about their genetics and biochemistry. The mutants in each class cease to develop at characteristic time points. The signaling system defined by each complementation group directs the expression of a distinct set of developmental genes in a temporal hierarchy (122). Kroos and Kaiser (80) determined the time of developmental arrest in these mutants by studying the expression pattern of a set of *lacZ* reporter fusions to development-specific transcriptional units. If a particular mutation did not inhibit the expression of the reporter gene, then it was presumed to interrupt the developmental process after the expression of the reporter. On the other hand, if the expression of the reporter was inhibited by a particular mutation, then it was assumed to interrupt the developmental process before the expression of the reporter. The fact that each complementation group arrested development at different time points suggested that each of these mutant classes was responsible for generation of different signaling molecules and not part of a biochemical pathway to generate a single signaling molecule. The A, B, C signaling systems act within the first six hours after the initiation of development, while D and S (95) systems act several hours later. The E signaling system seems to act after the A, B, and C systems

7

Table 1.1. Extracellular complementation groups in *M. xanthus* (Shimkets 1999).

The six extracellular complementation groups are listed with the genes defining them and

the respective complementing cellular fraction where known.

Complementation group	Gene	Function of gene product	Complementing cellular fraction
A	*asgA*	Histidine protein kinase/response regulator	Amino acid mixture
	asgB	Putative transcription factor	Amino acid mixture
	asgC	Sigma factor (σ^{70})	Amino acid mixture
	asgD	Histidine protein kinase	Amino acid mixture
	asgE	Amino hydrolase	Amino acid mixture
B	*bsgA*	ATP-dependent protease	Unknown
C	*csgA*	Short chain alcohol dehydrogenase	CsgA
	socA	Short chain alcohol dehydrogenase	
D	*dsgA*	Translation initiation factor IF-3	Unknown
E	*esg*	E1α subunit branched-chain keto acid dehydrogenase	Unknown
		E1β subunit branched-chain keto acid dehydrogenase	
S	*difA*	Methyl-accepting chemotaxis protein	Fibrils
	difE	CheA-like histidine protein kinase	Fibrils

but before D and S (31, 134). Figure 1.2 depicts the time scale for various morphological stages of development and the corresponding gene expression affected by the different signaling groups.

The A-signal:

Mutations in five different genes define the A-complementation group (23, 39, 86, 99). All the mutants in this group show decreased A-signal production and reduction of secreted proteins.

Genes required for A-signaling:

The *asgA* gene codes for an unusual member of a two-component regulatory system with an N-terminal response regulator domain and a C-terminal histidine protein kinase (HPK) domain (28, 111). The input and the output domains associated with ligand binding and DNA binding, respectively, are missing in AsgA and are presumed to be supplied by other unidentified proteins (111). Plamann et al. (111) suggest that AsgA participates in a phosphor-relay essential for sensing starvation, and the subsequent response results in A-signal generation.

asgB encodes a putative transcription factor with a C-terminal helix-turn-helix motif (109). AsgB may have an essential role during growth as suggested by failed attempts to create a null *asgB* allele (109). Hence, Plamann et al. (109) proposed that AsgB acts as a transcriptional repressor of early developmental genes whose expression during growth may have deleterious effects on vegetative cells.

asgC encodes the essential bacterial sigma factor σ^{70}. The mutant *asgC* phenotype is due to a single amino acid change in the highly conserved region 3, which is

Figure 1.2. Time scale indicating the various morphological stages and the earliest point where gene expression is arrested by mutants in the different extracellular complementation groups (Shimkets 1999). Earliest representative genes whose expression is completely dependent on the corresponding signaling group are indicated. (A-group Black; B-group Blue; C-group Red; D-group Grey; E-group White; S-group Green). The morphology of wild-type cells at various developmental times is represented above the time scale. Aggregates start to appear about 8-12 hr of development. Immature fruiting bodies without spores are formed by 24 hr, and sporulation is complete by 48 hr. Cells, fruiting bodies, and spores are not to scale.

Morphology

Reporter gene
expression

Time Scale

0   12   24   48

Hours
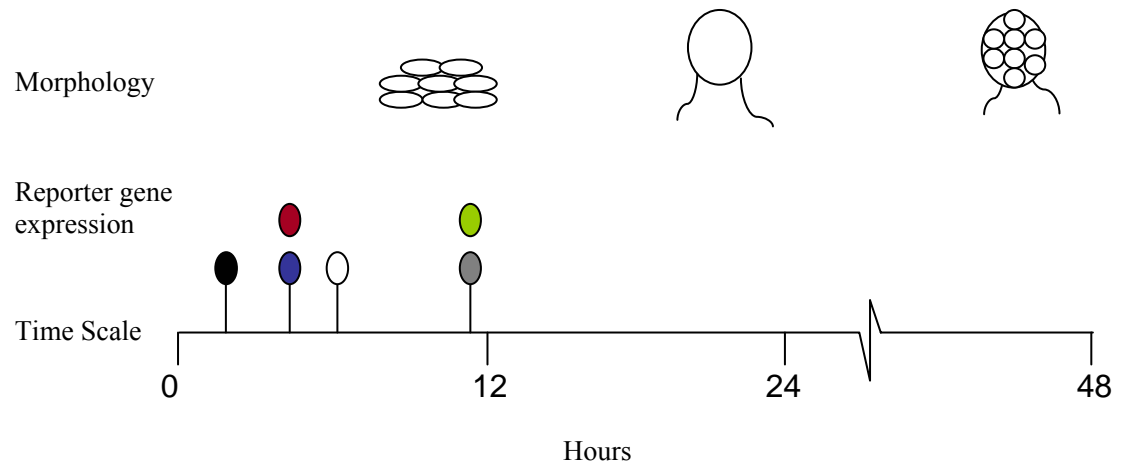
composed of 2 subregions. Subregion 3.2 is proposed to be involved in binding to core RNA polymerase and subregion 3.1 has a weak helix-turn-helix (HTH) motif. The *asgC* mutation is found immediately downstream of the putative HTH motif. This type of mutation in sigma factors is known to affect the interaction between RNA polymerase and transcription factors (56, 60, 85, 98). This led Davis et al. (28) to propose that the inability of AsgC to interact with a transcriptional regulator required for A-signal production results in the A-signaling defect. Alternately, the mutant sigma factor binds the core polymerase with increased affinity preventing an alternate sigma factor necessary for A-signal production to bind core polymerase.

asgD encodes an atypical HPK in which the receiver domain is at the N-terminus and a kinase domain is at the C-terminus (23). The receiver and the sensor domains of AsgD are separated by a 380-amino-acid-long intermediate region of unknown function. The *asgD* mutant has an interesting phenotype. Wild-type cells complete development upon starvation on low nutrient medium called CF (Clone Fruiting) medium that contains 10 mM MOPS (pH 7.6), 0.015% Casitone, 8 mM $MgSO_4$, 1 mM KH_2PO_4, 2% sodium citrate, 1% sodium pyruvate, and 1.5% Difco agar. The development of *asgD* mutant is severely compromised on this low nutrient medium. However, on a more stringent starvation medium with 10 mM MOPS, 4 mM $MgSO_4$, 2 mM $CaCl_2$ and 1.5% Difco agar, *asgD* sporulates at 35% of wild-type levels. This led Cho and Zussman (23) to propose that AsgD is involved in defining the nutrient threshold for sensing starvation leading to the initiation of development.

asgE encodes a putative aminohydrolase (39). Aminohydrolases catalyze the hydrolysis of substrates containing nitrogen-carbon heterocyclic rings. *asgE* mutants

produce only 4% of wild type spore levels. While *asgE* improved the sporulating efficiency of *asgA* in extracellular complementation experiments to about 4% of the wild-type, the converse is not true. *asgA* did not improve spore yields of *asgE*, suggesting AsgE acts downstream of AsgA in the A-signal transduction pathway, and the *asgE* gene could be one of the potential targets of AsgA (39).

Biochemical basis for A-signaling:

Plamann et al. (110) and Kuspa et al. (87) identified two sets of substances in the medium conditioned by prior incubation with *asg*$^+$ cells that restored developmental gene expression in *asg* mutants. They used a bioassay to measure the reporter gene activity of the A-signal-dependent transcriptional fusion of Ω4521 to *lacZ* in an *asgB* background. One factor was heat-sensitive and the other heat-stable. Plamann et al. (110) identified the heat-sensitive factor as two proteases of 27 kDa and 10 kDa. The 27 kDa protease had trypsin-like substrate specificity, hydrolyzing peptides on the carboxy terminus of arginine or lysine residues. In addition, the 27 kDa protease was able to rescue aggregation and sporulation in *asgB* mutants upon extracellular complementation. The substrate specificity of the 10 kDa protease has not been identified.

Kuspa et al. (87) determined that the heat-stable A-factor was composed of amino acids and peptides. Pure amino acids with highest A-factor activity include tyrosine, proline, tryptophan, phenylalanine, leucine, and isoleucine. These amino acids were present at concentrations of 11-22 μM in starvation medium conditioned by *asg*$^+$ cells. Below the threshold concentration of 10 μM, these amino acids did not rescue developmental gene expression individually or in mixtures. The specific activities of the peptides were the sum of the specific activities of their individual components.

Kuspa et al. (88) used *in vitro* experiments to simulate conditions of *in vivo* A-factor production. The crude A-factor was subjected to autodigestion followed by amino acid analysis of the free amino acid content. The concentration of each of the six amino acids with highest A-factor specific activity increased about 2-fold upon digestion. In addition, the timing of A-factor release from asg^+ cells coincided with the activation of gene expression by the A-factor conditioned medium (87). Also, Plamann et al. (110) found that proteases with substrate specificities different from trypsin also rescued the developmental gene expression in *asgB*. Finally, inhibition of the endogenous trypsin activity abolished A-factor production, strengthening the argument that amino acids are the A-signal.

Role of A-signaling during development:

Kuspa et al. (88) proposed that A-signal amino acids serve in cell density sensing. Transcription of the $\Omega 4521$ reporter decreased to 75-90% when wild-type cells were diluted below the threshold levels required for development. Transcription increased upon addition of amino acids added at the same levels required for $\Omega 4521$ expression in the *asgB* mutant. While *asgB* mutants produced 5-10% of wild-type levels of A-factor, increasing the cell density 10 to 20-fold restored $\Omega 4521$ expression and sporulation. Since the concentration of A-signal amino acids is directly proportional to the cell density, Kuspa et al. (88) proposed that A-signal determines whether an adequate density of starved cells is present to complete development. Hence, the A-signal defines a novel mechanism that regulates gene expression in response to changes in cell density.

A-signal transduction pathway:

Putative components of the A-signal sensory pathway have been identified based on the isolation of suppressor mutations capable of A-signal independent expression of genes that would otherwise require the A-signal. SasS, a putative histidine protein kinase, is proposed to positively regulate Ω4521 expression during early development by phosphorylating its cognate response regulator (143). A *sasS* null mutant shows abnormal aggregation and sporulation and is severely compromised in the expression of the Ω4521 reporter in spite of producing wild-type levels of the A-signal. *sasS* mutants do not respond to extracellular A-signal.

Gorski and Kaiser (46) proposed that SasR, a sigma-54 activator protein, is involved in sensing the A-signal. The *sasR* mutant is compromised in aggregation, sporulation, and expression of the A-signal dependent reporter Ω4521. The fact that this mutant makes wild-type levels of the A-signal was demonstrated by its ability to correct the *asgA* phenotype upon extracellular complementation. However, the *sasR* phenotype is not corrected by extracellular complementation with wild-type cells, suggesting its potential role in the A-signal response pathway. SasS is proposed to phosphorylate SasR in response to the A-signal, resulting in the expression of sigma-54-dependent genes under A-signal control (46, 49).

The A-signal paradox and stringent response:

Starvation sensing in *E. coli* is characterized by the initiation of a stringent response upon depletion of aminoacylated tRNA (18). When the ribosome pauses because of lack of charged tRNA, RelA, the ribosome associated stringent response protein, synthesizes the starvation signaling molecules guanosine pentaphosphate

(pppGpp) and guanosine tetraphosphate (ppGpp) (18). The reaction involves the transfer

of the β, γ -pyrophosphoryl group from ATP to the ribose 3' hydroxyl group of GTP or

GDP, respectively, by RelA (18). These effector molecules regulate growth by positively

or negatively influencing gene expression and inhibit DNA replication initiation (18). A

M. xanthus relA mutation prevents the accumulation of (p)ppGpp and inhibits

development (52). Furthermore, ectopic expression of *relA* induces the untimely

expression of early developmental genes (129). The stringent response activates

transcription of many developmental genes (129) and inhibits transcription of a

developmental repressor *socE* (26, 27). The stringent response also activates the

extracellular A (52) and C signaling systems (26, 27). The extracellular amino acid pool

generated during A-signaling reaches a high enough concentration (25 μM) to sustain

slow growth. However, cells continue development using the limited carbon and energy

generated by the A-signal for growth (110). This paradox is explained by a novel

regulatory mechanism suggested by Crawford and Shimkets (26, 27). They have

demonstrated that ectopic depletion of SocE results in growth arrest even in the presence

of nutrients. Growth arrest is achieved by the action of CsgA and the loss of SocE, which

maintains RelA-dependent (p)pp(G)pp production in spite of the influx of amino acids

(26, 27). It is not known how the two proteins maintain the RelA-dependent starvation

response.

The B-signal:

The mutants in the B complementation group are aggregation- and sporulation-

defective and are compromised in the expression of early developmental genes (43, 81).

The *bsgA* gene encodes an ATP-dependent protease similar to the Lon protease of *E. coli* (41, 42, 44). BsgA is localized in the cytoplasm (41), and the recombinant BsgA protein, partially purified from *E. coli*, has an ATP-dependent protease activity (44). The *E.coli* Lon protease degrades misfolded proteins and modulates the regulatory function of several cellular proteins (47). For example, SulA, a physiological substrate of the Lon protease, is induced by UV irradiation and aids in DNA repair by preventing premature segregation of damaged DNA into daughter cells (57, 58). SulA inhibits cell division by preventing self-assembly of FtsZ (12). Rapid degradation of SulA by Lon protease is essential for normal cell cycle progression.

Hager et al. (51) described a *bsgA* suppressor that was localized to *spdR*. *spdR* encodes a σ^{54}-dependent transcriptional activator that belongs to the NtrC family of transcriptional activators. The *spdR* mutants regained aggregation, sporulation, and expression of many early developmental genes (51, 136). The *spdR* mutants showed accelerated development, forming spore-filled fruiting bodies, about 8-12 hr earlier than the wild-type. These mutants also showed development in the presence of casitone concentrations (0.2%) high enough to suppress development. In addition, some of the developmental genes were expressed in the mutant background in vegetative cells. This led Hager et al. to propose that SpdR is a negative regulator of development. While their data are consistent with the idea that SpdR is the cellular target of BsgA, immunoblot analysis of wild-type and *bsgA* cells did not support this hypothesis. SpdR does not accumulate in *bsgA* cells, and SpdR did not decrease upon initiation of wild-type development. Furthermore, the *spdR* mutation does not exclusively suppress the *bsgA* defect. It also suppresses the requirement for A-signaling (136). Although these data

rule out the possibility that SpdR is the physiological target of BsgA, the mechanism of

B-signaling could still be due to the proteolytic processing of a protein by BsgA. Since

the substrate of BsgA has not been identified yet, the basis for extracellular

complementation remains to be established.

The D-signal:

The mutants in the D class show partial aggregation followed by delayed

sporulation. The aggregates are larger than fruiting bodies formed by wild-type cells and

less symmetrical. Gene expression is reduced or abolished after the first eleven hours of

development (20). Insertion mutations that completely inactivate *dsgA* are lethal

suggesting that *dsg* is essential for growth (21). Indeed, the *dsg* gene encodes translation

initiation factor IF3 (22, 70). *E. coli* IF3 is required for dissociating the 70S ribosomal

complexes upon completion of translation and for positioning the ribosome at the right

initiation codon on the mRNA. Dsg differs from its *E. coli* and *Bacillus*

stearothermophilus homologs in having 66 additional amino acids at the C-terminus (70).

In addition, Dsg also uses a rare AUC start codon, which is not known to initiate

translation of any known gene (22). In *E. coli*, the use of another atypical start codon

AUU is important for the autoregulation of IF3 at the level of translation. At high levels

of IF3, its corresponding mRNA is not translated because IF3 does not recognize AUU as

the start codon. However, at low levels of IF3, IF3 mRNA is translated because the

ribosomes lacking IF3 show low selectivity for typical start codons (17).

Kalman et al. showed that Dsg is a typical IF3 protein except for its use of a

different initiation codon (70). Dsg restored autoregulation of IF3 synthesis in an *E. coli*

IF3 mutant that does not distinguish between typical and atypical codons (70). The essential nature of this protein explains its requirement during growth in *M. xanthus*. Dsg may be involved in the recognition of a rare initiation codon required for generation of the D-signal.

The E-signal:

The *esg* mutants show reduced aggregation, sporulation, and expression of many developmentally regulated genes that express after six hours into development (31, 32). The mutations mapped to an operon of two genes that encode the E1α and E1β subunits of branched-chain keto acid dehydrogenase (BCKAD), a multienzyme complex involved in branched-chain amino acid metabolism. This complex is composed of E1, E2, and E3 proteins and converts branched chain keto acids derived from leucine, isoleucine, and valine to the coenzyme A derivatives of isovalerate, methylbutyrate, and isobutyrate, respectively. These CoA derivatives are used for the production of cellular carbon and energy. Some bacteria also use these fatty acid CoA derivatives for the synthesis of long branched-chain fatty acids for incorporation into membrane phospholipids. The fatty acids resulting from isovalerate include *iso*-15:0, *iso*-13:0 and *iso*-17:0, and unsaturated and hydroxy-modified forms of these fatty acids.

esg mutants grown in the presence of isovalerate showed developmental aggregation and sporulation indicating that the metabolic block caused by the absence of BCKAD is bypassed by the addition of a metabolic end product (134). The cell membrane phospholipids of the *esg* mutants have lower amounts of branched-chain fatty acids and proportionally increased levels of the unsaturated fatty acid 16:1 ω5c and the

saturated fatty acid palmitic acid (5, 134). Exogenous addition of isovalerate during growth also restored the wild-type levels of most *iso*-odd fatty acids with a concomitant decrease (3-fold) in the levels of 16:1 ω5c (72). This led Toal et al. (134) to suggest that the branched-chain fatty acids derived from the corresponding branched-chain amino acids are used to produce cellular components during growth that could be used as specific intercellular signals during development.

Kearns et al. (72) discovered that phosphatidylethanolamine (PE) preparations from *esg* mutants grown in the absence of isovalerate elicited a strong chemotactic response. They used metabolic engineering to identify the fatty acid component of chemotactic PE as 16:1 ω5c. This observation was confirmed by the ability of chemically synthesized PE containing 16:1 ω5c to elicit the same response. PE chemotaxis was only observed under starvation conditions, suggesting that PE containing 16:1 ω5c plays an important role in the directed movement of cells during fruiting body morphogenesis. This poses a paradox for the developmental defects of *esg* mutants since they produce increased levels of the developmental chemoattractant. The observation that the chemotactic response was found within a very narrow concentration range led Kearns et al. (72) to propose that the developmental defects manifested in *esg* mutants could be due to the presence of excess signal rather than the lack of it. This model does not explain the basis for the extracellular developmental rescue of *esg* mutants by wild-type cells or mutants of other complementation groups and may not be related to E-signaling.

The S-group:

     M. xanthus utilizes two genetically and mechanistically separate motility systems adventurous (A) and social (S). Cells with a mutation in the A motility system lack the ability to move as single cells but are capable of group movement. Conversely, cells bearing a mutation in the S motility system are compromised in their communal movement while still retaining the capacity to move as individuals. Mutants with both systems impaired are unable to move. Wolgemuth et al. (141) have proposed that A-motility is mediated by directed slime extrusion through nozzle-like structures located at the cell poles. According to this model, hydrated slime within the cell is extruded through the nozzles with concomitant cell propulsion in the opposite direction. Cell reversal is proposed to occur when slime extrusion occurs from the opposite pole (141). On the other hand, S-motility is driven by the retraction and extension of type IV pili (96, 133). Type IV pili are thin, long organelles that are found only on one of the cell poles (67). Loss of pili either by mutation or by mechanical shearing results in S-motility defects (114, 142). The tip of a pilus at the leading pole of one cell extends and attaches to a surface of another cell. Retraction of the pilus pulls the cell forward (96). Both motility systems are coordinated through the action of the G-protein MglA (53).

     In addition to type IV pili, S-motility depends also on two other surface molecules, lipopolysaccharide O-antigen (15, 145) and fibrils (2). The role of O-antigen in motility and development remains to be elucidated.

     Some S-motility mutants, particularly those defective in fibril production also show defective fruiting body formation and sporulation (54). Fibrils are polysaccharide organelles composed of galactose, glucosamine, glucose, rhamnose, and xylose, and a

tightly associated set of proteins (6, 8). They are peritrichous in distribution, 30-40 nm in diameter and about one cell length long (7). Fibrils interconnect adjacent cells and enable their adhesion to substratum (2). The S-system includes some of the proteins encoded by the *dif*/*dsp* locus that are involved in chemotactic sensory transduction (89, 144). These mutants do not exhibit the cohesiveness characteristic of *M. xanthus* and are compromised in fibril production (3, 123). Li et al. (96) have suggested that the fibril polysaccharide may be the pilus receptor during pilus retraction.

Several observations led Shimkets (122) to define the S-group as the sixth extracellular complementation group. Of the S mutants, only those that are defective in fibril synthesis are completely compromised in fruiting body development. These results argue that the fibrils play a specific role in development above and beyond their necessity for S motility. The wild-type cells rescued cohesion and development of *dsp* mutants in a contact-dependent manner (121). While *dsp* mutants formed normal aggregates in a 1:1 mixture with wild-type cells, their sporulation efficiency was not as high as that of wild-type cells. Fibrils extracted from wild-type cells restored cohesion and development to the *dsp* (19) and *dif* mutants (145) lacking fibrils. In addition, Chang and Dworkin (19) showed that wild-type fibrils restored partial expression of certain developmental genes while the complete restoration of gene expression in certain other cases showed a delayed response. These results suggest that the developmental defects manifested by the *dsp*/*dif* mutants are due to an inability to generate extracellular molecule(s). The biochemical basis of fibril-mediated complementation remains to be established. One function of fibrils is to mediate chemotaxis to PE (71).

The C-signal:

The C-signal is essential for all events occurring six hours after induction of development including rippling, aggregation, sporulation, and expression of late developmental genes (80, 127). All the mutations in this class have been mapped to the *csgA* gene which has significant homology with short chain alcohol dehydrogenase genes (4, 90, 91, 124). CsgA occurs in two forms, a full-length 25 kDa form (90) and a proteolytic product that is about 17 kDa (76). Native and recombinant versions of both forms of CsgA restore the ability of *csgA* cells to develop, though at different concentrations (76, 90, 97). Localization of CsgA to the cell membrane (97, 128) and the ability of anti-CsgA antibodies to prevent development of wild-type cells (120) suggest further that CsgA can act extracellularly.

An interesting feature of the C-signal is that it requires cell-cell contact for transmission. Separation of wild-type and *csgA* cells by a 0.45 μm nucleopore membrane filter prevents the developmental rescue of *csgA* cells (76). In addition, C-signal transmission requires cell motility (75). Although nonmotile cells produce CsgA at wild-type levels, they fail to complement the C-signal defect in *csgA* mutants (75). Mechanical alignment of nonmotile mutants on microscopic grooves created by abrasion restores the ability of nonmotile *csgA* cells to express C-dependent genes and sporulate (74). These experiments establish the contact-dependence for C-signal transmission and suggest that the C-signal is a paracrine (locally-acting) signal.

Mechanism of C-signal generation:

Although CsgA has been extensively studied, there is still ambiguity with regard to the nature of the C-signal. The role of the two different forms of CsgA in the

generation of the signal is the center of debate. It is not known if C-signal is generated by the enzymatic activity of full-length CsgA or if the 17 kDa proteolytic fragment is itself the signal. It is also not clear whether the two forms of the protein controls different aspects of development.

CsgA acts as a hormone:

The first model envisages CsgA as a protein hormone. Cell-free extracts from wild-type cells restored development to *csgA* mutants enabling a bioassay for purification of the bioactive molecule (76, 77). This assay involved resuspension of log phase *csgA* cells in a nutrient-free buffer containing 10 mM 3-(N-morpholino) propanesulfonate (MOPS), 1 mM $CaCl_2$, 4 mM $MgCl_2$, 50 mM NaCl (pH 7.2) and transfer of this cell suspension into the wells of a 24-well microtitre plate. After incubation at 32^0C for six hours in a humid chamber, which is when the morphological anomalies of these mutants become apparent, the buffer was replaced by pre-warmed fractions to be assayed. The active fractions restored the ability of the *csgA* mutants to form fruiting bodies and spores to wild-type levels (200-300 fruiting bodies and 2.5×10^6 spores per 2.5×10^8 input cells) and also to express C-signal-dependent genes. The C-signal rescue activity was found in the membrane fraction, and isolation of free C-factor required treatment of the membrane fraction with the zwitterionic detergent 3([3cholamidopropyl] dimethylammonio)-1-propane-sulfonate (CHAPS). This fraction was purified about 1000-fold by ammonium sulfate precipitation and anion exchange chromatography. Purified C-factor was identified as a 17 kDa polypeptide and was active at a concentration of 1-2 nM. Cleavage of the 17 kDa polypeptide with endoproteinase Lys-C resulted in two fragments. Edman degradation of the smaller of the two fragments revealed an amino

acid sequence that corresponded with an internal sequence of the *csgA* gene. The peptide

fragment was approximately the size of the carboxy terminus of the protein. The N-

terminal amino acid sequence of the larger fragment of the 17 kDa polypeptide was not

obtained, but the size of the peptide suggests that CsgA is processed to the 17 kDa form

at the N terminus. The exact site of truncation is unknown. While Kim and Kaiser

achieved a 1000-fold purification of the active fraction, the fraction contained other

higher molecular weight polypeptides (77) and exhibited a very narrow range of activity

(76).

Lobedanze and Sogaard-Andersen used antibodies raised against the N and C-

termini of the full-length CsgA to demonstrate the molecular difference between the two

forms (97). The antibodies against the N-terminus recognized only the full length CsgA

whereas antibodies against the C-terminus recognized both versions confirming that the

processed form lacks the N-terminus. A serine protease was implicated in truncation of

the full-length form. The 25 kDa protein as a MalE-CsgA fusion protein was incubated

with the total cell lysate from developing *M. xanthus*. Immunoblot analysis of this

extract detected the 17 kDa protein that was not seen when the cell lysate was subjected

to heat treatment at $70^{O}C$ for 10 minutes. In order to determine the specificity of the

protease, the 25 kDa protein was incubated with the *M. xanthus* cell extract in the

presence of protease inhibitors. The 17 kDa protein was not produced when serine

protease inhibitors were added but was observed with inhibitions of cysteine proteases,

aspartyl proteases, and metalloproteases. The exact site of processing remains to be

identified.

Lobedanze and Sogaard-Andersen demonstrated that a C-terminal 18.1 kDa of CsgA with an N-terminal MalE fusion was able to correct the developmental defects of *csgA* mutants upon extracellular complementation. The recombinant 18.1 kDa form purified from *E. coli* had a 2000–fold lower specific activity (97). The authors suggest that the low specific activity is due to the lack of an unknown posttranslational modification of the CsgA portion of the fusion protein. Expression of the truncated protein in the *csgA* mutant did not restore the wild-type developmental phenotype.

Lobedanze and Sogaard-Andersen (97) used Triton X-114 phase separation to obtain outer and inner membrane fractions of wild-type cells undergoing development. Immunoblot analysis was performed to determine which, if any forms were found in the outer membrane. They observed that both forms of CsgA were localized to the outer membrane. This led them to suggest that the truncated form acts as a paracrine hormone to signal the neighboring cell *via* a hypothetical receptor.

Simunovic and Shimkets (128) used a more refined approach to study the localization of CsgA in vegetative cells. They separated the cellular membranes from the spheroplast-enriched cells into inner, outer, and hybrid membrane fractions using a three-step sucrose gradient followed by further separation on discontinuous sucrose gradients. The purity of each fraction was assessed by unique protein markers. The succinate dehydrogenase assay was used to confirm the purity of the inner membrane, and the purity of the outer membrane fractions was determined from immunoblots performed with monoclonal antibodies against the LPS core and O-antigen. This method detected the full-length form of CsgA in the inner membrane and neither form in the outer membrane. This discovery does not support the role of the processed form as a paracrine

signal. However, Simunovic and Shimkets used vegetative cells, and there could be differential localization of CsgA during vegetative growth versus development. But then, there is no direct evidence for this being the case.

Taken together, the experiments from the Kaiser and Sogaard-Andersen laboratories appear to suggest that the processed form of CsgA acts as a protein hormone. However, the evidence provided is not sufficient to establish this beyond a reasonable doubt. The presence of some high molecular weight proteins in the initial preparation of the 17 kDa form by Kim and Kaiser does not necessarily exclude the possibility of developmental rescue by the full length form of CsgA. Although, the recombinant form of the truncated protein had developmental activity, the specific activity was about 2000-fold lower than the original preparation of Kim. In addition, expression of this protein in a *csgA* mutant did not result in developmental rescue. These observations lead one to question the validity of the 17 kDa form as the signal.

CsgA acts as an enzyme to generate the signal:

The second model suggests an enzymatic role for CsgA which shares significant homology with the short-chain alcohol dehydrogenase (SCAD) family (90). The members of the SCAD family utilize NAD(H) or NADP(H) to mediate the interconversion of secondary alcohols and ketones (105). The first line of genetic evidence for the enzymatic nature of CsgA comes from the isolation of the suppressor of *csgA* (*soc*) mutants containing transposon insertions in the *socABC* operon (91, 92). The first of the three genes in the *socA* operon, *socA*, encodes a short chain alcohol dehydrogenase that bears 28% amino acid identity to CsgA, primarily in the enzyme

active site (91). The second gene in this operon encodes SocB, an integral membrane

protein with homology to FrdD which anchors fumarate reductase to the membrane in

Proteus vulgaris. The third gene in the *socABC* operon encodes SocC, a negative

regulator of the operon (92). Two transposon suppressor mutations were discovered, one

between *socB* and *socC*, and another in *socC* (92). These insertions are polar and

inactivate the negative regulator of the operon resulting in the overexpression of *socA*.

Lee and Shimkets studied the role of SocC in the regulation of the *socABC* operon using

the *soc-lacZ* fusions in *socC*$^+$ and *socC* mutant backgrounds and found a 90-fold increase

in expression of *socAB* transcription in the absence of *socC* (92). Further, mRNA levels

also showed a 50-100 fold increase, confirming the role of SocC as the negative regulator

of the operon.

      The ability of *socA*-overproducing mutants to rescue the C-signaling defect of

csgA mutants was examined by extracellular complementation of *csgA* mutants with cells

bearing mutations in the *socA* operon and *csgA*. Vegetative cells were mixed in a 1:1

ratio, and allowed to develop at 32^0C for 4 days. Spores were enumerated by plating as

each strain has a unique antibiotic resistance profile. The restoration of development to

csgA cells suggested that the *socA csgA* double mutant produces the C-signal (92). This

led Lee and Shimkets to propose that the overlapping substrate specificity between CsgA

and SocA may result in production of the C-signal.

      Mutation of conserved CsgA residues provides further evidence in support of the

hypothesis that CsgA is an enzyme. The presumptive substrate binding site as well as the

coenzyme binding site are required for CsgA activity (90). Point mutations that cause

replacement of conserved active site residues, S135T and K155R, inactivated *csgA* (90).

A MalE-CsgA protein bearing the S135K mutation was unable to restore development to *csgA* mutants when extracellularly complemented. A point mutation that caused substitution of conserved arginine in the coenzyme binding region (R10A) with alanine resulted in inactive CsgA (90). Deletion of the entire coenzyme binding region resulted in an inactive protein that was unable to rescue development of *csgA* mutants (120). A conserved threonine residue stabilizes coenzyme-binding through hydrogen bonding (40), and the MalE-CsgA fusion protein bearing a threonine to alanine substitution (T6A) in the coenzyme-binding domain failed to complement the C-signaling defect in *csgA* mutants (90). This mutant protein showed reduced capacity to bind radiolabeled NAD^+ (90). Furthermore, the addition of NAD^+ and $NADP^+$ along with MalE-CsgA stimulated development while these nucleotides in their reduced forms delayed development (90) highlighting the importance of the coenzyme-binding region for CsgA activity.

The experimental evidence described above suggests a role for the coenzyme binding site as well as the substrate binding site of CsgA for the generation of the C-signal during *M. xanthus* development. Both CsgA and SocA are members of a family of short chain alcohol dehydrogenases that includes enzymes that catalyze the conversion of a wide range of substrates including sugars, steroids, prostaglandins, and aromatic hydrocarbons (105), making it difficult to predict putative substrates based on sequence similarity alone.

Role of C-signaling during development:

Rippling:

Rippling is the first of the various morphologically distinct events controlled by C-signaling. Shimkets and Kaiser (126) first observed that *csgA* null mutants are

completely compromised in their ability to ripple. The inability of *csgA* mutants to ripple was restored by codevelopment with a 1:1 mixture of wild-type cells (116). Dilution of wild-type cells with *csgA* mutants in different proportions led to an increased ripple wavelength suggesting a reduced frequency of cell-cell signaling. Each cell type was labeled with a different fluorescent dye, and fluorescence confocal microscopy revealed that the *csgA* cells were arranged end-to-end as for wild-type cells. Addition of partially purified CsgA resulted in increased reversal frequency of developing *csgA* cells. This observation combined with the already established requirement for end-end orientation of cells during C-signaling, led Sager and Kaiser (116) to propose that contact between cells in waves migrating in opposing directions initiates C-signaling, triggering cell reversals. Based on the above observations and those of Welch and Kaiser (138) who provided a quantitative basis for cell-behavior in ripples as described earlier, Igoshin et al. (59) developed a mathematical model of rippling in which C-signaling is proposed to be a biochemical oscillator that controls reversal of cell gliding. This model also suggests that the cell contact-dependent C-signaling increases the reversal probability by increasing the cycle phase velocity, which is followed by a brief non-responsive phase. This prediction has not been experimentally tested. The response to the C-signal is proposed to be dependent on local cell density suggesting the cooperative nature of C-signaling.

Aggregation:

    csgA mutants cannot form compact, hemispherical aggregates (125). *csgA* cells can be induced to form multicellular aggregates by extracellular stimulation with $csgA^+$ cells or by addition of either version of the C-signaling protein (50, 76, 90). Jelsbak and Sogaard-Andersen (62, 63) defined the motility parameters controlled by C-signaling by

analyzing the behavior of isolated cells as well as those in a population. In the first set of experiments, a high density of starving cells at the initiation of C-signaling was dispersed on a solid surface to enable monitoring of isolated cells using time-lapse video microscopy. The underlying assumption was that individual cells would already be C-signal-stimulated to exhibit specific behavioral patterns while at high cell density. The wild-type cells glided longer distances with an increased velocity and decreased stop frequency. In contrast, the motility profiles of *csgA* cells showed no increase in the gliding period or the velocity. However, *csgA* cells reacquired wild-type motility parameters upon exposure to purified full-length form of MalE-CsgA for 30 minutes before dispersal on starvation agar, suggesting that CsgA induces the changes in motility parameters directly or indirectly (62). This approach however did not allow for observation of cell behavior that depends on continuous cell-cell contact.

In order to overcome the limitation imposed by loss of contact, Jelsbak and Sogaard-Andersen (63) used fluorescent tagging to study the behavior of individual cells in a high density population. Green fluorescent protein (GFP)-expressing wild-type cells were mixed 1:400 with non-fluorescing wild-type cells, and the cell mixture was subjected to starvation-induced development at high cell density. The GFP-tagged cells showed increased speed, extended gliding intervals, and a decreased stop and reversal frequency. GFP-expressing *csgA* cells mixed with non-fluorescing *csgA* cells did not exhibit the same behavior. The gliding velocity of *csgA* cells decreased slightly, and the cells showed frequent periods of no cell movement. Also, the gliding interval, and the reversal frequency did not change significantly. The net distance traveled by the cells during the recording period was about 3-fold lower than that traveled by the wild-type

cells. GFP-expressing *csgA* cells mixed with non-fluorescing wild-type cells showed the same behavior as wild-type cells. Conversely, GFP-expressing wild-type cells mixed with non-fluorescing *csgA* cells exhibited the mutant motility parameters. These observations, along with the already established evidence for contact dependence of C-signaling transmission, led Jelsbak and Sogaard-Andersen (61) to propose that aggregation begins with end-end contact between two cells enabling exchange of the C-signal. This results in increased gliding velocity and reduced reversal frequency, enabling formation of chains of cells. The direction of gliding is proposed to be determined by the cell at the leading end of the chain. They suggest that the cells remain in chains because of their inherent cohesive nature (123) and also because of the continuing contact-mediated signaling. The primary chains of cells are proposed to give rise to secondary chains, finally resulting in the formation of streams of cells. Eventually, the streams of cells are proposed to be trapped in aggregation centers by an unknown mechanism.

Timing of development:

C-signal is an intrinsic timer that *M. xanthus* uses to spatially and temporally control rippling, aggregation, and sporulation. Kruse (84) have quantitatively demonstrated that an ordered increase in CsgA levels is required for the separation of these developmental processes. Overproduction of CsgA results in premature aggregation and sporulation and the uncoupling of the two events in space and time. Reduced CsgA levels caused delayed aggregation, and reduced sporulation (84). Li et al. studied the genetic basis for this observation by using nested deletions upstream from the *csgA* gene that resulted in reduced *csgA* expression. Successively larger deletions resulted

in cessation of development at stages prior to the onset of the next stage. 20%, 30%, and 82% *csgA* expression was required for rippling, aggregation, and sporulation, respectively (94). This suggests that the accumulation of CsgA at different threshold levels defines the corresponding morphological check-point.

Developmental rescue experiments involving addition of exogenous CsgA do not show the concentration-dependence for the temporal separation of the developmental events. Aggregation and sporulation occur with a 24 hour lag at 1 nM partially purified 17 kDa CsgA (76) or 100 nM 25 kDa MalE-CsgA (90). Uncoupling of these events would not be seen if they were defined merely by the accumulation of extracellular CsgA. This ambiguity might be explained if the short chain alcohol dehydrogenase activity of CsgA could catalyze the conversion of different substrates at different times to execute the different developmental events. Thus, CsgA could define a novel class of timers that work based on enzyme catalysis.

Regulation of csgA expression:

Temporal regulation of developmental *csgA* expression is important during fruiting body morphogenesis. *csgA* expression, which is relatively constant during vegetative growth, increases gradually during the course of development, peaking at about 72 hours (26, 94). Although the mechanism of *csgA* regulation has not been completely deciphered, different regulatory elements have been identified. Optimal *csgA* expression and sporulation requires an upstream region of about 400 bp from the transcriptional start-site under stringent starvation conditions (94). However, an extended region including another 530 bp further upstream is required for optimal C-signal activity in the presence of low nutrient levels, suggesting that this region is important for sensing

carbon, nitrogen, and phosphorus (94).

Transcription of *csgA* increases in the presence of the C-signal and FruA, a response regulator with a predicted HTH motif, suggesting that a potential positive feedback loop controls *csgA* expression (35, 131). Indeed, the four genes of the *act* operon control the timing and level of *csgA* expression. Mutations in *actA* and *actB*, which encode a response regulator and a sigma-54 activator protein, respectively, lower *csgA* transcription to about 25% of wild-type levels. Both these mutants show increased periods of rippling, delayed aggregation, and no sporulation. Although, this suggests that the sigma-54-dependent ActB response regulator affects *csgA* expression, Li et al. (94) have reported that the promoter upstream of *csgA* is of the sigma-70 type. This could suggest the existence of additional regulatory elements.

The other two genes in the operon, *actC* and *actD*, affect the temporal regulation of *csgA* expression. The *actC* mutant shows a premature peak in maximal *csgA* expression, while the *actD* mutant exhibits a 6 hour delay. Altered *csgA* expression is evident in the developmental phenotype of these mutants. *actC* cells begin aggregation earlier than wild-type cells, while *actD* cells show delayed aggregation relative to wild-type (48). Since development of the *act* mutants cannot be rescued by codevelopment with wild-type cells, it seems plausible that C-signal itself is the sensory input into the operon (45). Thus, the *act* operon could constitute a positive feedback loop to control the increase in *csgA* expression at appropriate times.

The C-signal transduction pathway:

Some components of the C-signal transduction pathway have been identified based on the isolation and characterization of mutants that arrest development

prematurely in spite of being C-signal-proficient. FruA is the earliest known protein required for C-signal transduction and is essential for rippling, aggregation, and sporulation (131). FruA belongs to the FixJ family of transcriptional regulators whose activity is modulated by phosphorylation of the conserved aspartate in the receiver domain. Mutants with a substitution of the conserved aspartate with alanine, aspargine, or glutamine were unable to aggregate or sporulate, suggesting the importance of this residue for FruA activity (35). Expression of *fruA* is developmentally induced and is first detected 6 hours after the onset of starvation (104). Expression of *fruA* is independent of C-signaling, but requires input from A and E signaling (35, 104). Ellehauge et al. (35) demonstrated that the *fruA* expression profiles of wild type cells and *csgA* mutants were the same, while the FruA accumulation was severely reduced in the *asg* and *esg* background as seen in immunoblot analysis. The cognate histidine kinase is unlinked and unknown, which is unfortunate as it could be the receptor for the C-signal.

The C-signal transduction pathway branches downstream of FruA. One branch regulates cell reversals while the other controls developmental gene expression, C-signaling, and sporulation. An important component of the motility branch of the pathway includes the cytoplasmic Frz proteins, which share homology with bacterial chemotaxis proteins and control cell reversals (137). Both C-signal and FruA cause increased methylation of FrzCD, a methyl-accepting chemotaxis protein (130). Increased methylation of FrzCD in turn reduces reversal frequency. This observation forms the basis of the model for aggregation proposed by Jelsbak and Sogaard-Andersen (61) but does not exclude other possibilities.

Components of the C-signal transduction pathway downstream of C-signal and FruA were identified by their reduced sporulation efficiency (35, 82, 83). The *devRS* mutants showed wild-type levels of rippling and aggregation and about 300-fold reduced sporulation efficiency compared to the wild-type cells (35). The expression of *devRS* in a *fruA* or a *csgA* mutant background was about 5-fold reduced relative to wild-type (35). Also, *devRS* expression was shown to be independent of *frz* (130). These observations provide evidence for the role of *devRS* downstream of C-signaling and FruA, and independent of *frz*.

DevT, which is also part of the *dev* operon, has no homology to any protein in the database. It appears to participate in a positive feedback loop in the C-signal response pathway. Phosphorylated FruA induces transcription of the *dev* operon (35) resulting in DevT synthesis, which in turn enhances the expression of *fruA* (16). The *devT* mutant ripples but exhibits delayed aggregation and reduced sporulation. DevT is required for FrzCD methylation during development suggesting that this protein is active before the FruA branch point. Although the *devT* mutant produced wild-type levels of the C-signal, the level of FruA according to immunoblot analysis was about five-fold lower than in corresponding wild-type cells. In addition, *fruA* transcription was about five-fold lower in the *devT* mutant as measured by *lacZ* transcriptional fusion suggesting that DevT was required for stimulating transcription of *fruA*. Apparently, FruA is made in sufficient amounts to allow rippling but not to sustain aggregation and sporulation.

A model for C-signaling:

Figure 1.3 describes a model for the perception and transmission of the C-signal. Briefly, the recognition of the C-signal by an unknown receptor, possibly the cognate

37

histidine kinase for FruA, triggers the cascade of events manifested by the signal. FruA, which is phosphorylated by an unknown HPK interacts with the Frz signal transduction system and initiates rippling and aggregation at low and intermediate levels of the C-signal. The level of C-signal increases as aggregation progresses, and active FruA along with the components of the *act* operon further increase *csgA* expression. At high levels of C-signal and active FruA, *devRST* and the rest of the late developmental genes are expressed, leading to sporulation.

Short chain alcohol dehydrogenase:

The short-chain alcohol dehydrogenase (SCAD) family is large, diverse, and includes proteins from three EC classes, including oxidoreductases (EC 1.1), dehydratases (EC 4.1) and epimerases (EC 5.1), with oxidoreductases forming the majority of those that have been studied in vitro (105). The oxidoreductases catalyze the interconversion of many different kinds of secondary alcohols and ketones using NAD(P)(H) as the cofactor. For example, hydroxysteroid dehydrogenases catalyze the reversible reduction of oxo/β-hydroxy groups at various positions of steroid hormones and bile acids (107). SCAD dehydratases include the NADPH-dependent nucleotide diphosphate (NDP)-sugar modifying enzymes that carry out an oxidation and subsequent reduction reaction involving the removal of a molecule of water. For example, GDP-D-mannose 4,6-dehydratase catalyzes the $NADP^+$ dependent oxidation of GDP-D-mannose to the ketomannose intermediate, which loses a molecule of water to result in the GDP-4-keto-5,6-ene intermediate. This intermediate is then reduced using NADPH to GDP-4-keto-6- deoxy-D-mannose (112). The SCAD epimerases catalyze the inversion of the

Figure 1.3. A model for C-signal transduction pathway. Upon initiation of development, the C-signal is sensed by an unknown receptor, and the cascade of downstream events follows. Phosphorylated FruA induces *dev* transcription, resulting in DevT accumulation. DevT stimulates *fruA* transcription by an unknown mechanism. Phosphorylated FruA and the *act* operon gene products enhance *csgA* expression. In the presence of low and intermediate levels of the C-signal, the Frz system carries out rippling and aggregation, while the presence of high levels of the C-signal stimulates *devRS* to result in sporulation.

Hypothetical C-signal
receptor

fruA

FruA

DevT

Frz

Rippling and Aggregation
(Low levels of C-signal)

C-signal input

act operon

FruA-P

csgA

devRST

Sporulation
(High levels of C-signal)

C-signal
output
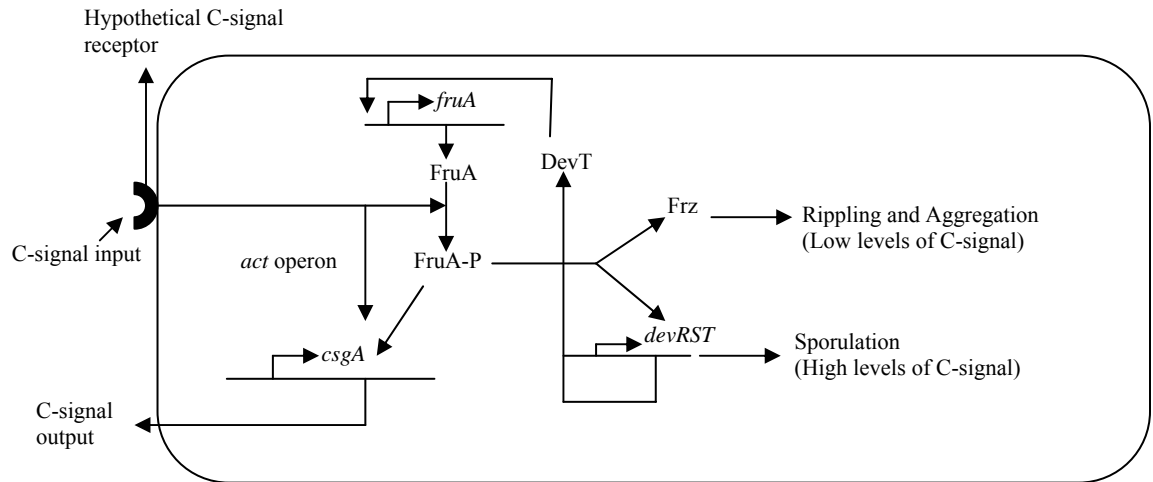
configuration around an asymmetric center of sugar substrates in a NAD^+-dependent manner. For example, UDP-galactose 4'-epimerase catalyzes the interconversion of UDP-galactose and UDP-glucose through the transient reduction of NAD^+. Catalysis involves a tyrosine base that abstracts the 4'-hydroxyl hydrogen of the substrate and mediates the subsequent hydride transfer to NAD^+. The resulting 4'-ketopyranose intermediate rotates 180° in the active site with the concomitant transfer of the hydride from NADH back to the opposite face of the sugar substrate generating the epimerized product (55). Thus, the SCAD family catalyzes reactions carried out by at least three of the six known enzyme classes.

SCAD substrates include a wide variety of biomolecules like amino acids, nucleotides, sugars, steroids, and xenobiotics. Because of their ability to act on many different classes of compounds, SCADs exhibit a great degree of functional diversity. They are involved in intermediary metabolism, biotransformation of xenobiotics, and lipid hormone signaling during cellular differentiation in higher eukaryotes to produce products such as steroids, prostaglandins and retinoids (105). Also, enzymes of this class whose function is not yet understood are involved in developmental processes such as *Anabaena* heterocyst differentiation (14), mouse adipocyte differentiation (139), and sex determination in maize (30). The broad substrate specificity of these enzymes and the lack of biochemical characterization of many of them have made it impossible to predict the substrate based on amino acid sequence alone. In spite of the low primary sequence identity between different enzymes in this family the tertiary structures display a similar α/β folding pattern with the coenzyme-binding fold being strictly conserved. Also, the critical residues involved in catalysis and coenzyme binding are conserved (69, 105).

41

With the exception of porcine and human carbonyl reductases, which are monomers (103, 140), SCAD enzymes are homodimers or homotetramers with 250-350 residues in each subunit. Each subunit has a single domain with an N-terminal coenzyme-binding region and a C-terminal substrate-binding region (105).

The architectures of SCAD active sites and coenzyme-binding regions have been deduced from over thirty crystal structures. These crystals have been prepared in either binary form, in which the enzyme is complexed with the coenzyme, or ternary form in which the enzyme is bound to both the coenzyme and the substrate or inhibitor. The proposed mechanism of catalysis is based on the structure of *Drosophila lebanonensis* alcohol dehydrogenase (DADH) (9). The PDB accession codes for the crystals deposited in Brookhaven Protein Data Bank are as follows: binary form (1B14), ternary form with NAD-acetone (1B15), ternary form with NAD-3-pentanone (1B16), and ternary form with NAD-cyclohexanone (1B2L). The indicated numbering is from DADH unless otherwise specified.

Coenzyme binding in SCAD:

The N-terminal coenzyme-binding region is defined by a highly conserved dinucleotide binding fold termed the "Rossmann fold" which consists of two βαβαβ motifs that form a central β-sheet flanked by α helices (Figure 1.4). The coenzyme binds to each of the two βαβαβ motifs (93, 115). Some enzymes show variation in the spacing and distribution of the glycine residues in the first βαβαβ motif (69, 108). This motif plays an essential role in maintaining the central β-sheet which is important for both coenzyme positioning and binding.

Figure 1.4. Rossmann fold topology. The arrows denote β-strands, and the rectangles

denote α-helices. The circles indicate the conserved glycine residues (Bottoms et al.

2002).
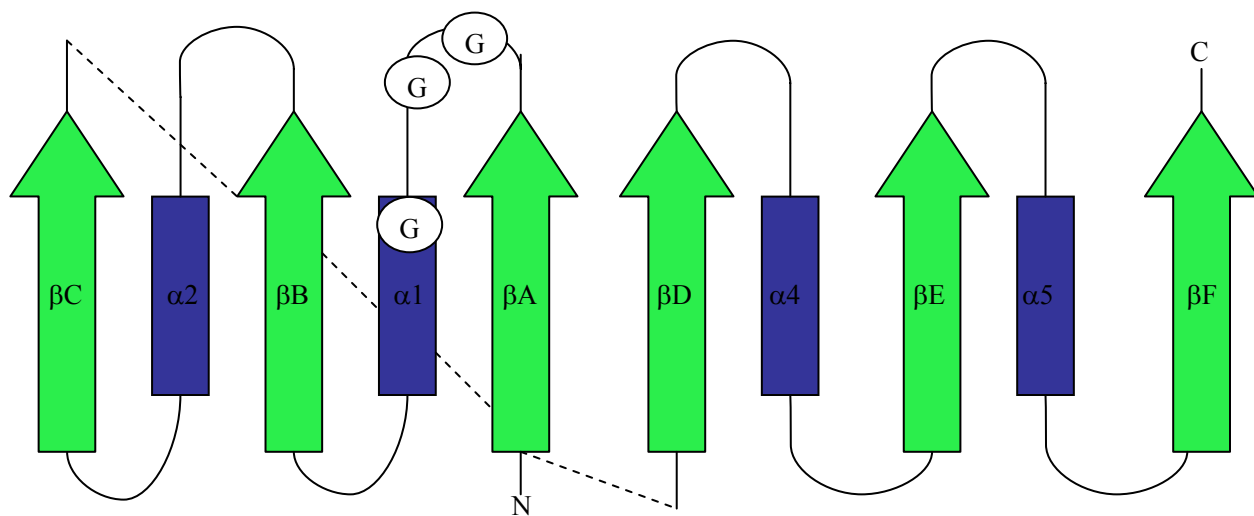
Conserved residues that don't interact directly with the coenzyme are preserved to provide a structural framework for its binding. Thr12 interacts with strand βD to keep the strands in the central β sheet for coenzyme positioning. A less conserved NNAG motif or HxAA motif in some SCAD enzymes also contributes to the secondary structure maintenance. The two aspargines [from 3β/17β-hydroxysteroid dehydrogenase (3β/17β-HSD) (PDB accession code 2hsd)] in this motif form critical side chain and backbone interactions through strands βD and βE respectively (Figure 1.5). The importance of these motifs has been demonstrated by several chemical modification studies, site-directed mutagenesis, and structure analysis. However, there is no evidence for the direct interaction of these residues with the coenzyme (11, 36, 106). Some of the conserved residues are thought to interact with the coenzyme by means of hydrogen bonding, electrostatic, and hydrophobic interactions (Figure 1.5). Thr188 (from 3β/17β-HSD) is proposed to stabilize the adenine-ribose end of the dinucleotide by hydrogen bonding with the carboxamide group of the nicotinamide ring. Asp60 (from 3β/17β-HSD) in βB, hydrogen bonds with the 2'- and 3'-hyroxyl groups of the adenine-ribose. However, the phosphate group on the 2'-hydroxyl of the adenosine-ribose of NADP$^+$ is repelled by this aspartate, which is usually the sole determinant of the coenzyme preference of the enzyme (36). There has also been a rare occurrence of glutamate as the critical acidic residue (108). Another role of this residue is proposed to be stabilization of the turn between βC and α4 in the adenine binding pocket. Finally, Ala88 (from 3β/17β-HSD) is proposed to maintain hydrophobic contacts with the adenine ring (36).

NADP(H)-binding enzymes have two conserved basic residues (arginine or lysine) that bind to the phosphate. The first of these is present in the glycine motif

Figure 1.5. Interaction of conserved residues from the central β-sheet with strands βA, βD, βE of 3β/17β-HSD with NAD$^+$. Hydrogen bond distances (in Å) are represented by dotted lines (Filling et al. 2002).
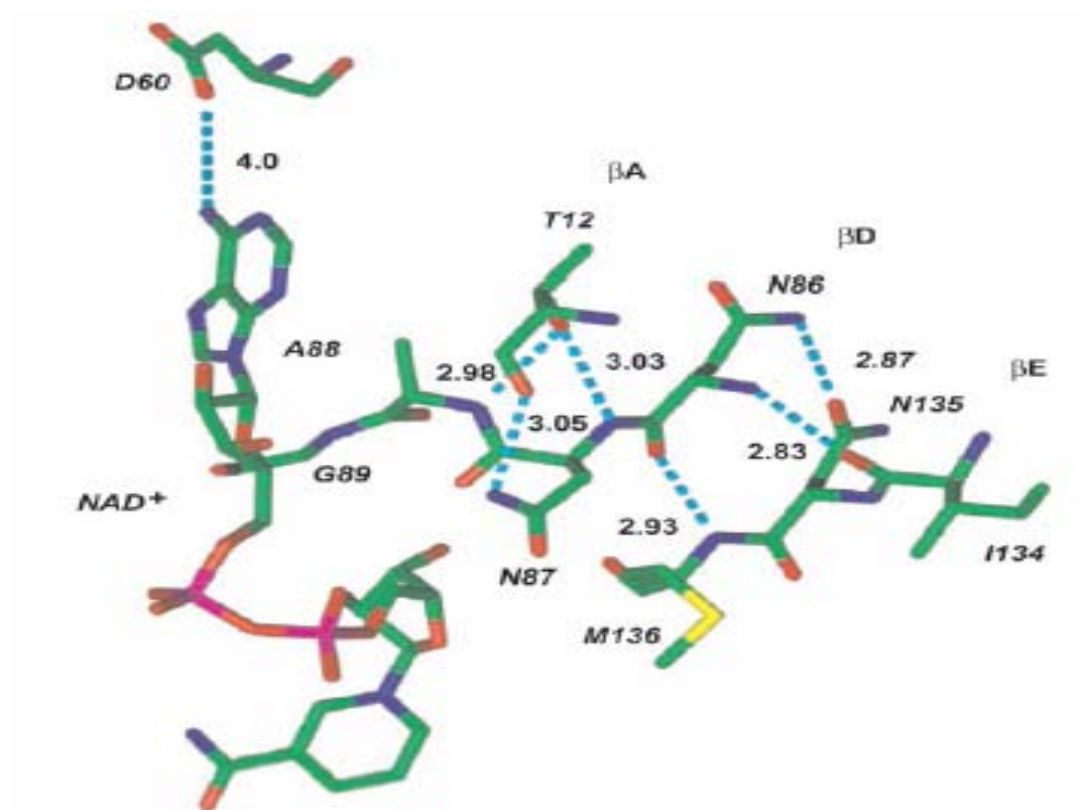
between βA and α1 immediately preceding the second glycine. The second basic residue is present directly after the critical acidic residue (βC and α3) in the NAD(H) binding enzymes. The requirement for these basic residues is not absolute, and there are NADP(H)-binding enzymes that have only one of the basic residues. These positively charged residues stabilize the bound NADPH via electrostatic interactions with the negatively charged phosphate moiety of the coenzyme (36). About 10% of the sequences analyzed do not have the typical pattern of charged residue distribution (108).

Active site structure and chemistry of catalysis:

The substrate binding site in the C-terminal region is the least conserved part of the dehydrogenase. Three important structural features define the active site, the first of which is a deep hydrophobic cavity. The residues in secondary structural elements βF to α7 are responsible for the substrate specificity and are therefore quite diverse. The hydrophobic cavity that constitutes the active site region consists of βD-βG, and is enclosed by a flexible loop formed by residues 181-211. This cavity is closed by the C-terminal residues 250-254 from the neighboring subunit upon coenzyme and substrate binding (10). Deletion of the C-terminal residues 250-254 severely affects enzyme activity (1).

The second important feature defining the active site is the presence of the catalytic triad formed by Ser138, Tyr151, and Lys155. Recent studies with 3β/17β-HSD have revealed that the conserved Asn111 also shows essential interactions with the catalytic triad (36). Ser138 is proposed to orient and stabilize the substrate by hydrogen bonding. Upon substrate binding, Tyr151 acts as a catalytic base and abstracts a proton from the hydroxyl group of the alcohol substrate and transfers it to the ε-amino group of

Lys155 *via* the O2' ribose hydroxyl of NAD$^+$ (65). Asn111 stabilizes the active site geometry by maintaining the position of Lys155 through an interaction with a water molecule (W41 in Figure 1.6). This water molecule along with seven other water molecules forms a hydrogen-bonded water chain which leads to the outside of the active site. The proton abstracted from the substrate is finally conveyed to the bulk solvent through this solvent channel. Thus, a proton relay is proposed to be formed at the active site involving the substrate, Tyr151, the 2'OH of nicotinamide ribose, Lys155, and the eight-membered water channel (Figure 1.6) (79).

Three well-ordered water molecules that interact with the catalytic residues constitute the third structural feature defining the active site. One water molecule is proposed to interact with Ser138 and Tyr151 until it becomes replaced by the substrate. The second water molecule links Tyr151 and Lys155 and is proposed to be involved in the deprotonation of the Tyr151 hydroxyl group and/or mimic the 2'O and 3'O atoms of the NAD ribose in the absence of the coenzyme. The third water molecule is proposed to play a structural role by linking Lys155 and the O atom of Asn107 (10).

Drosophila alcohol dehydrogenase follows the Theorell-Chance mechanism for substrate conversion (9). This is an ordered pathway as illustrated below, in which the coenzyme is the leading substrate and the dissociation of the binary enzyme-NADH complex is the rate limiting step:

Figure 1.6. The proposed proton relay chain in the binary complex (NAD$^+$) of *Drosophila lebanonensis* alcohol dehydrogenase. The ribbon diagram represents subunit A in pale red and subunit B in silver. Atoms are represented by red spheres (oxygen), blue spheres (nitrogen), green spheres (carbon). Distances are shown in Å units. The proposed proton relay path originating at the substrate (W144) and terminating at the end of the water channel is represented by dashed blue line. The hydrogen bond interactions between side-chain/main-chain atoms and the members of the proton relay bridge are represented by dashed gray lines (Koumanov et al. 2003). Consult text for more detailed explanation of proton relay.

$$E + NAD^+ \quad \Longleftrightarrow E \bullet NAD^+ + R\text{-}OH$$

$$\Longleftrightarrow E \bullet NAD^+ \bullet R\text{-}OH$$

$$\Longleftrightarrow E \bullet NADH \bullet R\text{=}O$$

$$\Longleftrightarrow R\text{=}O + E \bullet NADH$$

$$\Longleftrightarrow E + NADH$$
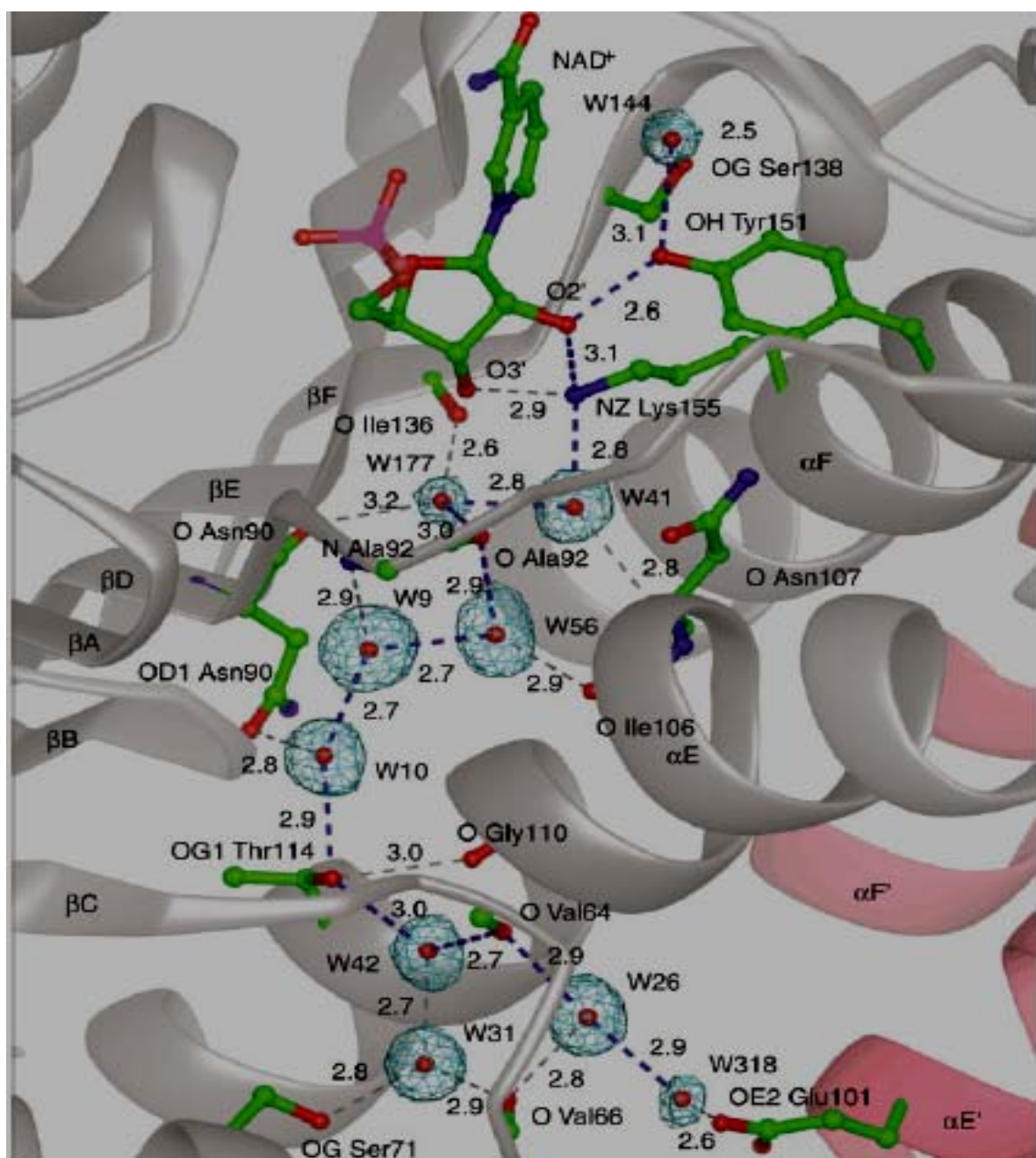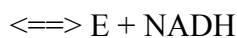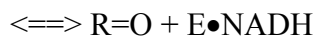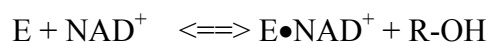
The coenzyme binding to the apo form (enzyme with unbound coenzyme and substrate) results in a conformational change that affects the relative positions of $\alpha 2$, $\alpha 3$, $\alpha 4$, and $\alpha 7$. This also results in a partially ordered structure of the entrance gate of the active site cleft. The binding of the substrate replaces the water molecule between the side chains of Ser138 and Tyr151. During the transition from the binary to the ternary form, the enzyme undergoes a second conformational change. Once the substrate is positioned in the active site cavity, the hydroxyl group of the substrate is placed between the oxygen atoms of the side-chains of Ser138 and Tyr151. This facilitates proton transfer from the alcohol group to the unprotonated Tyr151O$^-$ form, generating a partial positive charge on the C1 atom of the alcohol enabling hydride transfer from Ser138 to the C4 position (with a H at C4) of the coenzyme. Serine is proposed to orient the alcohol substrate, stabilize the transition state intermediate, or both. Lysine is proposed to serve the dual roles of orienting the coenzyme by formation of hydrogen bonds with the oxygen atoms of the nicotinamide-ribose moiety and lowering the pK_a of the tyrosine residue through ionic interactions. The positively charged nicotinamide ring is also proposed to lower the pK_a of tyrosine.

Classification of SCAD superfamily members:

Hidden Markov model analysis was used to classify the SCAD superfamily systematically into five families based on the chain length and the spacing and distribution of glycine residues in the coenzyme binding region (69, 108). Each of the five families is discussed in detail.

The classical family: The majority of SCADs fall into this family whose primary sequence consists of about 250 amino acids. The coenzyme-binding domain exhibits a typical glycine distribution pattern of TGxxxGxG in the coenzyme-binding region. There is also a conserved aspartate about thirteen positions downstream from the active site lysine residue that is involved in the stabilization of the adenine-binding pocket. The other conserved sequence in this family is the NNAG motif in the coenzyme binding region which is required for stabilizing the β-strands within the central β-sheet. Also, the aspargine residue responsible for maintaining the active site geometry is highly conserved throughout this family. This family includes oxidreductases like steroid dehydrogenases and carbonyl reductases. Most of the enzymes use NADP(H) as the preferred coenzyme.

The Extended family: Greater than 25% of the known SCADs are classified in this family, which is characterized by a chain length of about 350 amino acids. The coenzyme-binding motif TGxxGxxG differs from that of the classical enzymes in the position and distribution of the conserved glycines. A motif DxxD in the loop between βC and α3 contributes to the stability of the adenine-binding pocket. The coenzyme-binding NNAG motif in βD is replaced by a HxAA motif. The catalytic domain is characterized by the presence of a conserved proline immediately preceding the active

site tyrosine and a conserved negatively charged residue four residues downstream of the lysine residue. This family includes isomerases like UDP-galactose 4'-epimerase and lyases like UDP-D-mannose 4,6-dehydratase in addition to oxidoreductases like 3β-hydroxysteroid dehydrogenase. Also, these enzymes prefer NAD(H) as the coenzyme.

The Intermediate family: This family accounts for 6-13% of the known sequences. The glycines in the coenzyme binding region have been replaced by alanines. All the other characteristics resemble the classical enzymes except that the NNAG motif for coenzyme binding is replaced by NGAG. *Drosophila* alcohol dehydrogenase belongs to this family.

The Divergent family: These are NADH-dependent enzymes that exhibit certain deviations from the typical SCAD pattern. The second and the third glycines in the coenzyme binding fold have been replaced by serine and alanine, respectively. The catalytic tyrosine and lysine in the active site are spaced differently. The recurring motif in the active site of these enzymes is YxxMxxxK instead of YxxxK. This family is exemplified by the enoyl reductases from bacteria and plants.

The complex family: This family includes some fatty acid synthases that are parts of multifunctional enzyme complexes found in diverse living systems. The preferred coenzyme of this family is NADP(H) and the signature motif in the active site is YxxxN instead of YxxxK.

The divergent and the complex families together include fewer than 5% of all the known enzymes. Three percent of the enzymes lack at least one of the signature motifs to be classified under any family and hence remain unclassified.

The classical and extended families are further classified according to their coenzyme specificity based on the pattern of charged residues at key positions in the

Rossmann fold. NAD(H)-preferring enzymes have an acidic residue at the C-terminal end of βB while the NADP(H)-binding enzymes have two basic residues, the first of which is found immediately preceding the second glycine. The second one is located exactly after the crucial acidic residue of NAD(H)-binding enzymes. The former enzymes are classified under the subfamily cP1, while the latter enzymes are classified under the subfamily cP2. Enzymes with both of the basic residues are classified as subfamily cP3.

NAD(H) binding classical SCADs with aspartate as the acidic residue that determines coenzyme specificity are classified under the subfamily cD1d and those with glutamate as the crucial acidic residue are found under the subfamily cD1e. The position and the type of acidic residue are not strictly conserved and can be found one or two positions downstream. Thus, enzymes with either an aspartate or a glutamate one position downstream fall under cD2 and those that have the acidic residue two positions downchain are classified as cD3.

Extended SCAD also have an acidic residue at the end of the C-terminal end of βB as the sole determinant of the coenzyme preference of the enzyme. Enzymes with an aspartate or a glutamate at position 33 are classified as eD1 and those with the acidic residue two positions downstream are classified as eD2. NADP(H)-preferring enzymes of the extended family do not have the first of the two characteristic basic residues in the glycine motif. However, the second one is present in the defined position. These enzymes are classified as belonging to the subfamily eP1.

CsgA and SocA as SCAD members:

CsgA has conserved motifs typical of a SCAD (Figure 1.7). The coenzyme binding region is characterized by the motifs TGxxRGxG and the NNAG typical of classical SCADs. It has a glutamate at the C-terminal end of the second β-strand that could suggest a NAD(H) preference. CsgA could be classified under the classical subfamily cD1e. However, the glycine motif in the coenzyme-binding region has an arginine immediately preceding the second glycine, suggesting potential NADP(H) binding and classification of CsgA in subfamily cP1. The 229 amino acid primary structure of CsgA contains 34.7% identity with 11-*cis* retinol dehydrogenase from *Bos taurus* (X82262). The other close relatives include enzymes whose substrate specificity and biological function are unknown [*Bradyrhizobium japonicum* - P05406 (31.4); *Saccharomyces cereviceae* - Z28071 (33.2); *Maize* - L20621 (29.5%)]. Molecular modeling of CsgA with 3α/20β-HSD suggests that the overall shape of the protein is very similar to that of hydroxysteroid dehydrogenase. The conserved residues in the catalytic and coenzyme-binding regions are present, including all four catalytically important residues. CsgA with T6A or R10A replacements was biologically inactive in C-signaling (90). CsgA with a T6A replacement did not bind NAD$^+$ (90). CsgA has an unusual AY repeat in the YxxxK motif, the significance of which is not known. CsgA derivatives containing a K155R or S135T replacement were inactive, highlighting the importance of these active site residues for C-signal generation (90).

SocA has 28% identity with CsgA and exhibits all the primary and secondary structural features that define a short-chain alcohol dehydrogenase (Figure 1.7). The spacing and distribution of the glycine residues in the Rossmann fold, TGxxxGxG, is

Figure 1.7. An alignment of two *M. xanthus* SCAD CsgA and SocA with 3α/20β-

Hydroxysteroid dehydrogenase. The secondary structural elements are shown below the

sequence line based on the crystal structure of 3α/20β-Hydroxysteroid dehydrogenase.

Letters in red indicate the residues that are conserved in all the three proteins (Lee et al.

1995). The conserved residues in the coenzyme-binding region are indicated by a red

box and the conserved catalytic residues are indicated by a blue box. The predicted site

of processing of the 17 kDa form is indicated by a green arrow (Lobedanze and Sogaard-

Andersen, 2003).

```
       1                                                                    50
HSD    MNDLSGKTVI ITGGARGLGA EAARQAVAAG ARVVLADVLD EEGAAT....
SocA   MMAFSGKAAL VTGGTRGMGA AIVRHLAKGG ADVAFTYANS GDKAATRSVN
CsgA   ~~~~~~MRYV ITGASRGIGF EFVQQLLLRG DTV..EAGVR SPEGARRLEP

                βA              α2           βB          α3

       51                                                                  100
HSD    ARELGDAA.R YQHLDVTIEE DWQRVVAYAR EEFGSVDGLV NNAGIST.G
SocA   SRHSADGPLA IQADNGDPDA VRGAAVDRAA SELGRLDILV NNAGIFP.S
CsgA   LKQKAGNRLR IHALDVGDDD SVRAFATNVC T..GPVDVLI NNAGVSGLW

                βC              α4                     βD

       101                                                                 150
HSD    MFLETESVER FRKVVDINLT GVFIGMKTVI PAMKDAGGGS IVNISSA.AG
SocA   GPFEKVTLEE LDRTLAIHVR GVFVASQAAL AHMPQ..GGR IISIGSCFAQ
CsgA   CALGDVDYAD MARTFTINAL GPLRVTSAML PGLRQGALRR VAHVTSRMGS

                           α5                           βE

       151                                                      200
HSD    LMGLALTSSY G..ASKWGVR GLSKLAAVEL GTDRIRVNSV HPGMTYTPMT
SocA   RVPYGGVTLY S..MSKSALI GLTKGLAREV GERGITVNVI DPGSTDTDMN
CsgA   LAANTDGGAY AYRMSKAALN MAVRSMSTDL RPEGFVTVLL HPGWVQTDMG

                     α6                          βF

       201                                                      250
HSD    AETGIRQGEG NYPNTPMGRV GNEPGEIAGA VVKLLSDTSS YVTGAELAVD
SocA   PATGPAVA.A ELALMSVKHY A.QPEDIAAT VGHLASASGR FITGTSIAVD
CsgA   GPDATLPAPD SVRGMLRVID GLNPEHSGRF FDYQGTEVPW *~~~~~~~~~

                              α7                      βF

       251              265
HSD    GGWTTGPTVK YVMGQ
SocA   GGFSA~~~~~ ~~~~~
CsgA   ~~~~~~~~~~ ~~~~~
```

58

typical of a classical SCAD. The conserved aspartate between βC and α3 required for stabilizing the adenine binding pocket is present in addition to the NNAG motif in βD that provides the structural support for coenzyme binding. SocA lacks the crucial aspartate that blocks NADP(H) binding, suggesting that it can utilize NADP(H). Also, it has the first of the two basic residues immediately preceding the second glycine in the glycine motif and could be classified in the subfamily cP1. However, the aspartate in α3 at position 42 could enable NAD(H) binding in an atypical manner. The substrate binding region has the signature sequence YxxxK and the catalytically active serine. But the aspargine or serine (located in α5) that interacts with Lys155 via a water molecule for maintaining the active site geometry interaction is absent (92). None of the above observations about the significance of conserved SocA residues have been confirmed by mutational analysis because the gene appears to be essential for growth. The primary structure of SocA contains 39% identity with 3-oxoacyl-[acyl carrier protein] reductase from *Brassica napus* (P27582). The other close relatives include 3-oxoacyl-[acyl carrier protein] reductases from *E. coli* - P25716 (37.8%), *Cuphea lanceolata* (34.3%), acetoacetyl-CoA reductase from *Zoogloea ramigera* - P23238 (34.7%), 2, 3-Dihydro-2,3-dihydroxy-benzoate dehydrogenase from *E. coli* - P15047 (35.6%).

Functional heterogeneity of SCADs:

Presently about 3,000 SCADs have been identified based on their primary amino acid sequence, although the function(s) of the vast majority are unknown. Because of the myriad of physiological processes these enzymes are involved in and also because of the

59

diverse substrate spectrum these enzymes exhibit, it is not possible to predict the potential substrates based on amino acid sequence homology alone.

Analysis of completed genomes reveals the presence of SCAD-encoding genes in significant numbers. The *E. coli* genome encodes about 24 SCADs out of about 4200 ORFs (0.6% of genes). Similarly, *Mycobacterium tuberculosis* and *Bacillus subtilis* encode 57 and 32 SCADs, respectively (64). In the case of higher organisms, the human genome has 58 SCAD sequences while *Drosophila melanogaster, Caenorahbditis elegans,* and *Arabidopsis thaliana* genomes encode 62, 56, and 62, respectively (68). In all the cases, classical SCADs form the majority.

Most SCAD genes are defined based only on the presence of the conserved signature residues. For example, the *E. coli* genome encodes 17 classical SCADs and 7 extended SCADs out of which 11 sequences are annotated as hypothetical proteins broadly classified under sugar-utilizing SCADs. Seven *E. coli* enzymes have defined functions, including those that utilize hexose sugars or steroids, or are involved in fatty acid biosynthesis. Although extended SCADs are not as common as classical SCADs in Bacteria, they are the only SCADs in the Archaea *Methanococcus jannaschii* and *Pyrococcus horikoshii*. Bacteria with smaller genomes like *Mycoplasma sp.* or *Borrelia burgdorferi* also lack classical SCADs and encode at least one extended SCAD. The presence of these extended enzymes in even the most primitive of life forms suggests their evolutionary origin as sugar- or nucleotide-metabolizing enzymes that later evolved to utilize a wide diversity of other substrates.

Examples of functional diversity of SCAD:

SCADs can be grouped into two main categories based on their functional assignments as enzymes affecting intermediary metabolism or involved in intercellular signaling. Enzymes in the former category act on substrates such as sugars, amino acids, fatty acids, pteridines etc., while lipid substrates are the preferred choice for enzymes involved in lipid hormone mediated-cell signaling in Eukarya (107).

SCADs affecting intermediary metabolism: This group of enzymes exhibits a wide range of substrate specificity. Deficiency of many of these enzymes results in inherited metabolic disorders in higher animals. In *E. coli* and other bacteria, UDP-galactose epimerase is involved in galactose metabolism, catalyzing the interconversion of UDP-glucose and UDP-galactose. In humans, this enzyme is involved in the biosynthesis of glycoproteins and glycolipids by catalyzing the interconversion of UDP–*N*-acetylglucosamine and UDP-*N*-acetylgalactosamine. An impairment in the functioning of the human enzyme results in a severe metabolic disorder, epimerase-deficiency galactosemia.

Dihydropteridin reductase and sepiapterin reductase are involved in pteridine metabolism, the deficiency of which results in type II phenylketonuria. 3-hydroxy butyrate dehydrogenase catalyzes the interconversion of 3-hydroxybutyrate and acetoacetate during carbon metabolism in many bacteria that accumulate polyhydroxybutyrate. The mammalian counterpart of this enzyme is involved in ketone body metabolism during starvation (100). Many bacteria produce serine dehydrogenase which is the only known SCAD that acts on amino acid substrates (24). The physiological relevance of this enzyme is not known. SCADs also act on acylated

molecules like acyl carrier protein (ACP), coenzyme A, and cysteamine. β-Keto ACP reductase catalyzes the reversible reduction of 3-oxoacyl ACP to its hydroxy product during fatty acid biosynthesis (13, 119, 135).

SCADs involved in signaling and xenobiotic metabolism: Enzymes in this group act on structurally similar substrates but have different implications for the cell physiology of bacteria and higher animals. These SCADs mediate lipid hormone signaling during development in higher animals while carrying out xenobiotic carbonyl metabolism in bacteria. Some enzymes in this group have overlapping substrate specificity. These enzymes mediate intercellular signaling in mammals by activating or inactivating various bioactive molecules such as steroids and prostaglandins. Hydroxysteroid dehydrogenases (HSD) play an essential role in the biosynthesis of all classes of steroid hormones and bile acids. They catalyze the reversible reduction of oxo/β-hydroxy groups at various positions of steroid hormones and bile acids. 11β-HSD controls the access of glucocorticoids to their intracellular receptors (GR), thus preventing the nonspecific activation of mineralocorticoid receptors (MR). The glucocorticoid hormones have a high affinity for both GR and MR, while the mineralocorticoid hormone aldosterone binds only to MR. 11β-HSD reduces the glucocorticoid hormones cortisol and corticosterone to their corresponding inactive forms cortisone and 11-dehydrocorticosterone which are not recognized by either GR or MR, enabling recognition of MR by aldosterone (37). The 17β-HSD isoforms operate a similar metabolic switch to regulate the activity of androgens and estrogens. The microbial counterparts of these steroid hormone-metabolizing enzymes are involved in biotransformation of polyaromatic hydrocarbons in contaminated soils. *Comamonas*

testosteroni, which is able to utilize testosterone as the sole source of carbon, produces several enzymes such as 3α-HSD, 3β/17β-HSD, that are involved in the degradation of steroids.

Retinoids are the key photosensitive elements involved in visual sensation. Retinoic acids are chemical signals for cellular differentiation and proliferation. Retinol dehydrogenases catalyze the oxidation of retinol to retinal which is further metabolized into retinoic acid (107).

Unusual SCADs:

The SCAD family exhibits remarkable structural diversity, which contributes to the broad range of substrates converted. Some of these enzymes have novel structural features that lend themselves to novel functions. Haloalcohol dehalogenases catalyze the cofactor-independent dehalogenation of environmental contaminants like 1,3-dichloro-2-propanol to result in its corresponding epoxide, a halide ion, and a proton. These enzymes have the otherwise highly conserved catalytic triad of a SCAD but with lysine replaced by arginine. These enzymes also lack the ability to bind the coenzyme because of the replacement of the glycine-rich motif at the N-terminus by a NVKHFGG motif that provides a halide-binding site (29). The typical redox reaction mechanism of this SCAD is replaced by a substitutive dehalogenation. The catalytic tyrosine deprotonates the hydroxyl group of the substrate to generate an intramolecular nucleophile, which substitutes the halogen (29). Thus, this enzyme provides a striking example of the divergent evolution the SCAD family has undergone.

The SCAD fold is adapted for non-enzymatic functions such as transcriptional regulation as well. For example, NmrA, a negative transcriptional regulator involved in

the control of nitrogen metabolite repression in many fungi, has a two-domain structure including the Rossmann fold and shows significant homology with UDP-galactose 4-epimerase. However, this protein lacks the catalytic tyrosine and hence is not enzymatically active. The NAD$^+$ binding is suggested to have a regulatory role. Thus, the SCAD family exhibits diversity not just in terms of the range of substrates converted but also in terms of the diverse roles these enzymes play in the cell.

Conclusion:

Short-chain alcohol dehydrogenases form a large and evolutionarily ancient superfamily of enzymes that use NAD(P)(H) to catalyze redox reactions in addition to epimerization and dehydration reactions. In spite of low sequence identity at the primary amino acid level, they show a highly conserved secondary structure. The catalytically important residues as well as those involved in the coenzyme binding and positioning are conserved throughout the superfamily. They exhibit remarkable evolutionary divergence which has contributed to their ability to act on a wide spectrum of biomolecules implicating them in diverse cellular functions. Some of these functions are of biomedical and pharmacological interests in humans including metabolic disorders and hormone-dependent cancers. Then there are some proteins that deviate from the norm and perform non-enzymatic functions as fungal transcription factors. Thus, this enzyme superfamily exhibits extraordinary structural and functional diversity.

Statement of purpose:

The purpose of this dissertation is to examine the enzymatic role of CsgA in the generation of the C-signal. It is important to resolve the debate about the chemical nature of the C-signal. Genetic studies supporting the role of the full-length form as a short-chain alcohol dehydrogenase are striking. However, establishing the biochemical basis is complicated by the lack of significant sequence homology with enzymes of known substrate specificity. We propose to employ an in vitro dehydrogenase assay to screen for substrates prepared from whole cell extracts. The enzymatic activity of purified CsgA will be confirmed by repeating the assay with purified SocA to determine the extent of substrate overlap. Mass spectrometric methods will be employed to determine the identity of the active molecule(s) in the extract. Finally, the biological significance of the enzyme activity will be determined by the ability of the end product to reproduce the biological effects of the purified protein.

Reference:

1.   **Albalat, R., M. Valls, J. Fibla, S. Atrian, and R. Gonzalez-Duarte.** 1995. Involvement of the C-terminal tail in the activity of Drosophila alcohol dehydrogenase. Evaluation of truncated proteins constructed by site-directed mutagenesis. Eur. J. Biochem. **233:**498-505.

2.   **Arnold, J. W., and L. J. Shimkets.** 1988. Cell surface properties correlated with cohesion in *Myxococcus xanthus*. J. Bacteriol. **170:**5771-5777.

3.   **Arnold, J. W., and L. J. Shimkets.** 1988. Inhibition of cell-cell interactions in *Myxococcus xanthus* by Congo red. J. Bacteriol. **170:**5765-5770.

4.   **Baker, M.** 1994. *Myxococcus xanthus* C-factor, a morphogenetic paracrine signal, is similar to *Escherichia coli* 3-oxoacyl-[acyl-carrier-protein] reductase and human 17ß-hydroxysteroid dehydrogenase. Biochem. J. **301:**311-312.

5.   **Bartholomeusz, G., Y. Zhu, and J. Downard.** 1998. Growth medium-dependent regulation of *Myxococcus xanthus* fatty acid content is controlled by the *esg* locus. J. Bacteriol. **180:**5269-72.

6.   **Behmlander, R., and M. Dworkin.** 1994. Biochemical and structural analyses of the extracellular matrix fibrils of *Myxococcus xanthus*. J. Bacteriol. **176:**6295-6303.

7.   **Behmlander, R. M., and M. Dworkin.** 1991. Extracellular fibrils and contact-mediated cell interactions in *Myxococcus xanthus*. J. Bacteriol. **173:**7810-7821.

8.   **Behmlander, R. M., and M. Dworkin.** 1994. Integral proteins of the extracellular matrix fibrils of *Myxococcus xanthus*. J. Bacteriol. **176:**6304-6311.

9.   **Benach, J., S. Atrian, R. Gonzalez-Duarte, and R. Ladenstein.** 1999. The

catalytic reaction and inhibition mechanism of Drosophila alcohol dehydrogenase:

Observation of an enzyme-bound NAD-ketone adduct at 1.4A resolution by X-ray

crystallography. J. Mol. Biol. **289:**335-355.

10.   **Benach, J., S. Atrian, R. Gonzalez-Duarte, and R. Ladenstein.** 1998. The

refined crystal structure of *Drosophila lebanonensis* alcohol dehydrogenase at 1.9

A resolution. J. Mol. Biol. **282:**383-399.

11.   **Benach, J., C. Filling, U. C. Oppermann, P. Roversi, G. Bricogne, K. D.

Berndt, H. Jornvall, and R. Ladenstein.** 2002. Structure of bacterial

3beta/17beta-hydroxysteroid dehydrogenase at 1.2 A resolution: a model for

multiple steroid recognition. Biochem **50:**14659-14668.

12.   **Bi, E., and J. Lutkenhaus.** 1993. Cell division inhibitors SulA and MinCD

prevent formation of the FtsZ ring. J. Bacteriol. **175:**1118-1125.

13.   **Birge, C. H., and P. R. Vagelos.** 1972. Acyl carrier protein. XVI. Intermediate

reactions of unsaturated fatty acid synthesis in *Escherichia coli* and studies of *fab

B* mutants. J. Biol. Chem. **16:**4921-4929.

14.   **Black, T. A., and C. P. Wolk.** 1994. Analysis of a *Het*⁻ mutation in *Anabaena* sp.

strain PCC7120 implicates a secondary metabolite in the regulation of heterocyst

spacing. J. Bacteriol. **176:**2282-2292.

15.   **Bowden, M. G., and H. B. Kaplan.** 1998. The *Myxococcus xanthus*

lipopolysaccharide O-antigen is required for social motility and multicellular

development. Mol. Microbiol. **30:**275-284.

16. **Boysen, A., E. Ellehauge, B. Julien, and L. Sogaard-Andersen.** 2002. The DevT protein stimulates synthesis of FruA, a signal transduction protein required for fruiting body morphogenesis in *Myxococcus xanthus*. J. Bacteriol. **184:**1540-1546.

17. **Butler, J. S., M. Springer, and M. Grunberg-Manago.** 1987. AUU-to-AUG mutation in the initiator codon of the translation initiation factor IF3 abolishes translational autocontrol of its own gene (infC) in vivo. Proc. Natl. Acad. Sci. USA. **84:**4022-4025.

18. **Cashel, M., D. R. Gentry, V. J. Hernandez, and D. Vinella.** 1996. The Stringent Response, p. 1458-1496. *In* F. C. Neidhardt, R. I. Curtiss, J. L. Ingraham, E. C. C. Lin, K. B. Low, B. Magasanik, W. S. Reznikoff, M. Riley, M. Schaechter, and H. E. Umbarger (ed.), *Escherichia coli* and *Salmonella*: Cellular and Molecular Biology., vol. I. Am. Soc. Microbiol., Washington, DC.

19. **Chang, B.-Y., and M. Dworkin.** 1994. Isolated fibrils rescue cohesion and development in the *dsp* mutant of *Myxococcus xanthus*. J. Bacteriol. **176:**7190-7196.

20. **Cheng, Y., and D. Kaiser.** 1989. *dsg*, a gene required for cell-cell interaction early in *Myxococcus* development. J. Bacteriol. **171:**3719-3726.

21. **Cheng, Y., and D. Kaiser.** 1989. *dsg*, a gene required for *Myxococcus* development, is necessary for cell viability. J. Bacteriol. **171:**3727-3731.

22. **Cheng, Y., L. V. Kalman, and D. Kaiser.** 1994. The *dsg* gene of *Myxococcus xanthus* encodes a protein similar to translation initiation factor IF3. J. Bacteriol. **176:**1427-1433.

23. **Cho, K., and D. R. Zusman.** 1999. AsgD, a new two-component regulator required for A-signaling and nutrient sensing during early development of *Myxococcus xanthus*. Mol. Microbiol. **34:**268-281.

24. **Chowdhury, E. K., K. Higuchi, S. Nagata, and H. Misono.** 1997. A novel NADP($^+$)-dependent serine dehydrogenase from *Agrobacterium tumefaciens*. Biosci. Biotechnol. Biochem. **61:**152-157.

25. **Costerton, J. W., P. S. Stewart, and E. P. Greenberg.** 1999. Bacterial biofilms: a common cause of persistent infections. Science. **284:**1318-1322.

26. **Crawford, E. W. J., and L. J. Shimkets.** 2000. The *Myxococcus xanthus socE* and *csgA* genes are regulated by the stringent response. Mol. Microbiol. **37:**788-799.

27. **Crawford, E. W. J., and L. J. Shimkets.** 2000. The stringent response in *Myxococcus xanthus* is regulated by SocE and the CsgA C-signaling protein. Genes Dev. **14:**483-492.

28. **Davis, J. M., J. Mayor, and L. Plamann.** 1995. A missense mutation in *rpoD* results in an A-signalling defect in M*yxococcus xanthus*. Mol. Microbiol. **18:**943-952.

29. **de Jong, R. M., J. J. W. Tiesinga, H. J. Rozeboom, K. H. Kalk, L. Tang, D. B. Janssen, and B. W. Dijkstra.** 2003. Structure and mechanism of a bacterial haloalcohol dehalogenase: a new variation of the short-chain dehydrogenase/reductase fold without an NAD(P)H binding site. EMBO J. **22:**4933-4944.

30. **DeLong, A., A. Calderon-Urrea, and S. L. Dellaporta.** 1993. Sex determination gene TASSELSEED2 of maize encodes a short-chain alcohol dehydrogenase required for stage-specific floral organ abortion. Cell. **74:**757-768.

31. **Downard, J., S. V. Ramaswamy, and K.-S. Kil.** 1993. Identification of *esg*, a genetic locus involved in cell-cell signaling during *Myxococcus xanthus* development. J. Bacteriol. **175:**7762-7770.

32. **Downard, J., and D. Toal.** 1995. Branched chain fatty acids: the case for a novel from of cell-cell signaling during *Myxococcus xanthus* development. Mol. Microbiol. **16:**171-175.

33. **Dworkin, M.** 1962. Nutritional requirements for vegetative growth of *Myxococcus xanthus*. J. Bacteriol. **84:**250-257.

34. **Dworkin, M.** 1996. Recent advances in the social and developmental biology of the myxobacteria. Microbiol. Rev. **60:**70-102.

35. **Ellehauge, E., M. Norregaard-Madsen, and L. Sogaard-Andersen.** 1998. The FruA signal transduction protein provides a checkpoint for the temporal co-ordination of intercellular signals in *Myxococcus xanthus* development. Mol. Microbiol. **30:**807-817.

36. **Filling, C., K. D. Berndt, J. Benach, S. Knapp, T. Prozorovski, E. Nordling, R. Ladenstein, H. Jornvall, and U. Oppermann.** 2002. Critical residues for structure and catalysis in short-chain dehydrogenases/reductases. J. Biol. Sci. **277:**25677-23684.

37. **Funder, J. W.** 1997. Glucocorticoid and mineralocorticoid receptors: biology and clinical relevance. Annu. Rev. Med. **48:**231-240.

38.   **Garrity, P. A., and S. L. Zipursky.** 1995. Neuronal target recognition. Cell. **83:**177-185.

39.   **Garza, A. G., B. Z. Harris, J. S. Pollack, and M. Singer.** 2000. The *asgE* locus is required for cell-cell signalling during *Myxococcus xanthus* development. Mol. Microbiol. **35:**812-824.

40.   **Ghosh, D., Z. Wawrzak, C. M. Weeks, W. L. Duax, and M. Erman.** 1994. The refined three-dimensional structure of 3 alpha,20 beta-hydroxysteroid dehydrogenase and possible roles of the residues conserved in short-chain dehydrogenases. Structure. **2:**629-640.

41.   **Gill, R. E., and M. C. Bornemann.** 1988. Identification and characterization of the *Myxococcus xanthus bsg*A gene product. J. Bacteriol. **170:**5289-5297.

42.   **Gill, R. E., M. Cull, and S. Fly.** 1988. Genetic Identification and cloning of a gene required for developmental cell interactions in *Myxococcus xanthus*. J. Bacteriol. **170:**5279-5288.

43.   **Gill, R. E., and M. G. Cull.** 1986. Control of developmental gene expression by cell-to-cell interactions in *Myxococcus xanthus*. J. Bacteriol. **168:**341-347.

44.   **Gill, R. E., M. Karlok, and D. Benton.** 1993. *Myxococcus xanthus* encodes an ATP-dependent protease which is required for developmental gene transcription and intercellular signaling. J. Bacteriol. **175:**4538-4544.

45.   **Gorski, L., T. Gronewold, and D. Kaiser.** 2000. A sigma(54) activator protein necessary for spore differentiation within the fruiting body of *Myxococcus xanthus*. J. Bacteriol. **180:**2438-2444.

46. **Gorski, L., and D. Kaiser.** 1998. Targeted mutagenesis of sigma54 activator proteins in *Myxococcus xanthus.* J. Bacteriol. **180:**5896-5905.

47. **Gottesman, S.** 1996. Proteases and their targets in *Escherichia coli*. Annu. Rev. Genet. **30:**465-506.

48. **Gronewold, T. M., and D. Kaiser.** 2001. The *act* operon controls the level and time of C-signal production for *Myxococcus xanthus* development. Mol. Microbiol. **40:**744-756.

49. **Guo, D., Y. Wu, and H. B. Kaplan.** 2000. Identification and characterization of genes required for early *Myxococcus xanthus* developmental gene expression. J. Bacteriol. **182:**4564-4571.

50. **Hagen, D. C., A. P. Bretscher, and D. Kaiser.** 1978. Synergism between morphogenetic mutants of *Myxococcus xanthus*. Dev. Biol. **64:**284-296.

51. **Hager, E., H. Tse, and R. E. Gill.** 2001. Identification and characterization of *spdR* mutations that bypass the BsgA protease-dependent regulation of developmental gene expression in *Myxococcus xanthus.* Mol. Microbiol. **39:**765-780.

52. **Harris, B. Z., D. Kaiser, and M. Singer.** 1998. The guanosine nucleotide (p)ppGpp initiates development and A-factor production in *Myxococcus xanthus*. Genes Dev. **12:**1022-1035.

53. **Hartzell, P., and D. Kaiser.** 1991. Function of MglA, a 22-kilodalton protein essential for gliding in *Myxococcus xanthus*. J. Bacteriol. **173:**7615-7624.

54. **Hodgkin, J., and D. Kaiser.** 1979. Genetics of gliding motility in *Myxococcus xanthus* (Myxobacterales): Genes controlling movement of single cells. Mol. Gen. Genet. **171:**167-176.

55. **Holden, H. M., I. Rayment, and J. B. Thoden.** 2003. Structure and function of enzymes of the Leloir pathway for galactose metabolism. J. Biol. Chem. **278:**43885-43888.

56. **Hu, J. C., and C. A. Gross.** 1985. Mutations in the sigma subunit of *E. coli* RNA polymerase which affect positive control of transcription. Mol. Gen. Genet. **199:**7-13.

57. **Huisman, O., and R. D'Ari.** 1981. An inducible DNA replication-cell division coupling mechanism in *E. coli*. Nature. **290:**797-799.

58. **Huisman, O., R. D'Ari, and S. Gottesman.** 1984. Cell-division control in *Escherichia coli*: specific induction of the SOS function SfiA protein is sufficient to block septation. Proc. Natl. Acad. Sci. USA. **81:**4490-4494.

59. **Igoshin, O. A., A. Mogilner, R. D. Welch, D. Kaiser, and G. Oster.** 2001. Pattern formation and traveling waves in myxobacteria: theory and modeling. Proc. Natl. Acad. Sci. USA. **98:**14913-14918.

60. **Ishihama, A.** 1993. Protein-protein communication within the transcription apparatus. J. Bacteriol. **175:**2483-2489.

61. **Jelsbak, L., and L. Sogaard-Andersen.** 2003. Cell behavior and cell-cell communication during fruiting body morphogenesis in *Myxococcus xanthus*. J. Microbiol. Methods. **55:**829-839.

62. **Jelsbak, L., and L. Sogaard-Andersen.** 1999. The cell surface-associated intercellular C-signal induces behavioral changes in individual *Myxococcus xanthus* cells during fruiting body morphogenesis. Proc. Natl. Acad. Sci. USA. **96:**5031-5036.

63. **Jelsbak, L., and L. Sogaard-Andersen.** 2002. Pattern formation by a cell surface-associated morphogen in *Myxococcus xanthus*. Proc. Natl. Acad. Sci. USA. **99:**2032-2037.

64. **Jornvall, H., J. O. Hoog, and B. Persson.** 1999. SDR and MDR: completed genome sequences show these protein families to be large, of old origin, and of complex nature. FEBS Lett. **445:**261-264.

65. **Jornvall, H., B. Persson, M. Krook, S. Atrian, R. Gonzalez-Duarte, J. Jeffery, and D. Ghosh.** 1995. Short-chain dehydrogenases/reductases (SDR). Biochem. **18:**6003-6013.

66. **Kaiser, D.** 2004. Signaling in myxobacteria. Annu. Rev. Microbiol. **58:**75-98.

67. **Kaiser, D.** 1979. Social gliding is correlated with the presence of pili in *Myxococcus xanthus*. Proc. Natl. Acad. Sci. USA. **76:**5952-5956.

68. **Kallberg, Y., U. Oppermann, H. Jornvall, and B. Persson.** 2002. Short-chain dehydrogenase/reductase (SDR) relationships: A large family with eight clusters common to human, animal, and plant genomes. Protein Sci. **11:**636-641.

69. **Kallberg, Y., U. Oppermann, H. Jornvall, and B. Persson.** 2002. Short-chain dehydrogenases/reductases (SDRs): Coenzyme-based functional assignments in completed genomes. Eur. J. Biochem. **269:**4409-4414.

70. **Kalman, L. V., Y. L. Cheng, and D. Kaiser.** 1994. The *Myxococcus xanthus dsg* gene product performs functions of translation initiation factor IF3 in vivo. J. Bacteriol. **176:**1434-1442.

71. **Kearns, D. B., B. D. Campbell, and L. J. Shimkets.** 2000. *Myxococcus xanthus* fibril appendages are essential for excitation by a phospholipid attractant. Proc. Natl. Acad. Sci. USA. **97:**11505-11510.

72. **Kearns, D. B., A. Venot, P. J. Bonner, B. Stevens, G. J. Boons, and L. J. Shimkets.** 2001. Identification of a developmental chemoattractant in *Myxococcus xanthus* through metabolic engineering. Proc. Natl. Acad. Sci. USA. **98:**13990-13994.

73. **Keynes, R., and G. M. Cook.** 1995. Axon guidance molecules. Cell. **83:**161-169.

74. **Kim, S. K., and D. Kaiser.** 1990. Cell alignment required in differentiation of *M. xanthus*. Science **249:**926-928.

75. **Kim, S. K., and D. Kaiser.** 1990. Cell motility is required for the transmission of C-factor, an intercellular signal that coordinates fruiting body morphogenesis of *Myxococcus xanthus*. Genes Dev **4:**896-905.

76. **Kim, S. K., and D. Kaiser.** 1990. C-factor: A cell-cell signaling protein required for fruiting body morphogenesis of *M. xanthus*. Cell **61:**19-26.

77. **Kim, S. K., and D. Kaiser.** 1990. Purification and properties of *Myxococcus xanthus* C-factor, an intercellular signaling protein. Proc. Natl. Acad. Sci. USA. **87:**3635-3639.

78. **Klausen, M., A. Aes-Jorgensen, S. Molin, and T. Tolker-Nielsen.** 2003. Involvement of bacterial migration in the development of complex multicellular structures in *Pseudomonas aeruginosa* biofilms. Mol. Microbiol. **50:**61-68.

79. **Koumanov, A., J. Benach, S. Atrian, R. Gonzalez-Duarte, A. Karshikoff, and R. Ladenstein.** 2003. The catalytic mechanism of *Drosophila* alcohol dehydrogenase: Evidence for a proton relay modulated by the coupled ionization of the active site lysine/tyrosine pair and a NAD^+ ribose OH switch. Proteins: Str, func and gent. **51:**289-298.

80. **Kroos, L., and D. Kaiser.** 1984. Construction of Tn*5 lac*, a transposon that fuses *lacZ* expression to exogenous promotors, and its introduction into *Myxococcus xanthus*. Proc. Natl. Acad. Sci. USA **81:**5816-5820.

81. **Kroos, L., and D. Kaiser.** 1987. Expression of many developmentally regulated genes in *Myxococcus* depends on a sequence of cell interactions. Genes Dev **1:**840-854.

82. **Kroos, L., A. Kuspa, and D. Kaiser.** 1990. Defects in fruiting body development caused by the Tn*5 lac* insertions in *Myxococcus xanthus*. J. Bacteriol. **172:**484-487.

83. **Kroos, L., A. Kuspa, and D. Kaiser.** 1986. A global analysis of developmentally regulated genes in *Myxococcus xanthus*. Dev. Biol. **117:**252-266.

84. **Kruse, T., S. Lobedanz, N. M. Berthelsen, and L. Sogaard-Andersen.** 2001. C-signal: a cell surface-associated morphogen that induces and co-ordinates multicellular fruiting body morphogenesis and sporulation in *Myxococcus xanthus*. Mol. Microbiol. **40:**156-168.

85. **Kuldell, N., and A. Hochshild.** 1994. Amino acid substitutions in the -35 recognition motif of sigma 70 that result in defects in phage lambda repressor-stimulated transcription. J. Bacteriol. **176:**2991-2998.

86. **Kuspa, A., and D. Kaiser.** 1989. Genes required for developmental signaling in *Myxococcus xanthus*: Three *asg* loci. J. Bacteriol. **171:**2762-2772.

87. **Kuspa, A., L. Plamann, and D. Kaiser.** 1992. Identification of heat-stable A-factor from *Myxococcus xanthus*. J. Bacteriol. **174:**3319-3326.

88. **Kuspa, A., L. Plamann, and D. Kaiser.** 1992. A-Signalling and the cell density requirement for *Myxococcus xanthus* development. J. Bacteriol. **174:**7360-7369.

89. **Lancero, H., J. E. Brofft, J. Downard, B. W. Birren, C. Nusbaum, J. Naylor, W. Shi, and L. J. Shimkets.** 2002. Mapping of *Myxococcus xanthus* social motility *dsp* mutations to the *dif* genes. J. Bacteriol. **184:**1462-1465.

90. **Lee, B.-U., K. Lee, J. Mendez, and L. J. Shimkets.** 1995. A tactile sensory system of *Myxococcus xanthus* involves an extracellular NAD(P)$^+$-containing protein. Genes Dev. **9:**2964-2973.

91. **Lee, K., and L. J. Shimkets.** 1994. Cloning and characterization of the *socA* locus which restores development to *Myxococcus xanthus* C-signaling mutants. J. Bacteriol. **176:**2200-2209.

92. **Lee, K., and L. J. Shimkets.** 1996. Suppression of a signaling defect during *Myxococcus xanthus* development. J. Bacteriol. **178:**977-984.

93. **Lesk, M.** 1995. NAD-binding domains of dehydrogenases. Curr. Opin. Struct. Biol. **6:**775-783.

94.   **Li, S., B. Lee, and L. J. Shimkets.** 1992. *csgA* expression entrains *Myxococcus xanthus* development. Genes Dev. **6:**401-410.

95.   **Li, S. F., and L. J. Shimkets.** 1993. Effect of *dsp* mutations on the cell-to-cell transmission of CsgA in *Myxococcus xanthus*. J. Bacteriol. **175:**3648-3652.

96.   **Li, Y., H. Sun, X. Ma, A. Lu, R. Lux, D. Zusman, and W. Shi.** 2003. Extracellular polysaccharides mediate pilus retraction during social motility of *Myxococcus xanthus*. Proc. Natl. Acad. Sci. USA. **100:**5443-5448.

97.   **Lobedanz, S., and L. Sogaard-Andersen.** 2003. Identification of the C-signal, a contact-dependent morphogen coordinating multiple developmental responses in *Myxococcus xanthus*. Genes Dev. **17:**2151-2161.

98.   **Makino, K., M. Amemura, S. K. Kim, A. Nakata, and H. Shinagawa.** 1993. Role of the sigma 70 subunit of RNA polymerase in transcriptional activation by activator protein PhoB in *Escherichia coli*. Genes Dev. **7:**149-160.

99.   **Mayo, K. A., and D. Kaiser.** 1989. *asgB*, a gene required early for developmental signalling aggregation, and sporulation of *Myxococcus xanthus*. Mol. Gen. Genet. **218:**409-418.

100.   **McIntyre, J. O., L. A. Holladay, M. Smigel, D. Puett, and S. Fleischer.** 1978. Hydrodynamic properties of D-beta-hydroxybutyrate dehydrogenase, a lipid-requiring enzyme. Biochem. **20:**4169-4177.

101.   **McVittie, A., F. Messik, and S. A. Zahler.** 1962. Developmental biology of *Myxococcus*. J. Bacteriol. **84:**546-551.

102.   **Merz, A. J., and M. So.** 2000. Interactions of pathogenic *Neisseriae* with epithelial cell membranes. Annu. Rev. Cell Dev. Biol. **16:**423-457.

103. **Nakajin, S., S. Ohno, M. Aoki, and M. Shinoda.** 1988. 20 beta-hydroxysteroid dehydrogenase of neonatal pig testis: purification and some properties. J. Biochem. (Tokyo) **104:**565-569.

104. **Ogawa, M., S. Fujitani, X. Mao, S. Inouye, and T. Komano.** 1996. FruA, a putative transcription factor essential for the development of *Myxococcus xanthus.* Mol. Microbiol. **22:**757-767.

105. **Oppermann, U., C. Filling, M. Hult, N. Shafqat, X. Wu, M. Lindh, J. Shafqat, E. Nordling, Y. Kallberg, B. Persson, and H. Jornvall.** 2003. Short-chain dehydrogenases/reductases (SDR): the 2002 update. Chemico-Biol. Int. **143-144:**247-253.

106. **Oppermann, U. C., C. Filling, K. D. Berndt, B. Persson, J. Benach, R. Ladenstein, and H. Jornvall.** 1997. Active site directed mutagenesis of 3 beta/17 beta-hydroxysteroid dehydrogenase establishes differential effects on short-chain dehydrogenase/reductase reactions. Biochem. **1:**34-40.

107. **Oppermann, U. C. T., C. Filling, and H. Jornvall.** 2001. Forms and functions of human SDR enzymes. Chemico-Biol. Int. **130-132:**699-705.

108. **Persson, B., Y. Kallberg, U. Oppermann, and H. Jornvall.** 2003. Coenzyme-based functional assignments of short-chain dehydrogenases/reductases (SDRs). Chemico-Biological Interactions **143-144:**271-278.

109. **Plamann, L., J. M. Davis, B. Cantwell, and J. Mayor.** 1994. Evidence that *asgB* encodes a DNA-binding protein essential for growth and development of *Myxococcus xanthus*. J. Bacteriol. **176:**2013-2020.

110. **Plamann, L., A. Kuspa, and D. Kaiser.** 1992. Proteins that rescue A-signal-defective mutants of *Myxococcus xanthus*. J. Bacteriol. **174:**3311-3318.

111. **Plamann, L., Y. Li, B. Cantwell, and J. Mayor.** 1995. The *Myxococcus xanthus asgA* gene encodes a novel signal transduction protein required for multicellular development. J. Bacteriol. **177:**2014-2020.

112. **Rocchetta, H. L., L. L. Burrows, and J. S. Lam.** 1999. Genetics of O-antigen biosynthesis in *Pseudomonas aeruginosa*. Microbiol. Mol. Biol. Rev. **63:**523-553.

113. **Rosenberg, E., K. H. Keller, and M. Dworkin.** 1977. Cell density-dependent growth of *Myxococcus xanthus* on casein. J. Bacteriol. **129:**770-777.

114. **Rosenbluh, A., and M. Eisenbach.** 1992. Effect of mechanical removal of pili on gliding motility of *Myxococcus xanthus*. J. Bacteriol. **174:**5406-5413.

115. **Rossmann, M. G., D. Moras, and K. W. Olsen.** 1974. Chemical and biological evolution of nucleotide-binding protein. Nature. **463:**194-199.

116. **Sager, B., and D. Kaiser.** 1994. Intercellular C-signaling and the traveling waves of *Myxococcus*. Genes Dev. **8:**2793-2804.

117. **Shapiro, J. A.** 1998. Thinking about bacterial populations as multicellular organisms. Annu. Rev. Microbiol. **52:**81-104.

118. **Shapiro, J. A., and M. Dworkin (ed.).** 1997. Bacteria as Multicellular Organisms. Oxford University Press, New York.

119. **Sheldon, P. S., R. G. Kekwick, C. G. Smith, C. Sidebottom, and A. R. Slabas.** 1992. 3-Oxoacyl-[ACP] reductase from oilseed rape (*Brassica napus*). Biochim. Biophys. Acta. **2:**151-159.

120. **Shimkets, L., and H. Rafiee.** 1990. CsgA, an extracellular protein essential for *M. xanthus* development. J. Bacteriol. **172:**5299-5306.

121. **Shimkets, L. J.** 1986. Correlation of energy-dependent cell cohesion with social motility in *Myxococcus xanthus*. J. Bacteriol. **166:**837-841.

122. **Shimkets, L. J.** 1999. Intercellular signaling during fruiting-body development of *Myxococcus xanthus*. Annu. Rev. Microbiol. **53:**525-549.

123. **Shimkets, L. J.** 1986. Role of cell cohesion in *Myxococcus xanthus* fruiting body formation. J. Bacteriol. **166:**842-848.

124. **Shimkets, L. J., and S. J. Asher.** 1988. Use of recombination techniques to examine the structure of the *csg* locus of *Myxococcus xanthus*. Mol. Gen. Genet. **211:**63-71.

125. **Shimkets, L. J., R. E. Gill, and D. Kaiser.** 1983. Developmental cell interactions in *Myxococcus xanthus* and the *spoC* locus. Proc. Natl. Acad. Sci. USA **80:**1406-1410.

126. **Shimkets, L. J., and D. Kaiser.** 1982. Induction of coordinated movement of *Myxococcus xanthus* cells. J. Bacteriol. **152:**451-461.

127. **Shimkets, L. J., and D. Kaiser.** 1982. Murein components rescue developmental sporulation of *Myxococcus xanthus*. J. Bacteriol. **152:**462-470.

128. **Simunovic, V., F. C. Gherardini, and L. J. Shimkets.** 2003. Membrane localization of motility, signaling, and polyketide synthetase proteins in *Myxococcus xanthus.* J. Bacteriol. **185:**5066-5075.

129. **Singer, M., and D. Kaiser.** 1995. Ectopic production of guanosine penta- and tetraphosphate can initiate early developmental gene expression in *Myxococcus xanthus*. Genes Dev. **9:**1633-1644.

130. **Sogaard-Anderson, L., and D. Kaiser.** 1996. C factor, a cell-surface-associated intercellular signaling protein, stimulates the cytoplasmic Frz signal transduction system in *Myxococcus xanthus*. Proc. Natl. Acad. Sci. USA **93:**2625-2679.

131. **Sogaard-Anderson, L., F. J. Slack, H. Kimsey, and D. Kaiser.** 1996. Intercellular C-signaling in *Myxococcus xanthus* involves a branched signal transduction pathway. Genes Dev. **10:**740-754.

132. **Stewart, P. S., and J. W. Costerton.** 2001. Antibiotic resistance of bacteria in biofilms. Lancet. **358:**135-138.

133. **Sun, H., D. R. Zusman, and W. Shi.** 2000. Type IV pilus of *Myxococcus xanthus* is a motility apparatus controlled by the *frz* chemosensory system. Curr. Biol. **10:**1143-1146.

134. **Toal, D. R., S. W. Clifton, B. R. Roe, and J. Downard.** 1995. The *esg* locus of *Myxococcus xanthus* encodes the E1a and E1ß subunits of a branched-chain keto acid dehydrogenase. Mol. Microbiol. **16:**177-189.

135. **Toomey, R. E., and S. J. Wakil.** 1966. Studies on the mechanism of fatty acid synthesis. XV. Preparation and general properties of beta-ketoacyl acyl carrier protein reductase from *Escherichia coli*. Biochim. Biophys. Acta. **2:**189-197.

136. **Tse, H., and R. E. Gill.** 2002. Bypass of A- and B-signaling requirements for *Myxococcus xanthus* development by mutations in *spdR*. J. Bacteriol. **184:**1455-1457.

137.	**Ward, M. J., and D. R. Zusman.** 1997. Regulation of directed motility in *Myxococcus xanthus.* Mol. Microbiol. **24:**885-893.

138.	**Welch, R., and D. Kaiser.** 2001. Cell behavior in traveling wave patterns of myxobacteria. Proc. Natl. Acad. Sci. USA. **98:**14907-14912.

139.	**Wenz, H. M., L. Hinck, P. Cannon, M. Navre, and G. Ringold.** 1992. Reduced expression of AP27 protein, the product of a growth factor-repressible gene, is associated with diminished adipocyte differentiation. Proc. Natl. Acad. Sci. USA. **89:**1065-1069.

140.	**Wermuth, B.** 1981. Purification and properties of an NADPH-dependent carbonyl reductase from human brain. Relationship to prostaglandin 9-ketoreductase and xenobiotic ketone reductase. J Biol Chem **256:**1206-1213.

141.	**Wolgemuth, C., E. Hoiczyk, D. Kaiser, and G. Oster.** 2002. How myxobacteria glide. Curr. Biol. **12:**369-377.

142.	**Wu, S. S., and D. Kaiser.** 1995. Genetic and functional evidence that Type IV pili are required for social gliding motility in *Myxococcus xanthus*. Mol. Microbiol. **18:**547-558.

143.	**Yang, C., and H. B. Kaplan.** 1997. *Myxococcus xanthus sasS* encodes a sensor histidine kinase required for early developmental gene expression. J. Bacteriol. **179:**7759-67.

144.	**Yang, Z., Y. Geng, D. Xu, H. B. Kaplan, and W. Shi.** 1998. A new set of chemotaxis homologues is essential for *Myxococcus xanthus* social motility. Mol. Microbiol. **30:**1123-1130.

145. **Yang, Z., D. Guo, M. G. Bowden, H. Sun, L. Tong, Z. Li, A. E. Brown, H. B. Kaplan, and W. Shi.** 2000. The *Myxococcus xanthus* wbgB gene encodes a glycosyltransferase homologue required for lipopolysaccharide O-antigen biosynthesis. Arch. Microbiol. **174:**399-405.

CHAPTER 2

A Novel Lysophosphatidylethanolamine Dehydrogenase from *Myxococcus xanthus*

Introduction:

Myxococcus xanthus is a member of the delta proteobacteria that serves as a prokaryotic paradigm to study social behavior and multicellularity. In response to nutrient limitation, *M. xanthus* initiates a developmental program involving the directed movement of thousands of cells towards an aggregation center where they build a multicellular fruiting body. Within a fruiting body, the rod-shaped vegetative cells differentiate into spherical myxospores that are environmentally resistant and metabolically dormant. Development is governed by a series of extracellular signaling events carried out by biochemically diverse molecules (27). The A-signal is comprised of a mixture of amino acids (11). The extracellular concentration of the A-signal amino acids is directly proportional to the cell density and serves to determine whether an adequate density of starved cells is present to complete development (12). Phosphatidylethanolamine containing the unsaturated fatty acid 16:1 ω5c is a chemoattractant that is proposed to play a role in fruiting body morphogenesis (6). The protein that initiates C-signaling belongs to the short chain alcohol dehydrogenase family (SCAD) (14).

The C-signal is a concentration-dependent timer that controls the spatial and temporal expression of the morphologically distinct developmental events (8, 10, 16).

CsgA, a 25 kDa protein responsible for the manifestations of C-signaling, undergoes proteolytic processing into a 17 kDa fragment (9, 14, 17). Much debate has focused on whether the biologically active form is the 25 kDa protein or the truncated 17 kDa form. Both proteins have been shown to rescue development in *csgA* mutants upon extracellular complementation (9, 14). Although the 17 kDa form was purified 1000-fold from developing *M. xanthus* cells, the fraction that rescued development contained at least one other higher molecular weight polypeptide (9). Attempts to make a truncated form with a specific activity comparable to that of the full length form have failed. A *lacZ-csgA* fusion, lacking the N-terminal domain, does not rescue development of *csgA* mutants (26). Although a MalE fusion of the 17 kDa form corrected the developmental defects of *csgA* mutants, roughly 2000-fold more was needed than what the cells normally produce (17).

Genetic evidence that the 25 kDa form is an enzyme has come from isolation of a class of overexpression suppressor mutants. Overexpression of SocA, a SCAD with 28% identity to CsgA almost exclusively in the enzyme active site, restored C-signaling in *csgA* mutants (15). Mutational analysis of CsgA showed that conserved amino acids known to be essential for catalytic activity in other SCADs are also essential for C-signaling. These data raise the possibility that SocA can utilize the same substrate as CsgA to generate the C-signal. In fact, many SCAD enzymes play critical roles in hormone signaling during cellular differentiation in higher eukaryotes, producing products such as steroids, prostaglandins, and retinoids (21).

Enzymes belonging to the SCAD family catalyze the interconversion of secondary alcohols and ketones using NAD(P)(H) sequestered in the N-terminal

Rossmann fold (20). A single SCAD can act on structurally diverse biomolecules. For example, human type II hydroxyacyl-CoA dehydrogenase/amyloid-β binding alcohol dehydrogenase is an oxidoreductase that acts on 3-hydroxyacyl-CoA derivatives, hydroxysteroids, alcohols, and β-hydroxybutyrate (23). The varied substrate specificities of SCADs along with the lack of biochemical characterization of many of these enzymes make it difficult to predict the substrate based on amino acid sequence alone.

Several attempts to disrupt *socA* have failed suggesting that it is essential for growth (15). The potential role of SocA in synthesizing the C-signal made it an ideal candidate to attempt to identify the substrate. Here we use mass spectrometry to identify a substrate for SocA and then characterize the enzymatic activity. Our results indicate that SocA performs a novel biochemical reaction in oxidizing lysophosphatidylethanolamine.

Materials and methods:

Bacterial strains and growth conditions.

M. xanthus DK1622 (29) and LS523 (28) were used as the wild type and *csgA* mutant strains, respectively. Cells were grown at 32^OC in CYE (10 g L^{-1} casitone, 5 g L^{-1} yeast extract, 4 mM $MgSO_4$ 10 mM [N-Morpholino]propanesulfonic acid (MOPS), pH 7.6) broth or on CYE agar (CYE plus 15 g L^{-1} Difco agar). *E. coli* BL21Star (DE3), used for *socA* expression, was grown in Luria-Bertoni broth (10 g L^{-1} tryptone, 5 g L^{-1} yeast extract and 5 g L^{-1} sodium chloride) supplemented with 100 μg ml^{-1} ampicillin.

Expression and purification of SocA.

The *socA* gene was amplified by the polymerase chain reaction (PCR) using the following forward and reverse primers, respectively; 5' CACCATGATGGCGTTCAGT GGCAAG 3' and 5' AGCCGAAAAGCCCCATCGAC 3' (Gibco BRL Life Technologies, Gaithersburg, MD). The PCR fragment was cloned into different pET/D-TOPO expression vectors (Invitrogen Corporation, Carlsbad, CA) for generation of clones expressing SocA with different fusion tags. pLEE118 produces a SocA fusion protein with N-terminal HP Thioredoxin and a C-terminal V5 epitope followed by 6 histidines (tSocAh). pLEE112 produces a SocA fusion protein with an N-terminal Xpress epitope preceding a 6x histidine tag (hSocA). Expression from the pET promoter is regulated by T7 RNA polymerase, whose expression is in turn regulated by an IPTG inducible promoter. The expression host BL21StarDE3 is a derivative of *E. coli* B that is deficient in the Lon and OmpT proteases (7, 18).

Both versions of SocA were purified in a similar manner. Cells were lysed by 3 passes through a SIM-AMINCO French Pressure Cell (Spectronic Unicam, Rochester, NY) at 10,000 psi pressure and separated into soluble and insoluble fractions by centrifugation at 21,000 x g for 1 hour. Soluble protein was subjected to affinity chromatography on a Nickel column (Amersham Biosciences, Piscataway, NJ). Protein was eluted with 100 mM, 300 mM, and 500 mM imidazole. The fraction that eluted with 300 mM imidazole was used in these studies. The protein fractions were analyzed by sodium dodecylsulfate polyacrylamide gel electrophoresis (SDS-PAGE) and stained using Silver Stain Plus reagents (Bio-Rad Laboratories, Hercules, CA).

Protein concentration was determined using the biscinchoninic acid (BCA) assay (Pierce Chemicals Co., Rockford, IL) with bovine serum albumin standards.

Dehydrogenase assay.

The ability of recombinant SocA to oxidize partially pure cellular extracts or synthetic substrates was monitored at 340 nm using a spectrophotometer (DU 640B; Beckman Instruments Inc., Fullerton, CA) at 25^OC. The reaction mixture contained 100 mM sodium phosphate buffer, pH 6.8, 1 mM NAD^+, and various amounts of substrate and protein. The cellular extracts were solubilized in 100% methanol, and the final concentration of methanol in the reaction mixture was maintained at less than 2.5 %. The change in absorbance due to the production of NADH was monitored for at least 5 minutes or until the reaction plateaued. The specific activity was calculated from the initial rates by using a molar extinction coefficient of 6220 $M^{-1}cm^{-1}$ for NADH at 340 nm. Specific activity is defined as μmoles NADH formed per minute per mg protein. Specific activity was routinely determined from three independent protein preparations ± the standard deviation.

Synthetic lipids were purchased from Avanti Polar Lipids Inc. (Alabaster, Al). All the other substrates and chemicals were purchased from Sigma Chemical Co. (St. Louis, MO). Lysophosphatidylethanolamine (lysoPE) substrates with an unsaturated fatty acid were solubilized in 100% methanol and diluted in the reaction mixture to a final methanol concentration of 5%. Lysophospholipids with saturated fatty acids were solubilized in chloroform:methanol:water (65:25:4), added to the assay mixture, and the chloroform phase that separates from the aqueous assay medium was removed before

addition of the enzyme. Mixed micelles of the lysophospholipids and Trition X 100 were

prepared by equilibrating 2.5 mM lysophospholipid with 5 mM Triton X 100 in water at

room temperature overnight.

Preparation of 1-O-[11-(Z)-hexadecanoyl]-2-hydroxy-sn-glycero-3-

phosphoethanolamine.

       1-*O*-[11-(*Z*)-hexadecanoyl]-2-hydroxy-*sn*-glycero-3-phosphoethanolamine

(lysoPE 16:1 ω5c) was generated by treating 1,2-*O*-Bis[11-(*Z*)-hexadecanoyl]-*sn*-

glycero-3-phosphoethanolamine (PE-16:1 ω5c/16:1 ω5c)[Courtesy of A. Venot and G. J.

Boons] with phospholipase A2. 600 μg PE-16:1 ω5c/16:1 ω5c was incubated with 20 μg

phospholipase A2 from *Naja mossambica mossambica* (Sigma Chemical Co., St Louis,

MO) in the presence of 10 mM $CaCl_2$ and 200 mM Tris, pH 8.0 at 37^OC for 2 hours. The

lipid was extracted with chloroform:methanol:acetic acid (50:50:1) and purified by thin

layer chromatography on silica gel 60 (20 x 20 cm; layer thickness 250 μm; EM Science,

Gibbstown, NJ) with chloroform:methanol:water (65:25:4) as the mobile phase. The

same solvent was used for extraction of the lysoPE from the silica gel for subsequent use

in the dehydrogenase assay.

Extraction of oxidized lysophosphatidylethanolamine.

       The end-product of lysoPE oxidation was extracted with chloroform for analysis

of its chemical structure and also to study the biological relevance of oxidized lysoPE. A

10 ml aqueous enzyme assay mixture was vortexed with 2 ml chloroform for 1 minute at

25^OC and centrifuged at 10,000 x g for 1 minute to separate the chloroform phase from

the aqueous phase. The chloroform phase was dried under N_2 and the extract was

resuspended in 100 μl methanol.

Extraction of substrate molecule(s) from DK1622.

DK1622 cells grown in 2.85 L CYE to stationary phase were harvested by centrifugation at 10,000 x g for 10 minutes. The cell pellet was resuspended in 105 ml MOPS buffer (10 mM MOPS, pH 7.2, 1 mM $CaCl_2$, 4 mM $MgCl_2$ and 50 mM NaCl). Following 2 freeze thaw cycles (-20^OC and room temperature for 4 hours each), the cell suspension was subjected to sonication using ten 30 second pulses at 40 μW (W380, Heat Systems Ultrasonics). Three extraction methods were compared: extraction with acidified ethyl acetate (0.02% glacial acetic acid), extraction with ethyl acetate, and extraction with methanol/chloroform.

For extraction with acidified ethyl acetate, a 35 ml cell lysate was extracted with 25 ml acidified ethyl acetate at 37^OC for 30 minutes followed by centrifugation at room temperature for 45 minutes at 10,000 x g to separate the phases. The aqueous phase was reextracted with 25 ml acidified ethyl acetate, and the pooled ethyl acetate fractions were dried under N_2. The dried extract was dissolved in 1 ml methanol. Extraction with ethyl acetate was the same except for the omission of glacial acetic acid.

Extraction with methanol/chloroform was performed using the method of Bligh and Dyer as modified by Kearns and Shimkets (5). A 35 ml cell lysate was extracted with 15 ml methanol:chloroform (2:1) at 37^OC for 1 hour followed by centrifugation at room temperature for 5 minutes at 10,000 x g to separate the aqueous phase from the solvent phase. The pellet was reextracted with 5 ml methanol:chloroform:water (2:1:0.8, v/v/v), vortexed, and centrifuged again. The chlorform phase was removed, dried under N_2, and dissolved in 1 ml methanol.

91

The amount of substrate in each sample was determined using the dehydrogenase assay. The absorbance at 340 nm at the reaction plateau was used to calculate the amount of substrate converted, assuming a 1:1 molar ratio with the amount of NADH produced.

Partial purification of the substrate.

The crude extract was fractionated on a 500 mg LCSi silica gel Sep-Pak column (Supelco, Bellefonte, PA). The column was conditioned with 4 ml hexane:methyltertiarybutylether (MTBE) (96:4) followed by 6 ml hexane. The sample was loaded in hexane:MTBE (200:3). The column was then washed with solvents of increasing polarity in the following order: 10 ml hexane:MTBE (200:3), 10 ml hexane:MTBE (96:4), 10 ml hexane:acetic acid (100:0.2), 10 ml hexane:MTBE:acetic acid (100:2:0.2), 10 ml MTBE:acetic acid (100:0.2), 6 ml MTBE:methanol:ammonium acetate (25:4:1), 10 ml MTBE:methanol:ammonium acetate (10:4:1), 10 ml MTBE:methanol:ammonium acetate (5:4:1), 10 ml MTBE:methanol:ammonium acetate (5:8:2). The solvents were evaporated under N_2 and the dry extract resuspended in 500 µl methanol. 20 µl of each of these fractions was used in the dehydrogenase assay to quantify the amount of substrate recovered.

The active fraction from LCSi was subjected to reverse phase HPLC on a C18 column (3.9 x 150 mm; Waters, Milford, MA) equipped with a photodiode array detector. Elution was carried out using a methanol:acetonitrile (65:35) gradient with 0.1% triethylamine. Each fraction from the C18 column was assayed using the dehydrogenase assay. The peak corresponding to the active fractions was further analyzed by electrospray ionization mass spectrometry (ESIMS) in the negative mode.

Bioassay for developmental rescue.

A qualitative biological assay was employed to test the activity of the partially pure extracts and the synthetic lipids. The partially pure extract was oxidized with tSocAh and extracted by the modified method of Bligh and Dyer (5). Varying amounts (250 nmol, 100 nmol, 50 nmol, 25 nmol, 10 nmol, 1 nmol) of the oxidized and the reduced extracts (untreated with tSocAh) were dried on individual filter paper discs (Whatman 1; 0.5 mm diameter).

csgA cells were grown to mid-log phase in CYE and harvested by centrifugation at 10, 000 x g for 10 minutes at room temperature. The cell pellet was resuspended in fresh CYE to a final density of 5×10^9 ml^{-1}. Development was induced by spreading 200 μl of the cell suspension on TPM agar plates (150 mm diameter) [10 mM Tris, pH 7.6, 1 mM KH_2PO_4, and 10 mM $MgSO_4$, 1.5% (Difco) agar]. Plates were incubated at 32^OC. Whatman filter paper discs containing various amounts of the oxidized and reduced extracts were placed on the *csgA* cell lawn 6 hours later. Rescue of developmental aggregation and sporulation was monitored over the next 5 days using a dissection microscope.

LysoPE 16:0 and lysoPE 16:1 were oxidized by SocA, and varying amounts (100 μg, 50 μg, 25 μg, 10 μg, 5 μg, and 1 μg) of the oxidized and reduced forms of lysoPE 16:0 and lysoPE 16:1 were tested for their ability to rescue the developmental defects of *csgA* mutants.

Extraction and quantification of lysophosphatidylethanolamine.

   M. xanthus cells in CYE were harvested at a density of 5×10^9 ml^{-1} by centrifugation at 10,000 x g for 10 minutes, resuspended in fresh CYE, and spread on TPM agar at a final density of 2.8×10^6 cells (cm^2)$^{-1}$. After 24 hours at 32°C, the cells were removed from the agar and used as the source of developmental lysophospholipids. Vegetative *M. xanthus* cells grown in CYE to a density of 10^8 ml^{-1} were used as the source of vegetative lysophospholipids. The lysophospholipids were extracted in methanol:chloroform (5) and subjected to ESIMS. Synthetic lysoPE 16:0 and lysoPE 18:1 were used as standards for quantification of the saturated and unsaturated lysoPE, respectively.

Thin layer chromatography.

   Oxidized lysoPE 16:0 was subjected to thin layer chromatography (TLC) on silica gel 60 (20 x 20 cm; layer thickness 250 μm; EM Science, Gibbstown, NJ) using chloroform:methanol:water (65:25:4) as the mobile phase. The TLC plates were stained with iodine vapors to observe molecules containing fatty acids. The TLC plates were stained with ninhydrin (0.5% ninhydrin in 3% acetic acid in 1-butanol) and incubated at 100°C for 3 minutes to observe molecules containing amine group.

   The partially pure extract from the silica column was further purified by thin layer chromatography under the conditions mentioned above. Fifteen different fractions (1 cm tall x 3.5 cm wide), extending from the origin to the solvent front were extracted from the silica gel with 500 μl methanol. The silica gel and methanol mixture was vortexed for 15 seconds followed by centrifugation at 14,000 x g for 1 minute to separate the methanolic

supernatant, which was used as the source of substrate in the enzyme assay. The active fractions were subjected to mass spectrometry.

Nuclear magnetic resonance (NMR) spectroscopy of oxidized and reduced lysoPE 16:0.

LysoPE (reduced and oxidized) was dissolved in deuterated chloroform:methanol (2:1). 1-D Proton and 2-D gradient COSY spectra were recorded on a Varian Inova 500 MHz instrument at 25°C.

Gas chromatography-Mass spectrometric (GC/MS) analysis of oxidized lysoPE 16:0.

Oxidized lysoPE 16:0 was pertrimethylsilylated by treatment with Tri-Sil (Pierce Chemical Co, Rockford, IL) at 80°C for 20 minutes. Trimethylsilyalate (73 amu) reacts with the hydroxyl groups on the analyte enabling identification of the molecules based on a shift in the molecular mass. The analysis was performed by chemical ionization (CI) - GC/MS using an Agilent 6890N GC (Supelco, Bellefonte, PA; DB-1, 30 m $\times$ 0.25 mm ID) interfaced with a 5973 MSD with ammonia as ionizing gas.

Matrix assisted laser desorption ionization (MALDI) Mass spectrometry of oxidized lysoPE 16:0.

Oxidized lysoPE 16:0 was added to sinapinic acid matrix prepared in acetronitrile:water (50:50) with 0.1% trifluoroaceticacid and dried before analysis. A Bruker Autoflex mass spectrometer with a nitrogen laser was used to acquire the data. The analysis was also repeated in the presence of cesium chloride, which forms an adduct with the PE headgroup shifting the molecular mass of the analyte by 132 amu.

Results:

Purification of SocA:

SocA was overproduced in *E. coli* with an N- or C-terminal histidine (6x) fusion for enzymatic characterization. tSocAh and hSocA were purified on a nickel affinity column 8-fold and 5-fold respectively, to apparent homogeneity (Figure 2.1). The yields of tSocAh and hSocA were 24 mg L^{-1} and 9 mg L^{-1} respectively. Although, both tSocAh and hSocA had comparable specific activities, tSocAh was used in all the enzyme studies due to higher yield of purified protein.

Purification of SocA substrate:

The *M. xanthus* cell lysate was subjected to three different organic extractions to determine the most efficient extraction method. The amount of substrate in the solvent was quantified using a spectrophotometric assay in which NAD^+ is reduced to NADH by tSocAh, with the assumption that one molecule of substrate is oxidized for each molecule of NAD^+ reduced. The acidified ethyl acetate extraction gave the highest yield, 4.1 μmoles 10^{10} cells^{-1}. Extraction with ethyl acetate yielded 3.2 μmoles 10^{10} cells^{-1} (78% of that of the acidified ethyl acetate), and a modified Bligh and Dyer extraction yielded 1.1 moles 10^{10} cells^{-1} (26%). Acidified ethyl acetate was used for all subsequent extractions.

The acidified ethyl acetate extract was applied to a solid phase LCSi silica gel column and eluted stepwise with solvents of increasing polarity. Each fraction was assayed for dehydrogenase activity and the substrate was quantified based on the final yield of NADH. The substrate eluted with MTBE:acetic acid (100:0.2) in a single fraction of intermediate polarity, with 83% recovery of the original activity.

Figure 2.1. Silver stained gel showing tSocAh (lane 1), and hSocA (lane 2) purified by affinity chromatography on a Ni column. Each lane contains 30 μg protein.
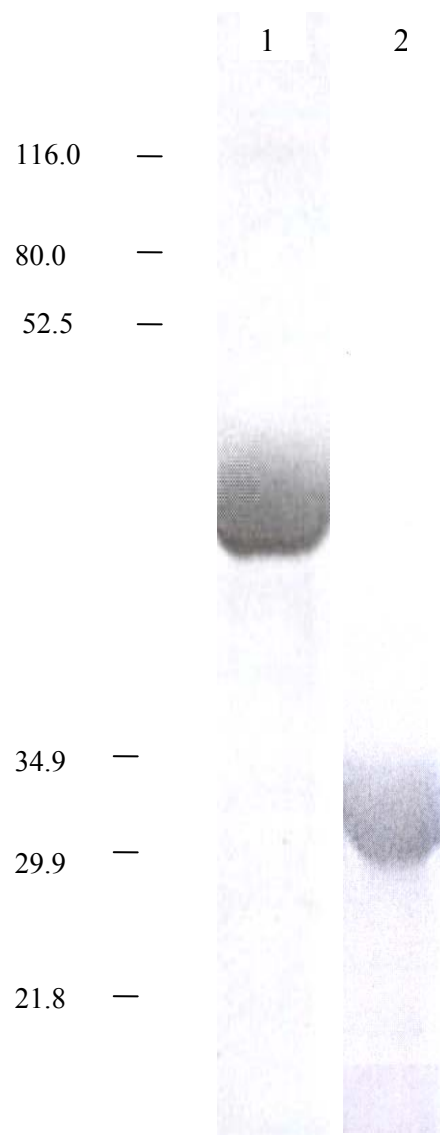
The partially pure extract from LCSi was subjected to reverse phase HPLC on a

C18 column, and the eluted fractions were used in the dehydrogenase assay. The

substrate had a retention time of 19-21 minutes (Figure 2.2A). There are at least two

sharp DAD spectral peaks that correspond to the broad substrate peak of SocA as

determined by the dehydrogenase assay (Figure 2.2B). One possible explanation is the

presence of multiple substrates. Attempts to devise another purification step with solid

phase separation on StrataX (Phenomenx, Torrance, CA) did not improve the

purification.

Identification of the SocA substrate.

Mass spectrometry of the active fractions was used to determine the masses of

compounds in the range of 140-500 amu (Figure 2.3). The most striking correlation was

with 1- acyl 2-hydroxy-*sn*-glycerophosphoethanolamine (lysoPE) containing a C16:1

fatty acid (m/z 450.7 amu). Previously it was found that 16:1 ω5c is one of the most

abundant fatty acids in *M. xanthus* (6).

SocA is a lysoPE dehydrogenase.

Since lysoPE 16:1 ω5c is not commercially available, biochemical analysis began

with lysoPE 16:0, which has a saturated fatty acid of identical length. Vesicles were

prepared by addition of chloroform:methanol:water (65:25:4)-solubilized lipid to the

aqueous assay mixture. The specific activities of tSocAh and hSocA with 100 μM

lysoPE 16:0 were 558 ± 69 and 461 ± 96 μmoles min^{-1} mg^{-1} respectively.

Figure 2.2. Total Wavelength Chromatogram of separation on C18 reverse phase column. The fractions with a SocA substrate (retention time of 19-21 minutes) are highlighted with vertical bars (A). Enzyme activity profile of corresponding fractions using the dehydrogenase assay (B).
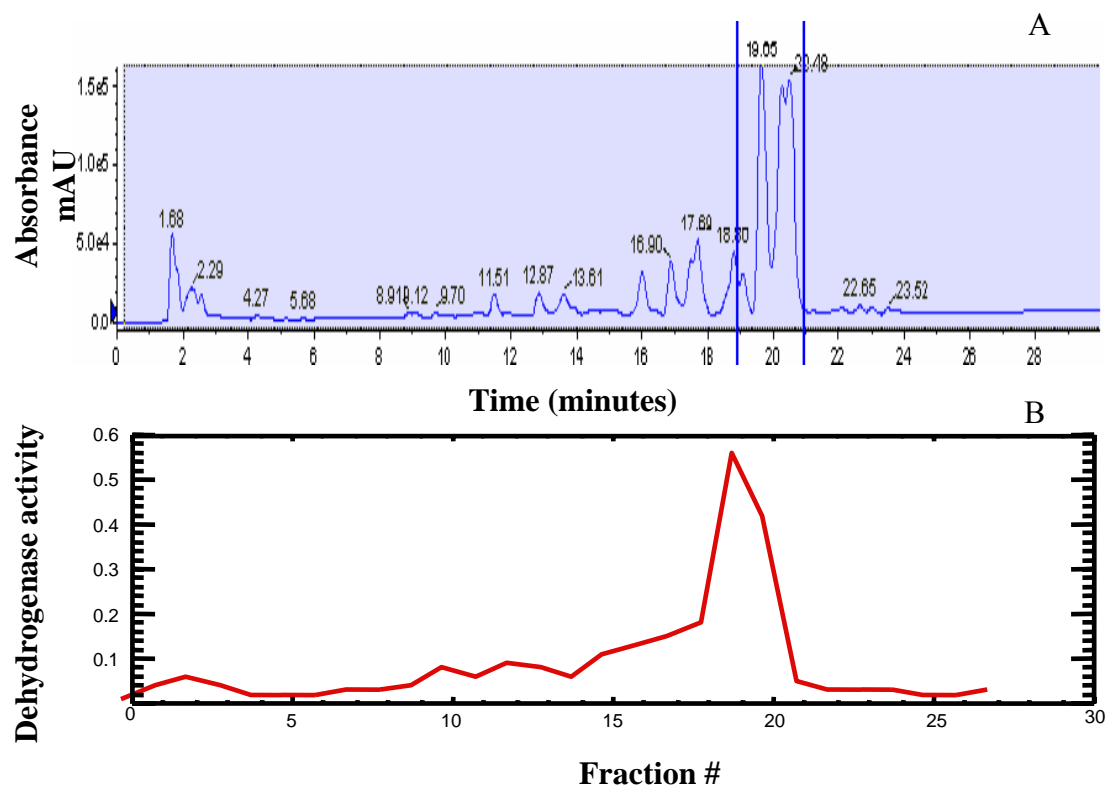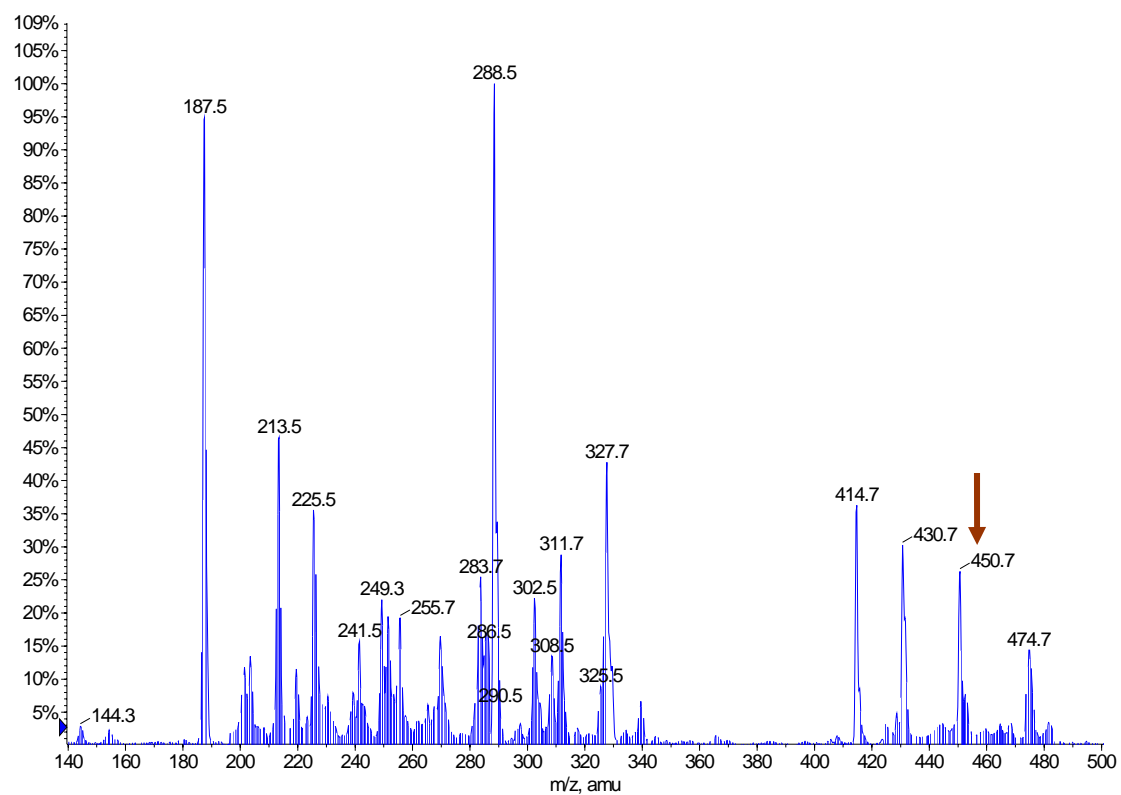
Figure 2.3. Mass spectrum of the fraction with highest enzyme activity (19-21 min). Intensity of individual masses plotted against respective m/z. The m/z indicated with a red arrow corresponds to the mass of lysoPE 16:1 in the negative mode.

SocA oxidized lysoPE16:0 over a greater than 100-fold pH range with maximal

activity at pH 7.0 (Figure 2.4). SocA utilized both NAD^+ and $NADP^+$ with comparable

efficiency (558 ± 69 and 652 ± 59 µmol min^{-1} mg^{-1}, respectively).

Substrate specificity and kinetics.

The dehydrogenase assay was used to oxidize various synthetic lysoPE species of

varying acyl chain length and saturation in order to determine the fatty acid specificity of

SocA (Table 2.1). Although SocA oxidizes lysoPE 16:0 with highest efficiency, it

oxidizes other lysoPE substrates with less than half-fold difference in specific activity.

However, a *sn*-1 fatty acid appears to be essential for oxidation as SocA was unable to

oxidize glycerophosphorylethanolamine. Although, lysophospholipids may be acylated

at either *sn*-1 or *sn*-2, the acyl chain in 1-hydroxy 2-acyl lysophospholipid rapidly

migrates to *sn*-1 resulting in the formation of 1-acyl 2-hydroxy lysophospholipid (22).

Hence this was the only form of the molecule available for examination. Because it was

more soluble in methanol, initial rates were analyzed with various concentrations of

lysoPE 18:1. Initial rates were fitted to the Michaelis-Menten equation, $V = V_{max}[S]/[S]$

$+ K_m$ using non-linear regression [SigmaPlot 8.0; SPSS Inc.] (Figure 2.5). V is the

velocity of the reaction, V_{max} is the maximal rate, [S] is the concentration of substrate and

K_m is the *Michaelis* constant. The apparent K_m and V_{max} were determined to be 116 µM

and 875 µmol min^{-1} mg^{-1}, respectively. The catalytic efficiency (K_{cat}/K_m) was calculated

to be 1 x 10^8 $(moles/L)^{-1}sec^{-1}$. The range of concentrations tested was limited by the

solubility of lysoPE 18:1 in methanol. Methanol inhibited protein activity at higher

concentrations, and the detection limits of the spectrophotometer did

Figure 2.4. Effect of pH on lysoPE 16:0 oxidation by SocA. Enzyme was assayed with 100 μM lysoPE 16:0 in sodium phosphate buffer.
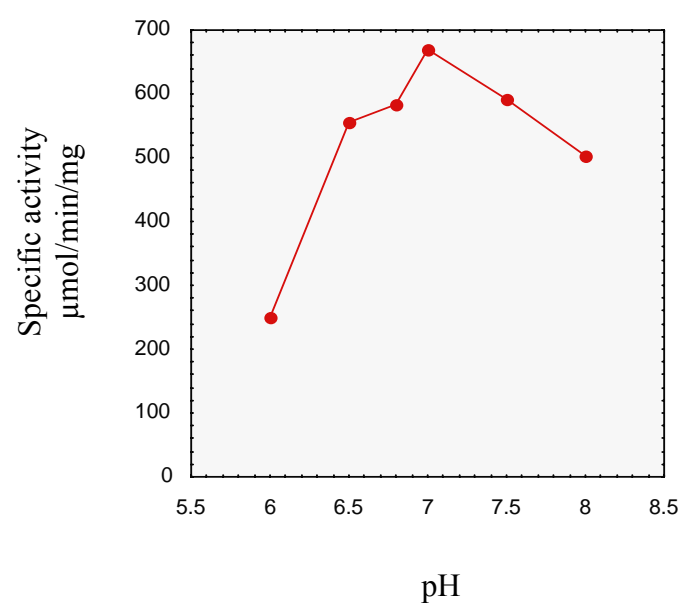
Table 2.1. Fatty acid specificity of SocA

Substrate	Specific Activity (μmol/min/mg)	% Converted in 10 min
Glycerophosphoryl-ethanolamine	10 ± 9	8
1-acyl 2-hydroxyPE 14:0	247 ± 61	39
1-acyl 2-hydroxyPE 16:0	558 ± 69	70
1-acyl 2-hydroxyPE 16:1 ω5c	345 ± 239	38
1-acyl 2-hydroxyPE 18:0	428 ± 164	40
1-acyl 2-hydroxyPE 18:1 ω9c	299 ± 69	32

Enzyme assays were carried out in the presence of 1 mM NAD$^+$, 100 μM substrate, and 200 μM sodium phosphate buffer, pH 6.8. Standard deviation of the mean was calculated from three independent experiments.

Figure 2.5. Double reciprocal plot of initial velocity versus lysoPE 18:1 concentrations.
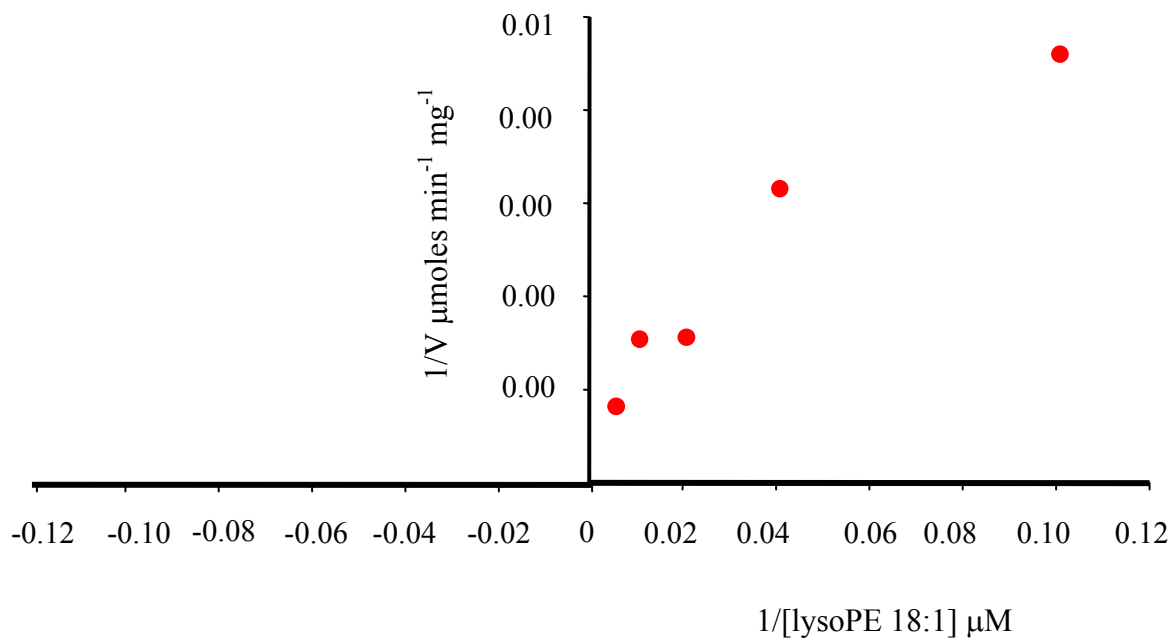
not allow for reliable readings at much lower substrate concentrations. Hence, the kinetic studies were performed over a narrow range of lipid concentrations. Interpretation of the results is made more difficult by the fact that the lipid is most likely in a heterogeneous mixture of states, including but not limited to micellar and unilamellar forms. When dispersed in excess water, phospholipids form vesicular membrane structures. The particular structures adopted by lysoPE have not been extensively examined with biophysical techniques, but under the conditions employed here it is likely that the lipid is present in micellar and unilamellar forms. The conversion by SocA is not complete, with only about 60-70% substrate conversion after 10 minutes when the enzyme velocity plateaued.

In order to develop a uniform method of lipid presentation, mixed micelles were created with lyso lipids and Triton X 100 (13). The specific activity of micellar 16:0 lysoPE was 3-fold lower than that formed by methanolic lipid (106 ± 43 μmol min^{-1} mg^{-1}), and the substrate conversion was about 20% in 10 minutes. The lowered specific activity could possibly be due to inhibition of protein activity by the detergent. These results indicate that micelles are adequate substrates, but still don't explain why only a fraction of the substrate is converted.

Detergent induced mixed micelles of individual lysophospholipids with varying head groups were examined with the dehydrogenase assay to determine if SocA exhibited head group specificity or if SocA acted on any lipid molecule with an ability to adopt a micellar form. SocA preferentially oxidized lysophospholipids with the ethanolamine head group. Parallel assays performed with lysophospholipids of varying head groups in the absence of Triton X 100 also indicated that SocA oxidized only lysophospholipids

110

Table 2.2. Head group specificity of SocA

Substrate	Specific Activity[a] (μmol/min/mg)	Specific Activity[b] (μmol/min/mg)
1-acyl 2-hydroxyPE 16:0	558 ± 69	106 ± 43
1-acyl 2-hydroxyPC 16:0	9 ± 4	3 ± 7.5
1-acyl 2-hydroxyPS 18:1	< 0.01	< 0.01
1-acyl 2-hydroxyPG 16:0	< 0.01	< 0.01
1-acyl 2-hydroxyPA 16:0	5 ± 8	< 0.01

Enzyme assays were carried out in the presence of 1 mM NAD^+, 100 μM substrate, and 200 μM sodium phosphate buffer pH 6.8. Standard deviation of the mean was calculated from three independent experiments. PE- Phosphatidylethanolamine; PC- Phosphatidylcholine; PS- Phosphatidylserine; PG- Phosphatidylglycerol; PA- Phosphatidic acid. [a]Specific activity determined in the absence of Triton X. [b]Specific activity determined in the presence of Triton X 100.

with the ethanolamine head group (Table 2.2).

Analysis of the oxidized lysoPE 16:0.

The proposed product of lysoPE oxidation is 1-acyloxy-3-(2-aminoethylphosphatyl) acetone. The NMR spectrum of the oxidation product indicated the absence of the phosphoethanolamine moiety. The dihydroxyacetone core of this molecule has the ability to rearrange *via* keto-enol tautomerism to glyceraldehyde, with the concomitant loss of both the phosphoethanolamine and the fatty acyl groups (Figure 2.6). Furthermore, the oxidized molecule could also be susceptible to potential acidic hydrolysis at the ester linkages, resulting in formation of glycerophosphorylethanolamine and a free fatty acid or monoacylglycerol phosphate and ethanolamine. Consistently, NMR spectroscopy and mass spectrometry indicated that oxidized lysoPE16:0 underwent further degradation (data not shown). TLC analysis of the oxidized lysoPE 16:0 showed two iodine stained spots with R_f values 0.35 and 0.93, indicating hydrolysis of the product (Figure 2.7A). The R_f value of 0.93 corresponds to that of the free fatty acid and monopalmitoylglycerol (data not shown) adding further evidence to the proposed breakdown of oxidized lysoPE. The identity of the iodine stained spot with R_f value 0.35 remains unknown. Ninhydrin staining revealed that neither product contained the ethanolamine group (Figure 2.7B). These results argue that the oxidized product is unstable and fragments into multiple products.

The oxidation product of lysoPE 16:0 was reduced by SocA in an NADH-dependent manner, with a specific activity of 733 ± 247 µmoles min^{-1} mg^{-1} suggesting that SocA reduces one or more products of hydrolysis. The possible substrates include 1-

Figure 2.6. Proposed keto-enol tautomerism and subsequent hydrolysis of oxidized

lysoPE. Keto form of oxidized lysoPE (6A) is converted to its tautomeric enol form

(6B). The enol form is unstable in an aqueous environment and is hydrolyzed into 1-

acylglyceraldehyde and phosphoethanolamine (6C). 1-acylglyceraldehyde rearranges

into 1-acyl-2-keto glycerol (6D) which isomerizes into the enol form, 1-acylglycerol

(6E). 1-acylglycerol subsequently hydrolyzes into free fatty acid and glyceraldehyde
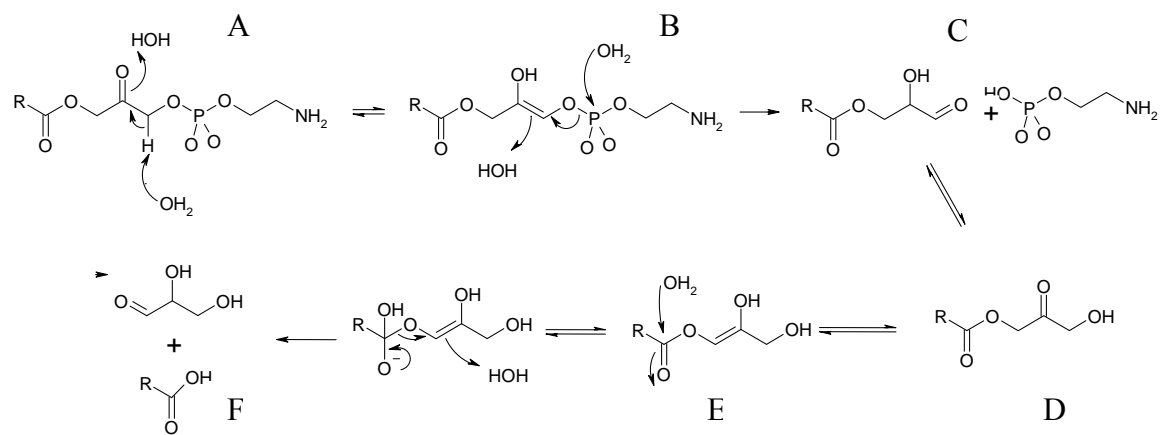
(6F).

Figure 2.7. Thin layer chromatography of lysoPE 16:0 (lane 1) and the enzymatically

oxidized lysoPE 16:0 (lane 2) stained with iodine (A) and ninhydrin (B). The reduced

form stains with both iodine and ninhydrin while the oxidized form stains only with

iodine.

acylglyceraldehyde, 1-acyl-2-keto glycerol, and glyceraldehyde. Since SocA did not reduce the commercially available glyceraldehyde, the likely substrate for reduction is 1-acyl-2-keto glycerol.

Bioassay for oxidized lysoPE 16:0 activity:

Bioassay involving the extracellular complementation of both the reduced and enzymatically oxidized forms of lysoPE 16:0 and lysoPE 16:1 was performed to determine the development rescue activity of these molecules. Both oxidized and reduced lysoPE 16:0 and lysoPE 16:1 did not correct the developmental defects of *csgA* mutants (data not shown).

SocA acts on multiple substrates.

The various lysoPE species were quantified during growth and development of wild-type *M. xanthus* cells (Table 2.3). The levels of lysoPE 16:1 and lysoPE 18:0 show a striking increase of 40-fold and 300-fold respectively during development. Quantification after partial purification on the LCSi column, using the dehydrogenase assay revealed the total number of substrate molecules per cell to be about 5×10^7. This is about 5 orders of magnitude higher than the total number of lysoPE 16:1 molecules present per cell, providing evidence for the presence of multiple SocA substrates.

The biologically active molecule is not likely to be a lysoPE. TLC was used to purify the biologically active substrate under conditions where all lysoPE species have a similar mobility, regardless of the type of associated fatty acid. LysoPE 16:0 identified by ninhydrin staining had an R_f value of 0.30, while the enzymatically active fractions

Table 2.3. Lysophosphatidylethanolamine species (molecules/cell) in vegetative and

developing   cells.

	15:0	15:1	16:0	16:1	**18:0**
Vegetative	5.8 x 10^4	2.8 x 10^2	4.4 x 10^4	9.6 x 10^2	6.0 x 10^1
Developmental	3.0 x 10^5	2.6 x 10^2	1.3 x 10^5	4.0 x 10^4	2.0 x 10^4

Cell samples were subjected to chloroform: methanol extraction followed by ESIMS; the

lysoPE species were quantified using calibration curves derived from known amounts of

lysoPE 16:0 for the saturated species and lysoPE 18:1 for the unsaturated species.

Figure 2.8. Rescue of developmental aggregation by the TLC fraction oxidized by SocA.

A single fruiting body (indicated by a box) is shown along the edge of the filter paper

disc. Bar is 50 µm.
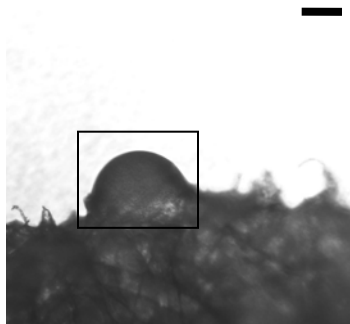
resolved at R_f 1.00, 0.93 and 0.80. Furthermore, 250 nmoles of SocA-oxidized fraction with an R_f 1.00, induced aggregation of *csgA* mutants along the edge of the filter paper disc (Figure 2.8). These results suggest that SocA oxidizes molecules other than lysoPE in the extract.

Discussion:

SocA is the first lysophosphatidylethanolamine dehydrogenase to be described. This enzyme acts on lysophospholipid substrates with fatty acids of different chain length and saturation, showing preference for lysophospholipids with an ethanolamine headgroup. The hydroxyl group at C2 on the glycerol backbone is proposed to be oxidized to the corresponding keto form. The efficiency of catalysis is 9×10^7 (moles/L)$^{-1}$ sec^{-1} and is comparable to other well characterized enzymes.

SocA has most of the sequence motifs that define the NADP(H) dependent classical SCADs (4). An aspargine residue found at the end of β4 in classical SCADs is absent in SocA. Also, SocA has a glutamate residue in place of the conserved aspartate, 13 positions downstream from the catalytic lysine. NAD(H)-binding SCADs have an aspartate in β2 that repels the negatively charged phosphate group on NADP(H) and hence confers NAD$^+$ specificity to such enzymes by preferential exclusion of NADP$^+$. SocA lacks the crucial aspartate in β2 and is predicted to utilize NAD$^+$ or NADP$^+$. SocA was able to utilize either coenzyme with comparable efficiency suggesting dual coenzyme specificity.

Lysophospholipids are generated by phospholipases and transacylases during phospholipid turnover in the cell membrane. *E. coli* phospholipase A, which is activated

upon damage to the cell membrane, hydrolyses the acyl chain at either *sn*-1 or *sn*-2 on the glycerol backbone generating 1-hydroxy 2-acyl glycerophosphoethanolamine or 1-acyl 2-hydroxy glycerophosphoethanolamine and a free fatty acid (30). Transacylases transfer the acyl chain from *sn*-1 of phosphatidylethanolamine, phosphatidylglycerol, or cardiolipin to lipoproteins generating the corresponding lysophosphatidylethanolamine, lysophosphatidylglycerol, or lysophosphatidylcardiolipin, respectively. In addition, palmitoyl transferase transfers the palmitate from *sn*-1 of a glycerophospholipid to the R-3-hydroxymyristoyl moiety during lipopolysaccharide biosynthesis. Regardless of the site of hydrolysis, the acyl chain migrates from *sn*-2 to *sn*-1 to generate 1-acyl 2-hydroxyglycerophosphoethanolamine (22).

The *M. xanthus* genome encodes putative lipases and transacylases that could potentially be involved in substrate generation for SocA (data not shown). At least nine of these are acyl transferases and seven are phospholipases. The phospholipases include five members of patatin-like (2), (25). These ORFs however have not been characterized.

Lysophospholipids serve as extracellular signaling molecules in mammals. In their capacity as autocrine or paracrine signals, they mediate differentiation of cells of the immune system as well as those involved in neurogenesis, angiogenesis, or carcinogenesis. For example, lysophosphatidic acid (LPA) stimulates ionic conductance changes in cortical neuroblasts during brain development (1). LPA is also produced by autotaxin, a metastasis-promoting factor, suggesting a potential role for LPA in carcinogenesis (19). Lysophospholipids exert their influence through specific G protein-coupled receptors (3). The binding of the ligand to these receptors results in GDP/GTP exchange on intracellular GTP-binding proteins, which then transmit the signal to

proteins involved in second messenger generation (24). While their role as mediators of signal transduction has been studied extensively in eukaryotes, a similar role for lysophospholipids in a bacterial system has not been reported.

Given a potential role for SocA in intercellular signaling during development of *M. xanthus*, and the intercellular signaling by lysophospholipids in mammals, it is tempting to speculate that SocA mediates lysoPE signaling in *M. xanthus*. Furthermore, lysoPE shows a striking increase during development. However, SocA appears to be substrate-limited as the physiological concentration of lysoPE is much lower than the apparent K_m of SocA, questioning the physiological relevance of lysoPE oxidation by SocA. The discrepancy between the lysoPE concentrations and K_m of SocA could be explained if the membrane-bound lysoPE substrate is sequestered by the enzyme. At this time, however, neither the distribution of lysoPE in the membrane nor the localization of SocA is known. In addition, extracellular complementation of both reduced and enzymatically oxidized lysoPE 16:0 and lysoPE 16:1 did not rescue the developmental defects of the *csgA* mutant.

Based on the data discussed above, it is not likely that oxidized lysoPE has a role in signaling during multicellular development of *M. xanthus* leading one to question the biological significance of oxidized lysoPE. Understanding the complex pattern of *socA* expression may illuminate the biological significance of SocA-mediated lysoPE oxidation. Lee and Shimkets (15) found that *socA* was expressed at high levels in vegetative cells during growth, and as development progressed, the expression levels steadily dropped in the rod-shaped cells. Conversely, *socA* expression increased in spores. This suggests that SocA may function during vegetative growth and also during

123

sporulation or spore germination. SocA could be part of the predatory machinery of *M. xanthus* enabling prey cell degradation and fatty acid catabolism. SocA also has a potential role in cell membrane remodeling during *M. xanthus* spore morphogenesis, which involves extensive phospholipid turnover (Shimkets, unpublished data). These possibilities appear to be attractive venues for exploring the significance of SocA-mediated lysoPE oxidation in future experiments.

socA appears to be essential for *M. xanthus* as numerous attempts to delete it have been unsuccessful. It is not clear that oxidized lysoPE has an essential function. Several lines of evidence support the possibility of multiple SocA substrates. First, the partially pure substrate extract that was oxidized by SocA, stimulated aggregation, while the corresponding reduced substrate stimulated sporulation of *csgA* mutants. These experiments seem to suggest that SocA controls different aspects of development by acting on different substrates. Second, partial purification of the crude extract containing the SocA substrate(s) yields about 5×10^7 molecules per cell. This is about five orders of magnitude higher than the number of lysoPE 16:1 molecules present per cell, suggesting the existence of more than one SocA substrate. Finally, the active molecules from the partially pure substrate extract migrate with R_f values of 1.00, 0.93 and 0.80, while lysoPE migrates with an R_f value of 0.30 under the same conditions. Thus, SocA appears to be acting on multiple substrates, which is not unusual for members of this family of enzymes.

.

Reference:

1. **Dubin, A. E., T. Bahnson, J. A. Weiner, N. Fukushima, and J. Chun.** 1999. Lysophosphatidic acid stimulates neurotransmitter-like conductance changes that precede GABA and L-glutamate in early, presumptive cortical neuroblasts. J. Neurosci. **19:**1371-1381.

2. **Hirschberg, H. J., J. W. Simons, N. Dekker, and M. R. Egmond.** 2001. Cloning, expression, purification and characterization of patatin, a novel phospholipase A. Eur. J. Biochem. **268:**5037-44.

3. **Ishii, I., N. Fukushima, Y. X, and J. Chun.** 2004. Lysophospholipid receptors: signaling and biology. Annu. Rev. Biochem. **73:**321-354.

4. **Kallberg, Y., U. Oppermann, H. Jornvall, and B. Persson.** 2002. Short-chain dehydrogenases/reductases (SDRs): Coenzyme-based functional assignments in completed genomes. Eur. J. Biochem. **269:**4409-4414.

5. **Kearns, D. B., and L. J. Shimkets.** 2001. Directed movement and surface-borne motility of *Myxococcus* and *Pseudomonas.* Methods Enzymol **9:**126-129.

6. **Kearns, D. B., A. Venot, P. J. Bonner, B. Stevens, G. J. Boons, and L. J. Shimkets.** 2001. Identification of a developmental chemoattractant in *Myxococcus xanthus* through metabolic engineering. Proc. Natl. Acad. Sci. USA. **98:**13990-13994.

7. **Kido, M., K. Yamanaka, T. Mitani, H. Niki, T. Ogura, and S. Hiraga.** 1996. RNase E polypeptides lacking a carboxy-terminal half suppress a *mukB* mutation in *Escherichia coli*. J. Bacteriol. **178:**3917-3925.

8. **Kim, S., and D. Kaiser.** 1991. C-Factor has distinct aggregation and sporulation thresholds during *Myxococcus* development. J. Bacteriol. **173:**1722-1728.

9.   **Kim, S. K., and D. Kaiser.** 1990. C-factor: A cell-cell signaling protein required for fruiting body morphogenesis of *M. xanthus*. Cell **61:**19-26.

10.   **Kruse, T., S. Lobedanz, N. M. Berthelsen, and L. Sogaard-Andersen.** 2001. C-signal: a cell surface-associated morphogen that induces and co-ordinates multicellular fruiting body morphogenesis and sporulation in *Myxococcus xanthus*. Mol. Microbiol. **40:**156-168.

11.   **Kuspa, A., L. Plamann, and D. Kaiser.** 1992. Identification of heat-stable A-factor from *Myxococcus xanthus*. J. Bacteriol. **174:**3319-3326.

12.   **Kuspa, A., L. Plamann, and D. Kaiser.** 1992. A-Signalling and the cell density requirement for *Myxococcus xanthus* development. J. Bacteriol. **174:**7360-7369.

13.   **Lambert, O., D. Levy, J. L. Ranck, G. Leblanc, and J. L. Rigaud.** 1998. A new "gel-like" phase in dodecyl maltoside-lipid mixtures: implications in solubilization and reconstitution studies. Biophys J. **74:**918-930.

14.   **Lee, B.-U., K. Lee, J. Mendez, and L. J. Shimkets.** 1995. A tactile sensory system of *Myxococcus xanthus* involves an extracellular NAD(P)$^+$-containing protein. Genes Dev. **9:**2964-2973.

15.   **Lee, K., and L. J. Shimkets.** 1996. Suppression of a signaling defect during *Myxococcus xanthus* development. J. Bacteriol. **178:**977-984.

16.   **Li, S., B. Lee, and L. J. Shimkets.** 1992. *csgA* expression entrains *Myxococcus xanthus* development. Genes Dev. **6:**401-410.

17.   **Lobedanz, S., and L. Sogaard-Andersen.** 2003. Identification of the C-signal, a contact-dependent morphogen coordinating multiple developmental responses in *Myxococcus xanthus*. Genes Dev. **17:**2151-2161.

18.   **Lopez, P. J., I. Marchand, S. A. Joyce, and M. Dreyfus.** 1999. The C-terminal half of
        RNase E, which organizes the *Escherichia coli* degradosome, participates in mRNA
        degradation but not rRNA processing *in vivo*. Mol Microbiol **33:**188-199.

19.   **Mills, G. B., and W. H. Moolenaar.** 2003. The emerging role of lysophosphatidic acid
        in cancer. Nat. Rev. Cancer. **3:**582-591.

20.   **Oppermann, U., C. Filling, M. Hult, N. Shafqat, X. Wu, M. Lindh, J. Shafqat, E.
        Nordling, Y. Kallberg, B. Persson, and H. Jornvall.** 2003. Short-chain
        dehydrogenases/reductases (SDR): the 2002 update. Chemico-Biol. Int. **143-144:**247-
        253.

21.   **Oppermann, U. C. T., C. Filling, and H. Jornvall.** 2001. Forms and functions of
        human SDR enzymes. Chemico-Biol. Int. **130-132:**699-705.

22.   **Pluckthun, A., and E. A. Dennis.** 1982. Acyl and phosphoryl migration in
        lysophospholipids: importance in phospholipid synthesis and phospholipase specificity.
        Biochem. **21:**1743-1750.

23.   **Powell, A. J., J. A. Read, M. J. Banfield, F. Gunn-Moore, S. D. Yan, J. Lustbader,
        A. R. Stern, D. M. Stern, and R. L. Brady.** 2000. Recognition of structurally diverse
        substrates by type II 3-hydroxyacyl-CoA dehydrogenase (HADH II)/amyloid-beta
        binding alcohol dehydrogenase (ABAD). J. Mol.Biol **303:**311-327.

24.   **Roberts, D. J., and M. Waelbroeck.** 2004. G protein activation by G protein
        coupled receptors: ternary complex formation or catalyzed reaction? Biochem.
        Pharmacol. **68:**799-806.

25.   **Rydel, T. J., J. M. Williams, E. Krieger, F. Moshiri, W. C. Stallings, S. M. Brown, J.
        C. Pershing, J. P. Purcell, and M. F. Alibhai.** 2003. The crystal structure, mutagenesis,

and activity studies reveal that patatin is a lipid acyl hydrolase with a Ser-Asp catalytic dyad. Biochem. **42:**6696-6708.

26. **Shimkets, L., and H. Rafiee.** 1990. CsgA, an extracellular protein essential for *M. xanthus* development. J. Bacteriol. **172:**5299-5306.

27. **Shimkets, L. J.** 1999. Intercellular signaling during fruiting-body development of *Myxococcus xanthus*. Annu. Rev. Microbiol. **53:**525-549.

28. **Shimkets, L. J., and S. J. Asher.** 1988. Use of recombination techniques to examine the structure of the *csg* locus of *Myxococcus xanthus*. Mol. Gen. Genet. **211:**63-71.

29. **Shimkets, L. J., and D. Kaiser.** 1982. Induction of coordinated movement of *Myxococcus xanthus* cells. J. Bacteriol. **152:**451-461.

30. **Snidjer, H. J., and B. W. Dijkstra.** 2000. Bacterial Phospholipase A: Structure and function of an integral membrane phospholipase. Biochim. Biophys. Acta. **1488:**91-101.

CHAPTER 3

CONCLUSION

Intercellular signaling systems consisting of diverse molecules coordinate the

formation of starvation-induced multicellular fruiting bodies in *Myxococcus xanthus*

(139). C-signaling is essential for the morphologically distinct events of rippling,

aggregation, and sporulation during the course of fruiting body formation. C-signaling is

initiated by CsgA, which has significant homology to short-chain alcohol dehydrogenases

(100). In addition to the full length form, a small proportion of CsgA also occurs as a

truncated 17 kDa form (83, 107). Much debate has centered on the role of these two

versions of CsgA in signal generation. The focus of this work initially was to establish

the biochemical basis for the mechanism of C-signal generation by identifying the

physiological substrate(s) of CsgA.

Previous work by Lee et al. (100) indicated that the full-length form of CsgA with

an N-terminal MalE fusion rescued development of *csgA* mutants at a concentration of

100 nM. The specific activity of the MalE fusion is roughly 1% of the native protein, and

the yields are low. In an attempt to obtain a protein with increased specific activity, we

expressed a non-fusion version of *csgA* under the control of the lambda promoter in *E.

coli*. However, the expression levels were low, compounding the problems associated

with purification of the recombinant protein. Varying the length of the induction period

and the concentration of the inducer did not improve expression levels. A 200-fold

purification of the protein was achieved by cation exchange followed by ADP-sepharose.

The partially pure protein from the ADP-sepharose column rescue development in *csgA* mutants at physiological concentrations (4 nM). Several attempts to purify CsgA further using various methods including anion exchange chromatography, hydrophobic interaction chromatography, and hydroxyapatite column chromatography were not successful, due ultimately to the low level of expression.

Attempts were made to explore other types of expression systems. Expression of *csgA* under the control of promoters like pBAD, pTrc, and pT_7 resulted in inhibition of *E. coli* growth. One possible explanation for the *csgA* expression-induced toxicity is that CsgA could oxidize or reduce a molecule required for cell viability. *csgA* expression was not detected when coexpressed with *hemN* (with which CsgA showed a strong interaction using the yeast two-hybrid assay). The idea behind this experiment was to see if CsgA-induced toxicity could be over come, by virtue of its presumptive association with HemN. Attempts to express *csgA* using an *in vitro* translation system were not successful. A *csgA* construct is ready to be tested for expression in the eukaryotic host *Pichia pastoris*. Transformation into the yeast is awaiting the availability of an anti-CsgA antibody to assess *csgA* expression. In summary, in spite of a promising start, biochemical characterization of CsgA had to be abandoned because of the lack of pure protein.

The focus of the project then shifted to enzymatic characterization of SocA. Complementation of developing *csgA* cells with *csgA$^-$ socA* over-expressing cells results in developmental rescue of the *csgA* mutants (102). Lee and Shimkets (102) proposed that the developmental rescue by SocA over-producing cells was caused by a substrate overlap between CsgA and SocA. SocA was expressed as a His-tagged protein and

purified to apparent homogeneity. SocA was found to oxidize lysophosphoethanolamine substrates with varying fatty acid chain length and saturation. The hydroxyl group at C2 on the glycerol backbone is proposed to be oxidized to 1-acyloxy-3-(2-aminoethylphosphatyl)acetone, which is unstable and breaks, losing both the phosphoethanolamine and fatty acyl groups. Attempts to identify the products of oxidation and subsequent hydrolysis using NMR spectroscopy and mass spectrometry were unsuccessful.

The identification of lysoPE as a substrate for SocA offers the attractive possibility that SocA mediates lysoPE signaling in *M. xanthus*. A direct link between developmental rescue by SocA complementation and its ability to oxidize lysoPE substrates *in vitro* still needs to be established. Although recombinant SocA with an N or C-terminal histidine (6x) fusion exhibited *in vitro* dehydrogenase activity, neither protein rescued the developmental defects of *csgA* mutants upon extracellular complementation. This could be due to the way SocA accesses the substrate under the conditions encountered in the bioassay. It could also be due to inactivation of SocA by the many proteases secreted during development. Also, the fusion tags used for purification could interfere with the interaction of SocA with the membrane-bound substrate.

Several lines of evidence argue against oxidized lysoPE as the C-signal. Although, the kinetic constants for SocA compare well with other well characterized enzymes, the apparent K_m is several orders of magnitude higher than the physiological concentration of lysoPE. In addition, oxidized lysoPE appears to be highly unstable in an aqueous environment. Cell-cell contact-dependence for C-signal transmission could be explained by a potentially unstable signal with a very short half-life. Nevertheless,

extracellular complementation of lysoPE or oxidized lysoPE did not rescue the developmental defects of the C-signaling mutant, and there is no evidence that it is a signal in *M. xanthus.* Several pieces of data suggest the possibility of multiple SocA substrates. Substrate(s) molecules in the partially purified extract were present at several orders of magnitude higher concentrations than the total number of lysoPE molecules present per cell. Extracellular complementation of the partially pure substrate extract oxidized by SocA stimulated aggregation of *csgA* mutants, while the corresponding reduced substrate stimulated sporulation. These experiments seem to suggest that molecule(s) with properties consistent with those of the C signal are present in the substrate extract.

In order to identify other SocA substrate(s), several potential targets were systematically tested using the *in vitro* dehydrogenase assay. The rationale behind testing each of the substrates differs for each set of compounds.

Crawford and Shimkets (26, 27) proposed that CsgA sustains the RelA-mediated stringent response in the presence of an influx of A-signal amino acids during development, possibly by oxidizing hydroxylated amino acids. SocA did not oxidize serine and threonine.

Stigmolone (2,5,8-trimethyl-8-hydroxy-nonan-4-one) is a pheromone that accelerates development in the closely related myxobacterium *Stigmatella aurantiaca* (61, 121). SocA did not reduce stigmolone and deoxystigmolone ('deoxy' at C8). CsgA has 34.7% identity to 11-*cis* retinol dehydrogenase from *Bos taurus* (X82262) (100). So the ability of SocA to oxidize both *cis* and *trans*-retinol was tested without success. *socB*, the second gene in the *socABC* operon, has 48% homology with *frdD* gene product

132

from *Proteus vulgaris*, which anchors fumarate reductase to the cell membrane. Fumarate reductase provides electrons and protons for the electron transport chain. SocA did not reduce menaquinone, an essential electron transport component. Furthermore, the *M. xanthus* genome was analyzed to explore the possibility that SocA could be involved in the TCA cycle or electron transport chain. The *M. xanthus* genome encodes a complete complement of genes involved in the essential electron transport components, leaving the perplexing question about the essential nature of SocA unanswered.

CsgA was found to have a strong interaction with HemN, a coproporphyrinogen-III oxidase involved in heme O biosynthesis, using the yeast two hybrid assay. In order to explore the possibility of metabolic channeling of substrates between HemN and CsgA, the ability of SocA to oxidize the hydroxyl group on the pyrrole ring of different hemes, Heme O and Heme A, (in the ferric state) was tested. SocA did not oxidize either of the two hemes. HemN requires *S*-adenosyl-L-methionine, NAD(P)H, and other unidentified components for conversion of coproporphyrinogen-III to protoporphyrinogen-IX, and 5'-deoxyadenosine is a by-product formed during the process (99). The ability of SocA to oxidize 5'-deoxyadenosine to possibly regenerate the NAD(P)H was tested. SocA did not oxidize 5'-deoxyadenosine.

Future directions:

In addition to its role in development in the absence of CsgA, SocA also appears to have essential vegetative function(s) as attempts to delete *socA* have been unsuccessful. The closest relatives of SocA with known substrates include the 3-oxoacyl-[acyl carrier protein] reductases (102). *M. xanthus* genome encodes 3-oxoacyl-

[acyl carrier protein] reductases in operon arrangements similar to *E. coli*, suggesting that SocA performs other essential function(s).

The dehydrogenase assay-based screen coupled with NMR and mass spectrometry will serve as a good tool for identification of the active molecule(s). Development of chromatographic methods to improve the purification of the substrate(s) with reduced background will enable identification of novel molecules with morphogenetic properties and essential vegetative properties.

Since it has not been possible to obtain a *socA* deletion mutant, ectopic depletion of SocA could be used to study the effect of the absence of SocA during growth and development. The ectopic depletion experiments can be performed by cloning the *socA* allele under the control of an inducible promoter in a plasmid vector capable of undergoing site-specific recombination in the *M. xanthus* genome.

Finally, the fact that the extract treated with SocA confers developmental rescue on *csgA* mutants suggests that the extract is enriched for a developmental morphogen, possibly the substrate(s) of CsgA. Eukaryotic protein expression hosts like the *Pichia pastoris* or baculovirus systems could be explored for achieving optimal expression of *csgA* to confirm the biochemical basis for C-signaling.

References:

1. **Crawford, E. W. J., and L. J. Shimkets.** 2000. The *Myxococcus xanthus socE* and *csgA* genes are regulated by the stringent response. Mol. Microbiol. **37:**788-799.

2. **Crawford, E. W. J., and L. J. Shimkets.** 2000. The stringent response in *Myxococcus xanthus* is regulated by SocE and the CsgA C-signaling protein. Genes Dev. **14:**483-492.

3. **Hull, W. E., A. Berkessel, and W. Plaga.** 1998. Structure elucidation and chemical synthesis of stigmolone, a novel type of prokaryotic pheromone. Proc. Natl. Acad. Sci. USA. **95:**11268-11273.

4. **Kim, S. K., and D. Kaiser.** 1990. C-factor: A cell-cell signaling protein required for fruiting body morphogenesis of *M. xanthus*. Cell. **61:**19-26.

5. **Layer, G., K. Verfurth, E. Mahlitz, and D. Jahn.** 2002. Oxygen-independent coproporphyrinogen-III oxidase HemN from *Escherichia coli*. J. Biol. Chem. **277:**34136-34142.

6. **Lee, B.-U., K. Lee, J. Mendez, and L. J. Shimkets.** 1995. A tactile sensory system of *Myxococcus xanthus* involves an extracellular NAD(P)$^+$-containing protein. Genes Dev. **9**:2964-2973.

7. **Lee, K., and L. J. Shimkets.** 1996. Suppression of a signaling defect during *Myxococcus xanthus* development. J. Bacteriol. **178**:977-984.

8. **Lobedanz, S., and L. Sogaard-Andersen.** 2003. Identification of the C-signal, a contact-dependent morphogen coordinating multiple developmental responses in *Myxococcus xanthus*. Genes Dev. **17:**2151-2161.

9.   **Plaga, W., I. Stamm, and H. U. Schairer.** 1998. Intercellular signaling in *Stigmatella aurantiaca*: Purification and characterization of stigmolone, a myxobacterial pheromone. Proc. Natl. Acad. Sci. USA. **95:**11263-11267.

10.   **Shimkets, L. J.** 1999. Intercellular signaling during fruiting-body development of *Myxococcus xanthus*. Annu. Rev. Microbiol. **53:**525-549.

Appendix A

Bioassays involving extracellular lipid complementation

Traditionally, bioassays involving extracellular complementation have been employed to study and identify signaling molecules. In *M. xanthus*, extracellular complementation experiments using reporter gene fusions or rescue of phenotypic properties have been used to study the biochemical basis for A and C signaling. In the case of A-signaling, a mixture of amino acids and proteases were partially purified using traditional chromatographic methods from media conditioned by cells producing the A-signal and added to cells compromised in A-signal production. The ability of individual fractions to enable expression of the A-signal-dependent reporter gene was monitored (95, 123). Kim and Kaiser (83) tested the ability of a partially purified protein fraction enriched in CsgA to correct the aggregation and sporulation defects of C-signaling mutants. Lee et al. (100) used a similar approach to study the developmental rescue properties of a MalE-CsgA fusion protein. In both the A signal and C signal, the molecules being tested were hydrophilic and were delivered to cells completing development under submerged culture.

In the current dissertation work involving the study of SocA-mediated signaling, the potential signal molecule(s) were contained in whole cell extracts prepared using organic solvents. Several approaches for the delivery of the hydrophobic molecules were tested as listed below:

137

Lipid delivery on polystyrene or agar surface under submerged culture:

Various amounts of the extract to be tested were spotted on the polystyrene surface of 24-well microtitre plates (Corning Inc. Corning, NY). After the solvent completely evaporated, the *csgA* cell suspension at a high density (2×10^8) in 400 μl MOPS buffer (10 mM MOPS, pH 7.2, 1 mM $CaCl_2$, 4 mM $MgCl_2$, and 50 mM NaCl) was added. The plates were incubated at 32° C for 5 days and analyzed for the presence of spore-filled fruiting bodies using a dissecting microscope. A similar approach involving lipid complementation on a thin layer of agar on the polystyrene was also tested. Neither method gave consistent results. The lipid was also delivered 6 hours into development [which was optimal for CsgA delivery (83)], but the time of lipid delivery did not improve the bioassay.

Exposure of the cells to the lipid before induction of development:

The lipid samples to be tested were mixed with *csgA* cells at a high density (2×10^8) in 400 μl MOPS to ensure uniform exposure of all the cells to the lipid before addition into the individual wells of a microtitre plate or before being plated at 1×10^9 cells per 150 mm diameter TPM agar plate (10 mM Tris, pH 7.6, 1 mM KH_2PO_4, 10 mM $MgSO_4$, 1.5% Difco agar). The plates were incubated at 32° C for 5 days and analyzed for the presence of spore-filled fruiting bodies using a dissecting microscope. This method of lipid complementation did not enable *csgA* development.

High density cell suspension spotted on lipid dried on agar surface:

This is a semi-quantitative method to study the effects of hydrophobic molecules on *csgA* development. Various amounts of the lipid were spotted on TPM agar and dried. Five microliters MOPS buffer containing 1×10^7 cells were placed on the lipid spots. The

plates were incubated at 32° C for 5 days and analyzed for the presence of spore-filled fruiting bodies using a dissecting microscope. This method did not enable developmental aggregation and sporulation.

Lipid delivery *via* filter paper discs:

This is a qualitative assay in which *csgA* cells at mid-log phase of growth were harvested by centrifugation at 10,000 x g for 10 minutes, resuspended in fresh CYE (casitone 1%, yeast extract 0.5%, MgSO$_4$ 0.1%, 10 mM MOPS), and plated on TPM agar plates at a density of 1 x 10^9 cells per plate. After 6 hours, various amounts of the lipids were spotted on sterile 0.5 mm diameter Whatman 1 filter paper discs. The dry discs were then placed on a lawn of *csgA* cells undergoing development. This method has so far been the only method to consistently allow for appropriate lipid presentation to the cells to enable developmental aggregation and sporulation.

Appendix B

Rescue of developmental aggregation and sporulation by a partially pure *E. coli* protein

preparation

Escherichia coli is a common host for the expression of recombinant proteins. *E. coli* G1724 was used as the host for the expression of a non-fusion *csgA* gene (Invitrogen Co., Carlsbad, CA). The total soluble protein from the recombinant expression host without the *csgA* expression vector was subjected to purification on the cation exchange SP-sepharose column. The partially pure protein served as a control to monitor the activity of the corresponding fraction with partially pure CsgA. Surprisingly, *E. coli* protein from the SP-sepharose column, without CsgA rescued development of *csgA* mutant. The activity of the *E. coli* protein preparation was found to peak at 100 nM, which is at least a 100-fold lower specific activity than partially pure CsgA. This suggests that *E. coli* makes a protein which has the potential to induce morphogenetic changes in *Myxococcus xanthus csgA* mutants. One possibility is that an *E. coli* protein shares substrate specificity with CsgA.

Materials and methods:

Bacterial strains and growth conditions.

M. xanthus DK1622 (143) and LS523 (141) were used as the wild-type and the *csgA* mutant strain, respectively. Cells were grown at 32°C in CYE broth [casitone 1%, yeast extract 0.5%, MgSO$_4$ 0.1%, 10 mM [N-Morpholino]propanesulfonic acid (MOPS),

140

pH7.6] or on CYE agar (CYE plus 1.5% Difco agar). *E. coli* G1724 was grown in Luria-Bertoni broth (tryptone 1% yeast extract 0.5%, and sodium chloride 0.5%) supplemented with 100 μg ml^{-1} ampicillin.

Partial purification of the E. coli protein:

    E. coli G1724 was grown in 1 l LB broth to late log phase (O.D$_{550}$- 1.14), and the harvested cells were subjected to lysis by French press and separated into soluble and insoluble fractions by centrifugation at 21,000 x g for 45 minutes. Soluble protein was subjected to cation exchange chromatography on SP-sepharose (Amersham Biosciences, Piscataway, NJ). Protein was eluted with a step-wise gradient using 90 mM, 250 mM, and 500 mM KCl in 50 mM phosphate buffer, pH 6.8. The protein fraction that eluted with 250 mM KCl was used in the bioassay. Protein concentration was determined using the biscinchoninic acid (BCA) assay (Pierce Chemicals Co, Rockford, IL) with bovine serum albumin standards.

Biological assay for protein activity:

    The biological activity of the protein preparation was tested for the rescue of *csgA* development under submerged culture as described previously (84, 93). After 5 days, the assay plates were analyzed for the presence of spore-filled fruiting bodies using a dissecting microscope. The spores were quantified using a Petroff-Hausser chamber.

Results:

Partially pure *E. coli* protein (without CsgA) used in the bioassay contains at least six proteins as seen on a silver-stained gel (Figure A.1). Two of the proteins are about the size of classical short-chain alcohol dehydrogenases (SCAD) (25 kDa). The *E. coli* genome encodes 17 classical SCADs, most of which have never been characterized, and matrix-assisted laser desorption ionization mass spectrometry (MALDI-MS) could possibly be used to identify these proteins.

E. coli protein restored wild-type levels of aggregation (Figure A.2) and 15% of wild-type levels of sporulation in *csgA* cells (Figure A.3). The *E. coli* protein-induced aggregates were much smaller than the wild-type aggregates. However, the distribution and spacing of the aggregates resembled those of wild-type. The bell-shaped curve for sporulation suggests that at protein concentrations 12.5 μg/ml and higher, development was inhibited possibly because the protein concentration was high enough to restore growth of *M. xanthus*. At protein concentrations 0.25 μg/ml and lower, developmental aggregation and sporulation were not observed. The fact that *csgA* cells aggregated but did not sporulate to wild-type levels suggests that the potential SCAD in the protein preparation may not be as catalytically active as CsgA, which restored aggregation and sporulation at 100-fold lower concentrations (with the same level of purity).

Figure A.1. Silver-stained gel showing partially pure *E. coli* protein purified by

cation exchange chromatography on SP-sepharose (20 μg protein).
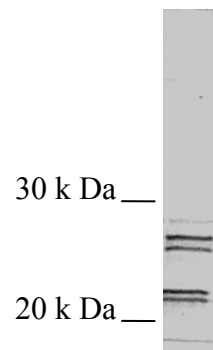
30 k Da __

20 k Da __

Figure A.2. Rescue of developmental aggregation by *E. coli* protein preparation. A.

Wild-type *M. xanthus*; B. *csgA*; C. *csgA* complemented with 2.5 µg/ml *E. coli*
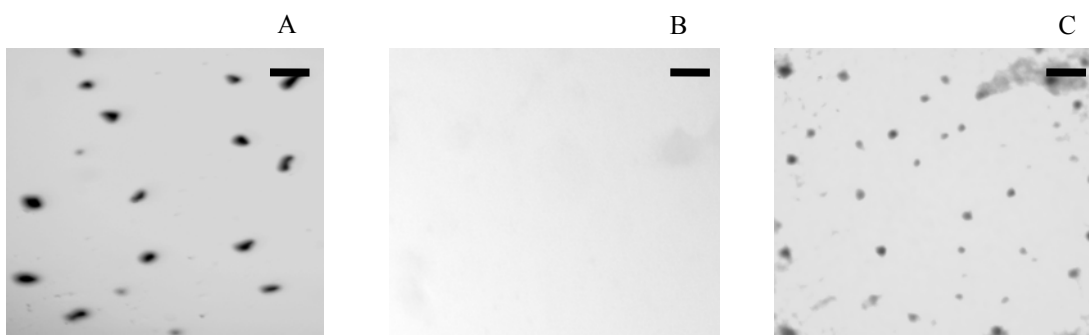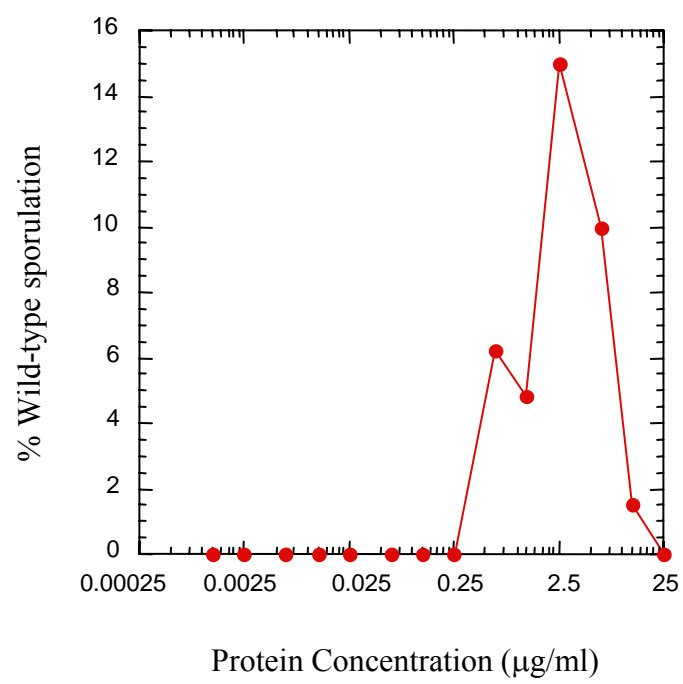
protein. Bar 620 µm

Figure A.3. Sporulation rescue by *E. coli* protein.

References:

1. **Kim, S. K., and D. Kaiser.** 1990. C-factor: A cell-cell signaling protein required for fruiting body morphogenesis of *M. xanthus*. Cell. **61:**19-26.

2. **Kim, S. K., and D. Kaiser.** 1990. Purification and properties of *Myxococcus xanthus* C-factor, an intercellular signaling protein. Proc. Natl. Acad. Sci. USA **87:**3635-3639.

3. **Kuner, J. M., and D. Kaiser.** 1982. Fruiting body morphogenesis in submerged cultures of *Myxococcus xanthus*. J. Bacteriol. **151:**458-461.

4. **Kuspa, A., L. Plamann, and D. Kaiser.** 1992. Identification of heat-stable A-factor from *Myxococcus xanthus*. J. Bacteriol. **174:**3319-3326.

5. **Lee, B.-U., K. Lee, J. Mendez, and L. J. Shimkets.** 1995. A tactile sensory system of *Myxococcus xanthus* involves an extracellular NAD(P)$^+$-containing protein. Genes Dev. **9:**2964-2973.

6. **Plamann, L., A. Kuspa, and D. Kaiser.** 1992. Proteins that rescue A-signal-defective mutants of *Myxococcus xanthus*. J. Bacteriol. **174:**3311-3318.

7. **Shimkets, L. J., and S. J. Asher.** 1988. Use of recombination techniques to examine the structure of the *csg* locus of *Myxococcus xanthus*. Mol. Gen. Genet. **211:**63-71.

8. **Shimkets, L. J., and D. Kaiser. 1982.** Induction of coordinated movement of *Myxococcus xanthus* cells. J. Bacteriol. **152:**451-461.